Further Studies with a Double-Focussing Beta Spectrometer

the Beta-Spectrum of Yttrium-91 and

the Internal Conversion Spectrum of Cerium-144.

by

A. H. Cuttler.

Ph.D. Thesis,
University of Liverpool.

Synopsis

The investigations discussed in this thesis are concerned with a β-spectrometer. The work may be divided into four distinct projects:-

1) To devize an apparatus to measure the magnetic field in the spectrometer to one part in ten thousand.

2) To investigate the behaviour of the spectrometer over a wide range of fields and the effect of setting the field by different methods.

3) To measure the β-spectrum of Y-91 and to look for small deviations from the predicted shape for a unique first-forbidden transition.

4) To measure the internal conversion lines produced in the decay of Ce-144 to establish the nature of the more prominent transitions and to establish the level scheme of Pr-144 following the β-decay of Ce-144.

The method chseen to measure the magnetic field in the spectrometer was a null method. A frame was built on which two pairs of coils were mounted to provide a reference field. Two synchronous motors were used to spin two coils, one in the spectrometer field and the other in the reference field. The outputs from the coils were fed into a sensitive narrow band-width amplifier and the spectrometer field was set by adjusting it until the output was a minimum. Because of the need to study the behaviour of the spectrometer, I did not assemble the final slip-rings and brushes but my successor did so and obtained an accuracy of one part in twenty-five thousand.

The resolution of the spectrometer was found to depend on the strength of the field and a careful study of the resolution, the position of the centroids of β-lines and the areas of the β-lines was made setting the spectrometer both on the initial magnetization curve and on a hysteresis cycle. It was found that the output of the spinning coil was proportional to the momentum only when the spectrometer was set on the initial magnetization curve. It was also found that if the spectrometer was set on the initial magnetization curve the resolution was greater than if the spectrometer was set using a hysteresis cycle and that the transmission depended on how the field was set.

From the measurements, it was concluded that the field changed shape as the strength varied. Some measurements were made to measure these changes in field shape and it was found that the field shape changed more when the spectrometer was set using a hysteresis cycle than when it was set on the initial magnetization curve. The choice of method by which to set the field is discussed.

The end point of the Y-91 β-spectrum was determined to be 1547 ± 5 Kev. and the spectrum was found to fit the theoretical shape of a ubique first-forbidden transition within the limits $-0.03 < b < 0.05$, where b is a Fierz type interference term.

In the decay of Ce-144, the K-shell conversion lines of γ-rays with energies of 80.1 and 133.6 Kev. and the L-shell conversion lines of transitions with energies of 33.7, 40.6, 53.2, 59.1, 80.1 and 133.6 Kev. were measured. The α_K/α_L and $\alpha_{L_1}/\alpha_{L_2}$ / α_{L_3} ratios indicated

that all the transitions expepting the 59.1 Kev. transition are M1 transitions and the 59.1 Kev. transition is a M3 transition. The intensities of the conversion lines were measured and a decay scheme has been proposed in which the ground state has spin (0^-) and levels at 59.1 Kev. (3^-), 80.1 Kev. (1^-), 92.8 Kev. (2^-) and 133.5 kev. (1^-).

Acknowledgements.

I wish to thank the late Professor H. W. B. Skinner for allowing me to pursue a course of research into Beta-spectroscopy at Liverpool University. I would also like to thank him for arranging a supplement to my grant for two years. I would like to thank the Senate of the University of Liverpool for awarding me a Postgraduate Studentship and the Minister of Education for a State Scholarship. I am indebted to Mr. D. G. E. Martin for guidance and much helpful advice and to Dr. J. F. Barry for many helpful discussions.

CONTENTS.

	Page.
Acknowledgements	i
Chapter I. Introduction.	
1. Beta- and Gamma-ray spectra	1
2. The development of Magnetic Spectrometers	6
Chapter II. The Magnetic Field	
1. Design of the Spectrometer	14
2. Production of the Magnetic Field	19
3. Measurement of the Magnetic Field	25
Chapter III. Apparatus and Techniques	
1. Apparatus	40
2. Source Preparation	45
3. Calibration of the Spectrometer and Errors in Measurements	48
Chapter IV. Behaviour of the Spectrometer	
1. Performance	52
2. Changes in the Field Shape	58
Chapter V. The Beta-spectrum of Yttrium-91 and the Internal Conversion Spectrum of Cerium-144	
1. The Beta-spectrum of Yttrium-91	65
2. The Internal Conversion Spectrum of Cerium-144 . .	71
Appendix A	81
Appendix B	83
Bibliography	84

Chapter I.

Introduction.

1. Beta- and Gamma-ray Spectra.

It is just over sixty years since Becquerel (1), discovered radioactivity. Following the discovery of X-rays by Roentgen, several workers had the idea that the origin of these rays may be connected with the phosphorescence of the glass of the X-ray tube which accompanied their emission. They made investigations to see whether other substances, phosphorescent when illuminated by ordinary light, also emitted penetrating rays of a nature similar to X-rays.

After several experiments of this kind with negative results, Becquerel remembered some experiments he had made with a uranium salt fifteen years previously. He had shown that it gave a brilliant phosphorescence when irradiated by ultra-violet light. When he exposed the salt to light, wrapped it in black paper and placed it on a plate of silver above a photographic plate, he found that after a time the photographic plate was affected. Soon he was able to show that the blackening of the photographic plate was independent of the phosphorescence of the salt. Becquerel then proceeded to show that the rays emitted, like X-rays, possessed the property of discharging electrified bodies.

Not long after this, Mme. Curie, in an investigation to see if

radioactivity was a general property of matter, found that thorium was also radioactive. In the same year, 1897, she isolated radium and polonium and in the following year, actinium.

As a result of studies of the penetrating power of these rays, Rutherford showed that they could be divided into two types. These he called alpha (α) -rays and beta (β) -rays. Alpha-rays are easily absorbed but produce dense ionization whereas beta-rays are more penetrating but do not produce the same density of ionization. When radium was found to emit still more penetrating rays, Villard named them gamma (γ) -rays. Gamma-rays were soon shown to possess properties similar to X-rays.

Both α-rays and β-rays are really charged particles moving at high speeds. Rutherford, in a brilliant series of experiments, showed that α-rays were helium nuclei travelling at very high speeds. β-rays were shown to be electrons; conclusive evidence coming from their charge and charge/mass ratio.

Early measurements on β-rays were carried out by absorption methods and it appeared possible to resolve the emission into components each of which was absorbed exponentially. When von Baeyer, Hahn and Meitner discovered the existence of homogeneous groups of β-rays using magnetic fields, it seemed obvious that these groups were associated with the components in the absorption experiments. Using magnetic deflection also, Wilson showed that a homogeneous group of β-rays was not absorbed exponentially. From this and the

absorption experiments, he suggested that the β-rays must have a continuous distribution of energies.

The true explanation was given by Chadwick in 1913. He discovered that the spectrum consisted of two parts, a line spectrum and a continuous spectrum which contained the greater number of electrons. Rutherford then showed that the homogeneous groups forming the line spectra were due to the conversion of γ-rays in the electronic shells of the atom disintegrating. The continuous distribution of β-rays was confirmed by Ellis and Wooster who measured the mean energy of the β-rays by a calorimetric method. They showed that although no energy was lost, the mean energy was less than the maximum energy.

No serious attempt was made to measure the energy distribution of the β-rays accurately because the way in which the rays were produced was not understood. In 1928, Pauli suggested that a light neutral particle might be involved, but it was Fermi, in 1934, who put the theory on its present basis. He postulated a light or massless particle, the neutrino (Pauli's designation), which had to fulfil certain conditions. From these, he was able to deduce the shapes of β-spectra. When β-spectra were then measured, experimental techniques were not good enough to obtain the correct shapes. Since then, the theory has been modified and experimental techniques have improved so that the theory has been tested with increasing accuracy.

Gamma-rays cannot be observed directly but only through observation of some secondary process. The first measurements of their wavelengths were made by Rutherford and Andrade who used rock-salt to diffract them. Another accurate method, suggested by Ellis, is to use the β-lines produced by internal conversion or by the photoelectric expulsion of electrons from a heavy element. An electron ejected from the excited atom itself is called an internal conversion electron.

The strengths of the various conversion lines arising from the different atomic shells or sub-shells can now be predicted with some accuracy. In atomic spectroscopy, usually it is only the electric dipole transition which is important because other transitions have a much longer lifetime. In nuclear spectroscopy on the other hand, while nuclear spin changes may forbid an electric dipole transition, because the energy of the transition is very much greater than in atomic spectroscopy, the nucleus may de-excite itself by a higher order multipole transition. The nature of the transition may be determined if the relative intensities of the conversion lines can be measured accurately. While in some cases the agreement with theory is not good, the difference between different transitions is usually sufficient to identify the nature of the transition being measured.

β-spectra have been measured in six different ways:-

1. Calorimetric methods to measure the mean energy.
2. Absorption methods.
3. By using electric fields to focus or retard the rays.
4. By using magnetic fields, either with a cloud chamber or in a spectrometer which focusses the rays.
5. By using proportional counters.
6. By using scintillation crystals.

Results from cloud chambers require much more analysis than results from magnetic spectrometers. Electric fields are not often used for focussing because it is difficult to maintain the high electric fields necessary. The most common difficulties are those of insulation, and the prevention of surface contamination, corona discharge and secondary emission from the surfaces of the apparatus. Retarding fields may only be used for low energy spectra.

Proportional counters are most useful for studying spectra from gaseous sources and, because it is possible to obtain almost 4π geometry with them, they are useful when low intensity sources have to be measured. Absorption methods are commonly used to identify spectra but the method cannot easily be used to determine the energy distributions of spectra. Scintillation crystals are now used extensively in the measurement of β-spectra. The great advantage in their use is the good solid geometry which can be obtained. With two crystals, the geometry may be made nearly 4π, hence thin sources may be used and source scatter kept to a minimum.

Gamma-spectra may be measured in three ways, by:-

1. Measuring conversion, photo-electrons or Compton electrons with a magnetic spectrometer.
2. Diffracting the γ-rays by a crystal lattice.
3. Using a crystal scintillator.

The spectrometers used in the first method are similar to the ones used in measuring β-ray spectra. The crystal diffraction method, whilst being very accurate, requires strong sources of the order of 100 times those used in the measurement of conversion spectra. Scintillation crystals have a high efficiency for the detection of γ-rays, up to 15% being possible. Since the γ-rays can only be detected by a secondary process, the pulse height is not constant for a γ-ray of given energy but depends on whether all the energy of the γ-ray is converted into light. Because of this, the energy spectrum of a single γ-ray is not simple, hence great care must be taken in interpreting any spectrum which is measured.

The two most accurate methods used to measure γ-ray spectra cannot be used if the radiation is weak. Then scintillation crystals become useful because their resolution is sacrificed in favour of their greater sensitivity.

2. The Development of Magnetic Spectrometers.

The first use of magnetic fields to measure the energy distribution of β-rays was by Wilson in 1906. He did not, however, use the principle of focussing. More accurate results were obtained

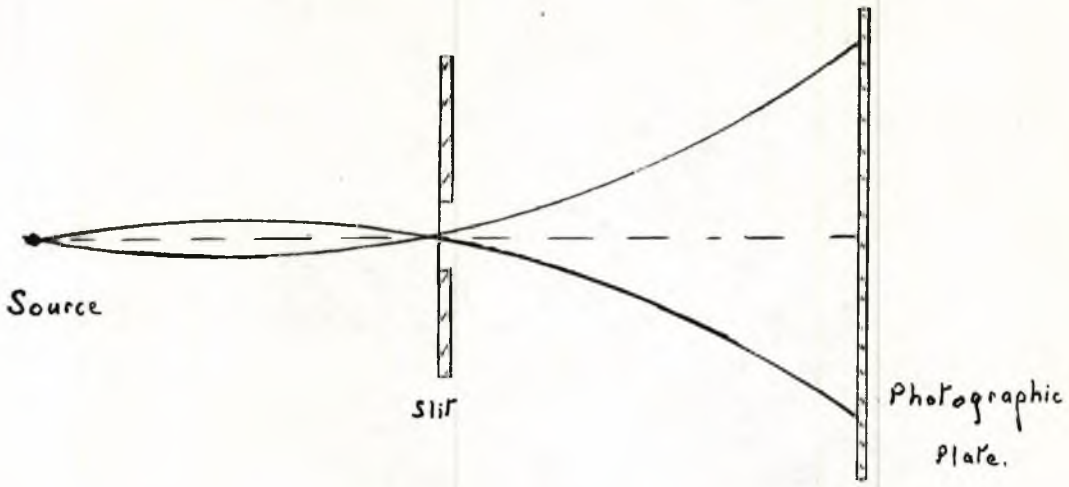

FIG. 1.1 The Principle of the Direct Deflection Spectrograph.

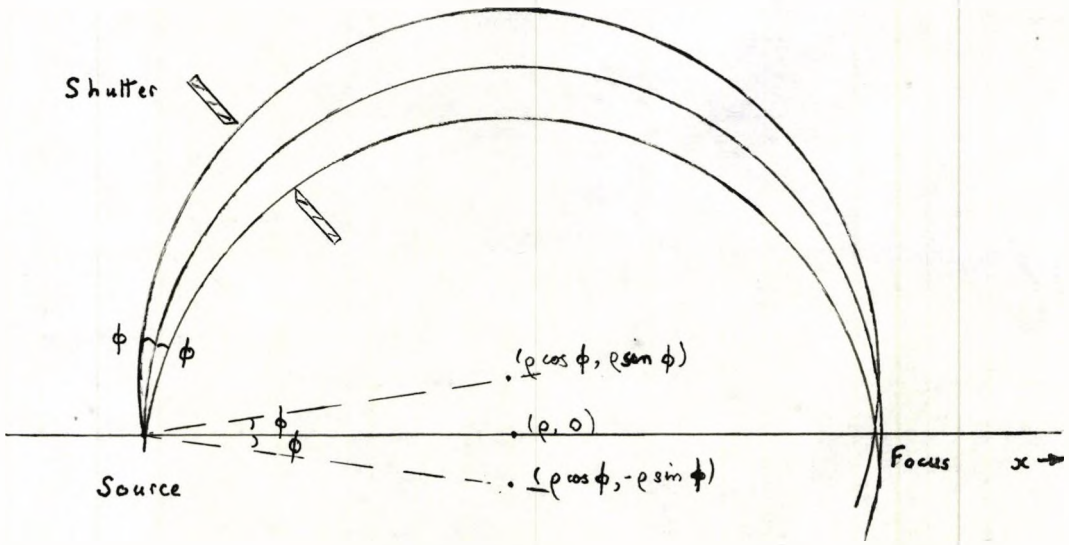

FIG. 1.2 The Principle of Semicircular Focussing.

by von Baeyer, Hahn and Meitner using the direct deflection method. The principle of this method is shown in Fig. 1.1. A narrow source is placed in a strong magnetic field and the rays pass through a narrow slit and then strike a photographic plate. Because of the magnetic field, rays with different energies will describe circular arcs with different radii of curvature. These rays will thus strike the photographic plate at different points. From the positions of the lines produced, the energies of the β-rays may be calculated if the field strength is known.

The first spectrograph utilising the principle of semi-circular focussing was designed by Danysz (2) in 1911 (the difference between a spectrograph and a spectrometer is that in a spectrograph the β-rays are detected by photographic means while in a spectrometer the rays are detected by any other means). Fig. 1.2. illustrates the principle of semi-circular focussing which is applicable to either instrument. The source, S, is placed in a strong homogeneous magnetic field, B, and rays emitted into a range of angles $\pm\phi$ are accepted by the first shutter. The mean ray travels along the arc of a circle defined by the equation

$$B\rho = p/e$$

where ρ is the radius of the circle, p is the momentum of the β-ray and e is the electronic charge. The mean ray intersects the x-axis at a distance 2ρ from the slit. The limiting rays intersect the x-axis at a distance of $2\rho(1 - \cos\phi)$. If the source

has a width, s, and if the axial angle of emission is $\pm\psi$, then the width of the image is

$$s + 2\rho(1-\cos\phi) + 2\rho(1-\cos\psi) = s + \rho(\phi^2 + \psi^2)$$

if ϕ and ψ are small. The base resolution R_o is:-

$$R_o = \frac{s+w}{\rho} + \phi^2 + \psi^2 \qquad (1.1)$$

where w is the width of the image detector.

A spectrometer has three important characteristics, they are the resolution, the transmission and the luminosity. These characteristics serve as useful criteria with which to judge the respective merits of different spectrometers. The resolution is the ability to resolve two rays with nearly equal energies. The transmission is a measure of the collecting power of the instrument and is defined as the fraction of a sphere into which the rays are emitted. The luminosity is the product of the source area and the transmission. The luminosity is important because, for a given activity, the source thickness is inversely proportional to the source area if the transmission is held constant. For an isotope with low specific activity, the thinner the source, the less will be the effect of line-broadening due to source thickness.

The transmission may be written:-

$$T = \frac{2\phi \cdot 2\psi}{4\pi} \qquad (1.2)$$

The luminosity is:- $L = s.h. \frac{(4\phi\psi)}{4\pi}$ (1.3)

where h is the height of the source.

The conditions for high resolution differ from those for high transmission so that one has to be sacrificed at the expense of the

other.

A fourth criterion sometimes used with a spectrometer is the dispersion, which expresses the rate of change of the image position with change in momentum. In the case of the semi-circular spectrometer, the dispersion is:-

$$\delta = \frac{\Delta\rho}{\Delta(B\rho)} = \frac{2\rho}{(B\rho)} \qquad (1.4)$$

Whilst high resolution may be obtained with a semi-circular spectrometer, the main disadvantage of the instrument is that it has a low transmission because there is no focussing in the axial direction. This low transmission is partly offset in a spectrograph by its ability to focus a range of energies.

Experimentally, during the 1930's, use was made of cloud chambers which were placed in magnetic fields. Although the cloud chamber has proved an extremely useful tool in the realm of high energy nuclear physics and in the discovery of the neutron and positron, with β-spectra the need to record and analyse thousands of tracks to obtain good statistical accuracy make the method tedious.

In the early 1940's, two spectrometers were designed which used the principle of focussing of the rays by an axial magnetic field. This idea had been tried, unsuccessfully, by Kapitza and by Tricker in 1922. Busch, in 1926, showed that an axial magnetic field behaved like a lens in that it could focus electrons. He derived a formula for the focal length, f, of such a field,

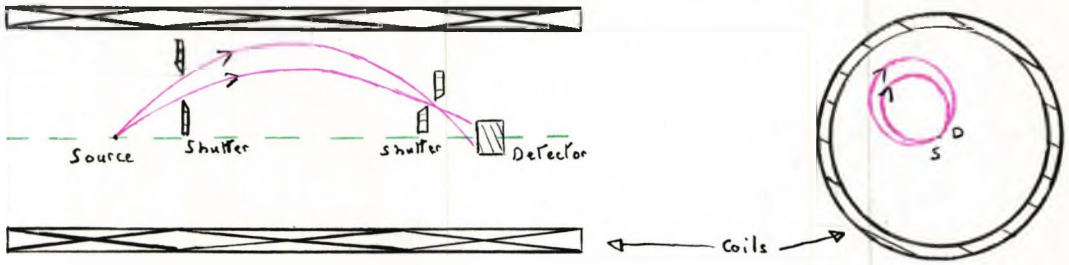

(a) The "Solenoidal" Spectrometer.

(b) The "Short Lens" Spectrometer.

FIG. 1.3 The Focussing Principles of two Lens Spectrometers.

$$\frac{1}{f} = \frac{1}{4(B\rho)^2} \int_{-\infty}^{+\infty} B_z(z,0)\, dz \qquad (1.5)$$

where B_z is the field along the z-axis and $B\rho$ is the momentum of the electron. For a uniform field, B_0, such as that produced by a long straight solenoid, the distance between the source and image is:-

$$Z = \frac{2\pi B\rho}{B_0} \qquad (1.6)$$

In 1941, Witcher (3), designed a spectrometer using a solenoid, a "solenoid" spectrometer. He also used ring focussing to improve the resolution. In the same year, Deutsch (4), designed a "short lens" spectrometer in which the β-rays were focussed by a short coil. The designs of these two spectrometers are shown in Fig. 1.3. The traces along and perpendicular to the axis are shown in each case. Both these spectrometers have a higher transmission than the semi-circular spectrometer but their resolutions are much poorer. Again, the luminosity is low for high resolution because the source has to be circular and the area is thus proportional to the square of the radius whereas the resolution is inversely proportional to the radius.

Good resolution is not necessary in the measurement of β-spectra where the number of rays does not vary rapidly with energy. High intensities are more important to ensure good statistical accuracy, especially at the low and high energy ends of the spectrum where the number of rays is small. Lens spectrometers

have been used extensively since 1941. The use of ring focussing in the solenoid spectrometer improves the resolution, but the optimum resolution achieved depends on the angle of emission of the rays, the angular aperture, the source dimensions and the width of the ring focus. The theory of the solenoid spectrometer has been given by Dumond (5), and Persico (6). In the solenoid spectrometer in this laboratory, both ring focussing and axial focussing immediately in front of the detector, are used.

The performance of a lens spectrometer can be improved greatly by allowing the rays to form an image between two short coils, the final image being formed beyond the second coil. This type is known as an "intermediate image" spectrometer, and has a very much higher resolution for a given transmission than the short lens spectrometer.(7)

Improvements to the semi-circular spectrometer were made by Langer and Cook (8), and by Deiduk and Kowalinski (9). They shimmed the field to alter its shape slightly, thus reducing the third order aberrations. In the same year, 1949, Siegbahn and Svartholm (10), published a paper on the use of non-homogeneous magnetic fields for focussing β-rays. They analysed the behaviour of β-rays in a circularly symmetrical, non-homogeneous, magnetic field determining under what conditions the rays would be focussed. The result was, that for a suitable field shape, β-rays leaving the source would be focussed both radially and axially at the same point. This property gave the spectrometer its name, a double focussing spectrometer. The shape of field required and its production are discussed in Chapter II. In

order to verify their conclusions, Siegbahn and Scartholm built a small model which gave very promising results. From these results, they decided to construct a large spectrometer with a mean radius of 50 cms. (11).

Because it has both radial and axial focussing, the transmission is greater than that of a semi-circular spectrometer with the same resolution. It would be possible to construct a semi-circular spectrometer with a large axial aperture to increase the transmission but then, the resolution would be decreased.

The resolution of a double focussing spectrometer is dependent on the parameters which describe the field shape,

$$R_o = \frac{s+w}{\rho} + \frac{|4\alpha_2 - 3|}{12}\frac{s^2}{\rho^2} + \frac{|2-16\alpha_2|}{12}\phi^2 + \frac{|16\alpha_2 - 6|}{12}\psi^2 \qquad (1.7)$$

α_2 is a variable parameter and may be chosen to reduce either the radial or axial aberrations. ϕ, ψ, ρ, etc., stand for the radial and axial angles of emission, the radius of curvature, etc., as before.

The transmission and luminosity are still defined as before. It will be seen that if ϕ and ψ have the same values as in a semi-circular spectrometer the resolution will be almost half that of the latter. Alternatively, larger source dimensions may be used for the same resolution so that the luminosity is higher. The dispersion is also greater by a factor two, being:-

$$S = \frac{4\rho}{(B\rho)} \qquad (1.8)$$

With such large instruments as the one mentioned on page 12, the source area may be quite large. The spectrometer discussed in this thesis is a double focussing spectrometer with a mean radius of 40 cms. and in it, source areas of 1 sq. cm. were often used with a resolution of 1%. The production and measurement of the field in a double focussing spectrometer are discussed in Chapter II. The auxiliary apparatus and techniques are described in Chapter III. Chapter IV describes the effect of the use of iron in the construction of the magnet and Chapter V gives some results obtained with this spectrometer.

Chapter II.

The Magnetic Field.

1. Design of the Spectrometer.

The field in the spectrometer may be produced by one of two methods. Either a permanent field, which is usually the remanent field of the spectrometer, or a variable field, produced by a current flowing through a number of coils with or without the assistance of iron, may be used. If the field of a permanent magnet is used, the spectrometer must be able to accept a range of momenta. A semi-circular spectrograph is the instrument to which this method is best suited.

The range of momenta which can be accepted is limited by the design of the spectrograph and cannot be made to cover the entire range of momenta emitted from a high energy β-transition. Mladjenovic (12), has recently built a semi-circular spectrograph in which the range of momenta accepted may be changed by remagnetizing the magnet. Slätis (13), used three semi-circular spectrographs to cover the same range of energies, namely 1 Kev. to 3 Mev.. For accurate work, it is desirable to keep the temperature constant so that the strength of the field does not alter. A regular measurement of the field strength in necessary to check its constancy.

Most spectrometers in use today have a variable field, produced by passing a current through one or more coils. These are either used

by themselves or with iron. A field produced solely by a number of coils is directly proportional to the currents flowing in those coils provided that the relative magnitudes of the currents in the coils is constant. It is then possible to calculate the field strength if the current is measured accurately. The passage of current through the coils will cause them to expand due to the heat generated. For accurate measurements, allowance must be made for the effect of this expansion on the magnitude of the field. Stray magnetic fields are undesirable and must be kept to a minimum. Since there is always a residual magnetic field, due to the earth's magnetism, it must either be compensated or allowed for in one's calculations.

A field produced by iron is not proportional to the exciting current and must be measured. The effect of the iron is such that it gives the field greater stability, both against stray fields and, because of the increased thermal capacity, against temperature changes. The stray field produced by the magnet is less extensive than that produced when no iron is used so that nearby equipment containing valves, photomultipliers, etc., is less likely to be upset.

The absence of a proportional relationship between the field and the current is not as inconvenient as the dependence of the field upon the previous history of the iron. In some of the most recent designs of spectrometers, for example, the double focussing spectrometer and the intermediate image spectrometer, non-homogeneous fields are required and, because of this dependence on the previous history

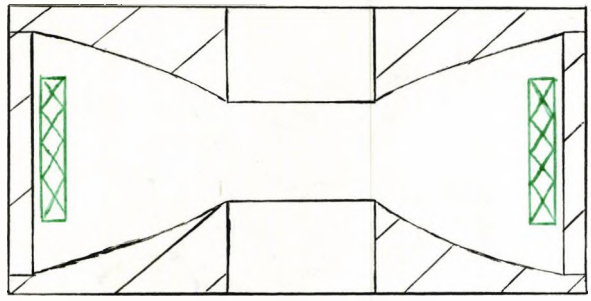

(a)

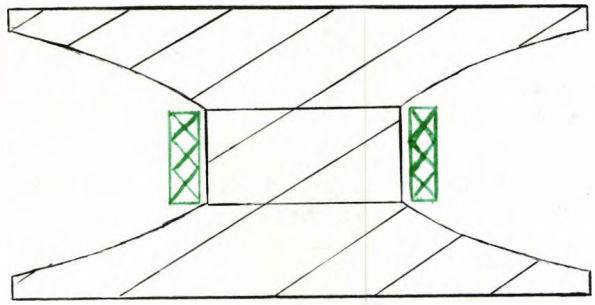

(b)

FIG. 2.1 Two Designs for a Double Focussing Spectrometer.

of the iron, there is a tendency for the shape of the field to alter at low field strengths.

The spectrometer in use in this laboratory is a double focussing spectrometer employing iron in its construction. The exciting coils are outside the poles and the vacuum chamber as shown in Fig. 2.1(a). An alternative design, shown in Fig. 2.1(b), has been used in the construction of a similar spectrometer at Uppsala (11). The advantages of design (a) are:-

1) There is no limitation on the space available for the coils.
2) There is no limitation on the thickness of the iron yoke, thus avoiding problems which may arise due to the saturation of the iron.
3) It is easy to make connections to the coils.
4) The fringing fields are easy to handle.
5) The yoke also serves to screen the spectrometer from stray fields.

As it has turned out, it is possible to gain access to both the centre and the periphery of the vacuum chamber. This was found to be extremely useful when setting the spectrometer and when making adjustments.

The theory of double focussing spectrometers has been developed in several papers (10), (14) to (19) and has been summarised in a few reviews (2), (20), (21), (22). It is not proposed to give this theory again, but only to quote such formulae as required.

The field at a point (r,z) may be expressed in terms of the axial field, B_z, at the mean radius, r_o, and the radial and axial coordinates, r and z. In the median plane, (z = 0), the field, B_z, may be written,

$$B_z(r) = B_z(r_o)\left[1 + \alpha_1\left(\frac{r - r_o}{r_o}\right) + \alpha_2\left(\frac{r - r_o}{r_o}\right)^2 + \ldots\right] \qquad (2.1)$$

where α_1 and α_2 are the first and second field coefficients which determine the shape of the field. In the radial direction, the field, B_r, is given by the equation

$$B_r(z) = z\, B_z(r_o)\left[-\frac{\alpha_1}{r_o} + 2\alpha_2\frac{(r_o - r)}{r_o^2} + \ldots\right] \qquad (2.2)$$

For double focussing to occur, the necessary condition is that $\alpha_1 = -\frac{1}{2}$.

The value chosen for α_2 only affects the second order focussing properties of the field and, usually is allowed to have one of the values $\frac{1}{8}$, $\frac{1}{4}$, $\frac{3}{8}$. If one chooses the value $\alpha_2 = \frac{1}{8}$, the radial aberration is eliminated. For $\alpha_2 = \frac{3}{8}$, the axial aberration is eliminated; this value also has the advantage that there is no astigmatism hence the equations are still valid if one wishes to use another mean radius for the spectrometer. The case where $\alpha_2 = \frac{1}{4}$ may be likened to the circle of least confusion in optics, while neither the radial nor axial aberration is zero, for equal apertures in both directions, the aberrations in this case will be less than in either of the two previous cases.

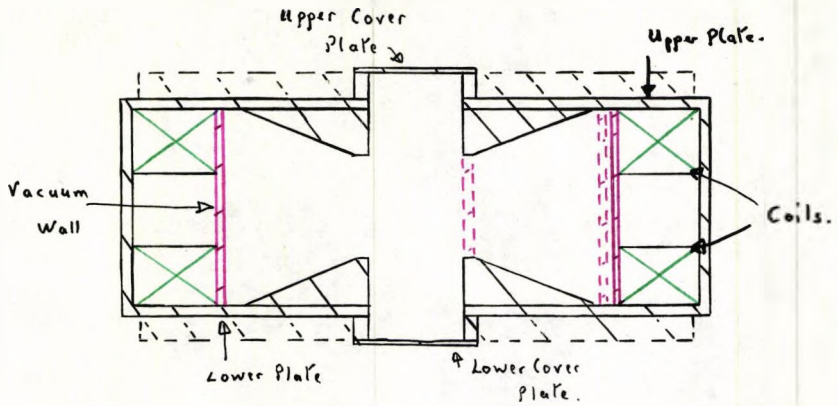

Elevation.

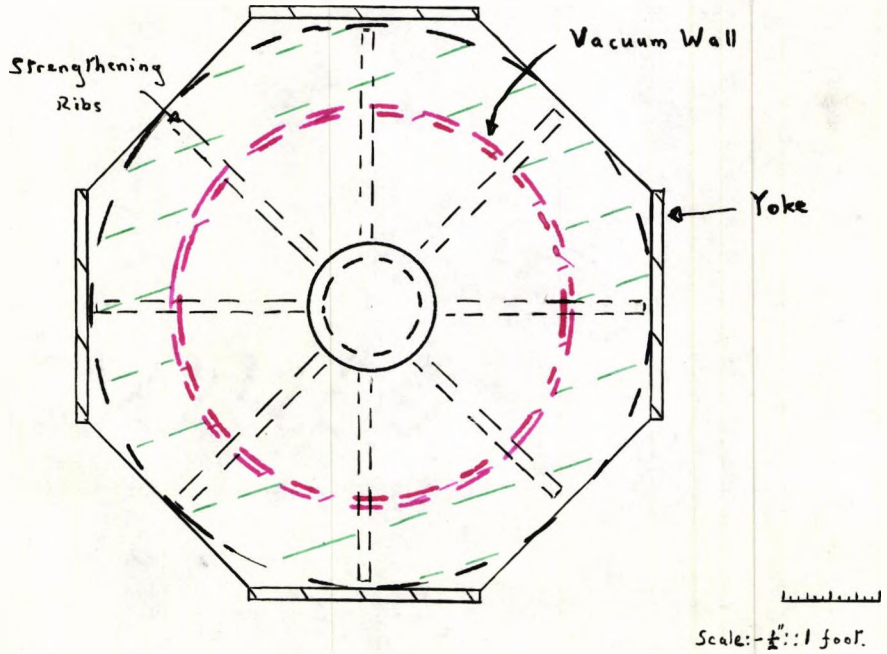

Plan View.

FIG. 2.2 The Design of the Spectrometer used.

α_1 and α_2.

The shape of the field is governed by the parameters, and the shape correspondin to $\alpha_1 = -\frac{1}{2}$, $\alpha_2 = \frac{1}{4}$ may be realised between conical pieces of iron. Since the machining of these faces is easy and because the field shape lies between the shapes for values of $\alpha_2 = \frac{1}{2}, \frac{3}{5}$, it had been decided to construct the spectrometer with conical poles and to shim the field to produce the shape corresponding to one of these values. The unshimmed field was nearly the shape corresponding to $\alpha_2 = \frac{1}{3}$, so it was shimmed to agree with this value (23).

The design is shown in Fig. 2.2. Fig. 2.2(a) shows a sectional view of the elevation and Fig. 2.2(b) a plan view. The whole assembly rests on the lower plate which is supported by four concrete pillars. The poles are separated by six brass tubes and may be removed as a single unit. The lower pole rests on three steel ball bearings on the lower plate. There is a small gap between the upper pole and the top plate, thus, if bowing of the top plate occurs on evacuation of the vacuum chamber, the field shape will not be affected.

The vacuum wall is of brass and lies inside the exciting coils. The return yoke consists of four iron slabs arranged round the magnet on alternate sides of an octagon. The chamber is evacuated through a pumping line connected to a small cover plate in the centre of the lower plate. There are two exciting coils, each consisting of six double layers of 32 turns, $\frac{1}{2}$" square aluminium conductor containing a central hole 5/16" diameter to allow cooling water to be passed when necessary.

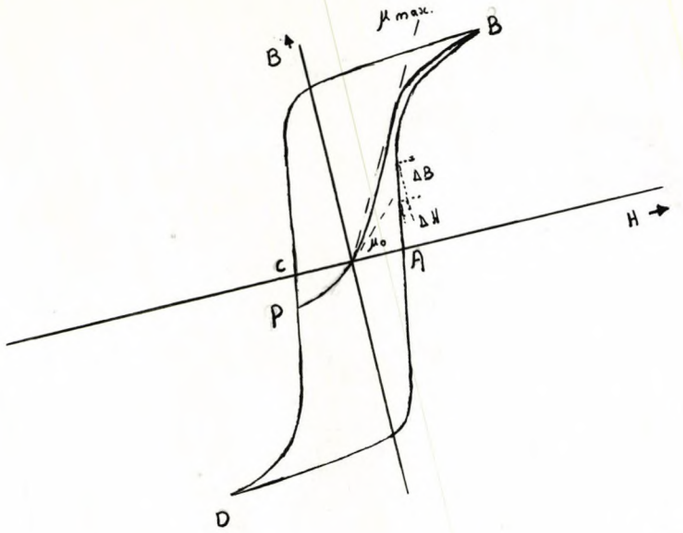

FIG. 2.3 A Hysteresis Loop with the Initial Magnetization Curve.

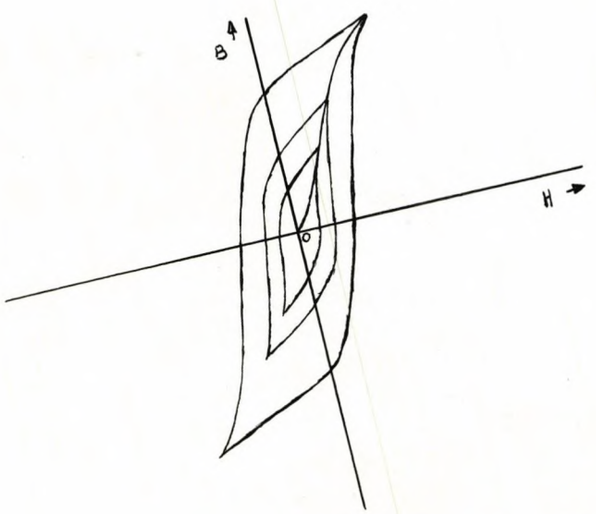

FIG. 2.4 The Normal Magnetization Curve.

2. The Production of the Magnetic Field.

There are three ways in which the desired field may be set, these are:-

1) To use the initial magnetization curve, curve OB in Fig. 2.3.

   a) using a.c. to demagnetize the magnet

   b) by reversing the exciting field to such a value that when it is removed, the magnetization curve will pass through the origin, point P in Fig. 2.3.

2) By working on one branch of a well established hysteresis loop, e.g., Branch I in Fig. 2.3. (i.e. on the curve AB).

3) By establishing a cycle in which the maximum field is the desired field, see Fig. 2.4. This is known as the normal magnetization curve.

To understand the behaviour of the spectrometer, it is necessary to consider carefully the relationship between the magnetic induction, B, and the magnetizing field, H, at any setting of the field. The behaviour will be considered for two cases, 1(a) and 2 above. The normal magnetization curve is very similar to the initial magnetization curve if the field changes slowly, but, since I did not use this method, I shall not discuss it.

It is necessary to consider the effects which may arise from:-

1) A change in the permeability of the iron.

2) The interaction between the exciting field and the induced field.

3) The possibility that different parts of the iron may follow different hysteresis cycles.

Consider the initial magnetization curve, OB in Fig. 2.3. At the origin, the curve has a finite slope which increases as the field increases. Eventually, the slope reaches a maximum and then decreases. The spectrometer was used between the origin and a point well below the maximum slope. Although in Fig. 2.3., the slope of the curve appears to increase rapidly, it is because it has been so drawn for emphasis, in practice, the change in slope is barely perceptible.

The change in slope, which is due to a change in permeability, implies that the change in permeability must also be small. Because the initial permeability of the iron is large one would not expect these small changes in the permeability to affect, to any great extent, the shape of the field. If one considers the interaction between the exciting field and the induced field one would expect, since the induced field is nearly proportional to the exciting field, that the interaction between them should be almost constant and thus not alter the field shape appreciably.

The same conclusion may be reached if one supposes each part of the iron to follow its own hysteresis loop. The reasoning is, that although each part of the iron is following its own hysteresis

cycle, the induced field in each will be nearly proportional to the current. As the current is increased, the field in each part will increase in almost the the same proportion. The combined effect will thus be nearly the same at all values of the field.

Thus, from all three considerations, it would appear that, if the field is set by using the initial magnetization curve, the shape should not alter appreciably.

The normal permeability, μ, is defined as the ratio B/H for the maximum value of H on the hysteresis cycle, at any other point on the curve, one can only define the differential permeability, $\mu_\Delta = \Delta B/\Delta H$, which relates the change in the induction, ΔB, to the change, ΔH, in the field. Because the differential permeability is constant along the lower portion of Branch I of the hysteresis curve, the field was set on this part of the curve. If one makes an analysis of the behaviour of the field using the differential permeability one may conclude that the field shape should not change. However, this is contrary to experimental evidence.

The interaction between the exciting and the induced fields is certainly different from the case for the initial magnetization curve. A current must flow through the coils to nullify the field due to the remanence of the iron point **A** on Fig. 2.3. To produce a given field, a larger current is required than in the case where the initial magnetization curve is used. Because of this, the interaction must be different. The hysteresis curve approaches the initial magnetization curve as the field increases and at high fields, the two curves become indistinguishable.

Since in the case of the initial magnetization curve, the field shape is not expected to alter much, it must be expected that when Branch I of a hysteresis cycle is used, the field shape will alter for low values of the field.

The same conclusion can also be deduced from the third supposition that each part of the iron follows its own hysteresis cycle. One may assume either, that each part of the iron is at a similar point on its hysteresis cycle or, that each part is at a different point. In the former case, the argument used in the preceding paragraph may again be applied and one would again conclude that the field shape should alter. If one assumes each part of the iron to be at a different point on its cycle, one would expect the combined effect to alter as the field increases, becoming constant at high fields, when the curve approaches the initial magnetization curve.

From this brief discussion, it would appear that it would be better to set the field using the initial magnetization curve than to use Branch I of a hysteresis cycle.

The circuit diagram for the production of the field is shown in Fig. 2.5 and was the same as that used by Barry. The current is provided by a bank of low resistance accumulators with a capacity of 120 Amp-hours. The maximum number of accumulators required was twenty, and these were capable of giving currents up to 30 Amps. In order to keep the current constant, the voltage across a 0.1 ohm standard resistance was measured with a Tinsley potentiometer (model 4363). The output was fed to a sensitive galvanometer, in

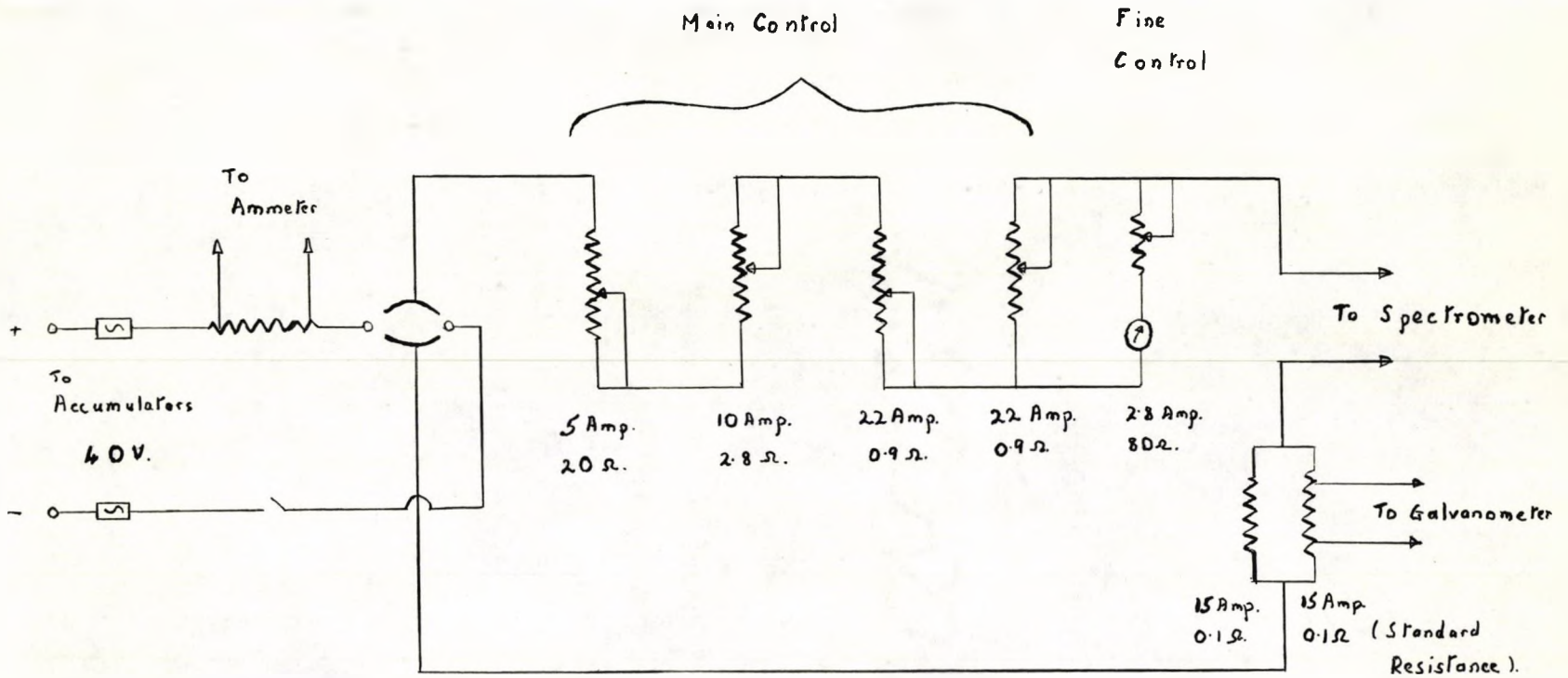

FIG. 2.5

The Current Control Circuit.

parallel with which several resistances were placed to allow the sensitivity to be controlled. The current was kept constant by adjusting the resistance of the circuit to bring the spot of the galvanometer to a fixed mark.

At first, the field was set using Branch I of a hysteresis cycle with a maximum current of 30 Amp. Later, both this method and the method using the initial magnetization curve were used. In either case, the starting point was the de-magnetization of the spectrometer. The two standard methods for de-magnetizing iron, those of heating the iron or using an a.c. field large enough to saturate the magnet, could not be used. The following practice was adopted and found to be satisfactory.

The current was increased to the maximum value previously used and then the spectrometer was taken round a series of hysteresis loops in which the maximum current drawn in each cycle was decreased by 1 Amp. When the lowest current which could be drawn was reached, the leads to the spectrometer were disconnected and a small Variac was used to supply lower a.c. currents. This a.c. current was increased to 2 Amps. (the lowest value which could be drawn from the accumulators using the circuit shown in Fig. 2.5.), and then decreased to zero. The field was measured to check that it was small. The largest value measured was 0.1 gauss and, since the direction of the field was not always the same, it was thought to be due to some slight variation in the cycling procedure.

Once the spectrometer had been de-magnetized, the field could be set straight-away if it was to be set on the initial magnetization curve. If I wished to work on a hysteresis cycle, the magnet was ready for the hysteresis cycle to be established. The cycle used had a maximum current of 30 Amps. which was established by taking the magnet round a series of hysteresis cycles in each of which the maximum current was $\frac{1}{2}$ Amp. greater than in the previous cycle. Once the maximum current reached 30 Amps., the spectrometer was taken round that hysteresis cycle several times to ensure that it was well established.

The setting of the field was much quicker once a hysteresis cycle had been established because the current could be increased above the value desired. This allowed the coils to warm and reach thermal equilibrium more quickly than when the spectrometer was used on the initial magnetization curve. When thermal equilibrium had been attained, the current remained constant; all that was then necessary to set the field was to take the spectrometer round the hysteresis cycle to the desired point.

The disadvantage when setting the field on the initial magnetization curve was that the current could not be increased above the required value. Besides taking longer for thermal equilibrium to be attained, a high field could not be used and then a low one, that is, I had either to work with an increasing field or de-magnetize the spectrometer between measurements of high and low energies.

It is found that the field shape changes more when the field is set on Branch I of a hysteresis cycle than when it is set on the initial magnetization curve. The choice between which of the two methods to use depends on the type of measurement it is desired to make and is discussed in Chapter IV where the behaviour of the spectrometer is described.

3. Measurement of the Magnetic Field.

The choice of method by which to measure the magnetic field is governed by several factors - the strength of the field, its uniformity, the accuracy desired, whether one wants a continuous or discontinuous measurement and also whether one wishes to make an absolute or a relative measurement. If iron is not used in the construction of the spectrometer, the field may be calculated from the strength of the current which can be measured very accurately. When iron is used, as in this spectrometer, it is necessary to measure the field strength.

With this spectrometer, high accuracy is essential because resolutions of the order of 0.1% have been achieved for internal conversion lines. In order to measure the momentum and energy of a line accurately, it must be possible to set and measure the field at intervals smaller than this figure, a value of 0.01% would be satisfactory. This accuracy is not easy to achieve and is made more difficult by the non-uniformity of the field. The change in the field is 1.25%/cm., at the mean radius. The field strengths most frequently used lay between 15 gauss and 250 gauss.

Theoretically, several methods are possible but experimentally, most of them are not accurate enough. Each of the methods will be summarised briefly, they are:-

1. The measurement of the force on a conductor carrying a current.
2. The use of nuclear magnetic resonance.
3. The use of magneto-resistance (e.g. the bismuth spiral).
4. The use of the Hall effect.
5. The measurement of the change in induction of a thin magnetic strip due to a change in its permeability.
6. The use of a flip coil and galvanometer.
7. The use of generator methods.

1. The measurement of the force on a conductor carrying a current.

This method is very simple in theory. A known current is passed through a straight conducting wire supported in the field. The force on the wire causes it to move, the deflection being measured. This method is best suited to the measurement of high fields and has been used by Chang and Daunblum, (24), to measure fields of the order of 10^4 gauss. The accuracy is limited by friction at the knife edges (or by torsion if a wire suspension is used), and the need to limit the deflection to be able to measure it over a wide range of fields.

This method will yield continuous readings of the field but it is subject to zero drift. For low fields, in order to obtain reasonable deflections, a large current must be passed through the coil; this will

cause heating for which a correction must be applied.

2. Nuclear magnetic resonance.

This is an absolute method and can be made accurate if the field gradient is small. The signal to noise ratio is dependent on the 3/2 power of the field and is inversely proportional to the bandwidth (25). For low fields, both these factors reduce the ratio considerably. Dumond (26), describes a system used to measure uniform fields of the order of 15 gauss, the volume of the sample being 70 c.c.s. In our spectrometer the field gradient is such that the size of the sample would have to be so small that a signal would not be detected. Where nuclear magnetic resonance may be used, the accuracy can be made better than 0.1% (27).

3. Magneto-resistance.

If a bismuth wire is placed in a magnetic field, its resistance increases. This effect is known as magneto-resistance. Newton and de Grazia (28) have discussed the use of this effect in the measurement of magnetic fields. To improve the sensitivity, the bismuth wire is kept at the temperature of liquid nitrogen. The increase in resistance over the range 0 to 1,000 gauss is only 33% and is greatest at 1,000 gauss. The accuracy is determined by the noise level of the resistances which becomes too great at low field strengths. Again, this method allows continuous readings to be taken.

4. The Hall effect.

If a current is passed along a strip of conducting material, an e.m.f.

is developed across the strip. This e.m.f. is proportional to the product of the current and the field strength. Even with a semi-conductor which has a large Hall coefficient, the e.m.f. developed is small for fields of the order of tens of gauss. So far, the accuracy which has been obtained is about 1%, which is not good enough for use with this spectrometer.

5. The measurement of changes in induction due to a change in the permeability of a thin magnetic strip.

A thin strip of permalloy placed in a steady magnetic field will be given a bias. When an a.c. field, sufficient to saturate the permalloy, is applied, the output will be distorted and a 2nd harmonic content, proportional to the d.c. bias will appear. This method is only applicable in the case of fields in the range from 0 to 1,000 gauss, but there is a tendency above 10 gauss for the strip to become magnetized thus upsetting the balance (29). The accuracy again is only about 1%.

Another method using the change in permeability is that using 'peaking' strips. A strip with high initial permeability is placed in the centre of two coils the axes of which are at right angles. If a current is passed through one coil, a pulse is developed in the other when the field generated by the current becomes greater than the field to be measured. The method is discussed by Symonds (30) as a means of measuring rapidly varying fields, such as those produced in a synchrotron. The accuracy he quotes is 1%.

6. The flip coil and galvanometer.

In this method, a coil is rotated through a known angle. The charge generated is passed through a special galvanometer, called a fluxmeter, which is electromagnetically damped. The deflection is proportional to the change in flux because the torsional damping is made very small. The zero is subject to erratic drift, while air damping and the slight torsional damping present limit the accuracy by reducing the deflection for large flux changes.

To overcome damping and torsion, and to give quicker responses, electronic fluxmeters have been designed (31), (32), but these are still subject to zero drift. The disadvantage with this method is that it is not a continuous one. Fechter and Reuben (33) used a null method in which two coils were rotated, one in the field to be measured and the other in a reference field. The outputs were compared by feeding them into a bridge circuit. Again the method does not yield continuous readings although a reading can be made automatically at a known frequency. The accuracy quoted is 0.02%. This method does not depend on the speed of rotation of the coils nor the phase between the outputs provided that both coils rotate through their angles in a much shorter time than the period of the galvanometer.

7. Generator methods.

If instead of rotating a coil through a known angle the coil is rotated at constant speed, an e.m.f. will be generated. This e.m.f. may either be measured as an a.c. signal or converted to and measured as a d.c. signal.

Martin and Richardson (34) and Cork, Shreffler and Shull (35) have used the latter method converting the output to d.c. by means of a commutator. There are difficulties with this method. They are the elimination of brush noise, contact resistance and thermo-e.m.f.'s. The brush noise and contact resistance may cause erroneous readings, the thermo-e.m.f. will only give false readings if the commutator is heated unevenly. Cork et al. quote a figure of 0.01 gauss as the smallest increment in the field strength which could be detected. This would yield an accuracy of 0.1% at the lowest field used.

The a.c. method is a null method, hence at the balance point no current flows as it does in the d.c. method. A second coil is rotated in a reference field at the same speed as the coil in the field to be measured. The two outputs are balanced either using a bridge (36), (37), or an amplifier which indicates the minimum value of the difference voltage (38), (39). The methods using amplifiers are capable of giving results with an accuracy better than 0.01%. The main troubles which arise are those of phasing the coils and brush noise.

Because these generator methods seemed so promising, it was decided to investigate their possibilities. The best method seemed to be the null recording system using two spinning coils and an amplifier, so it was decided to build a similar system. While this was being developed, a single coil was used to produce a d.c. voltage which was measured with a potentiometer. To enable methods to be

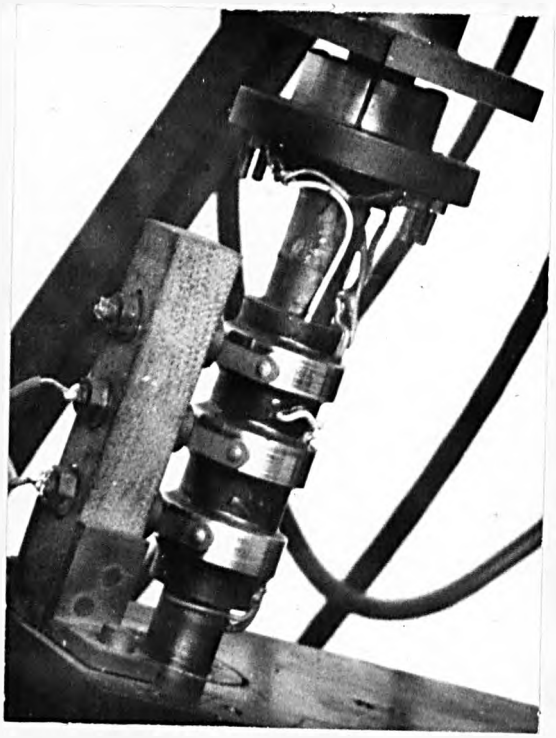

FIG. 2.6 The final Set of Slip-rings and Brushes with the Commutator above them.

used at the same time, a set of slip rings and a commutator were put on the same shaft supporting the coil. The arrangement is shown in Fig. 2.6., a similar arrangement was used on the shaft supporting the coil in the reference field.

The circuit for the d.c. method was constructed by Barry. A condenser was placed across the brushes to reduce the brush noise. The signal was then fed through a filter, with a cut-off frequency of 10 c/s, to a voltage divider and from this to a potentiometer (Tinsley, model 33876). The position of the brushes was adjusted relative to the coil to give a maximum output. With silver-graphite brushes, the output was extremely steady and there was little need to clean the commutator as the brushes were self-lubricating.

When two coils were used, the outputs were backed off and fed into a sensitive amplifier with a narrow band-width. The phase of the two coils must be adjustable to enable the outputs to be balanced exactly. Langer and Scott (36) used two synchronous motors, with a three phase supply and two variacs, to alter the phase of the two coils. Hedgran (38) placed both coils on the same shaft and used a small magnetic field to alter the direction of the reference field, thus changing the relative phase of the two coils.

With the latter method, for accurate work, the strength of the phasing field must be added vectorially to the main reference field. Since it is desirable to keep the reference field as far away as possible from the spectrometer field, Hedgran used a rotating shaft

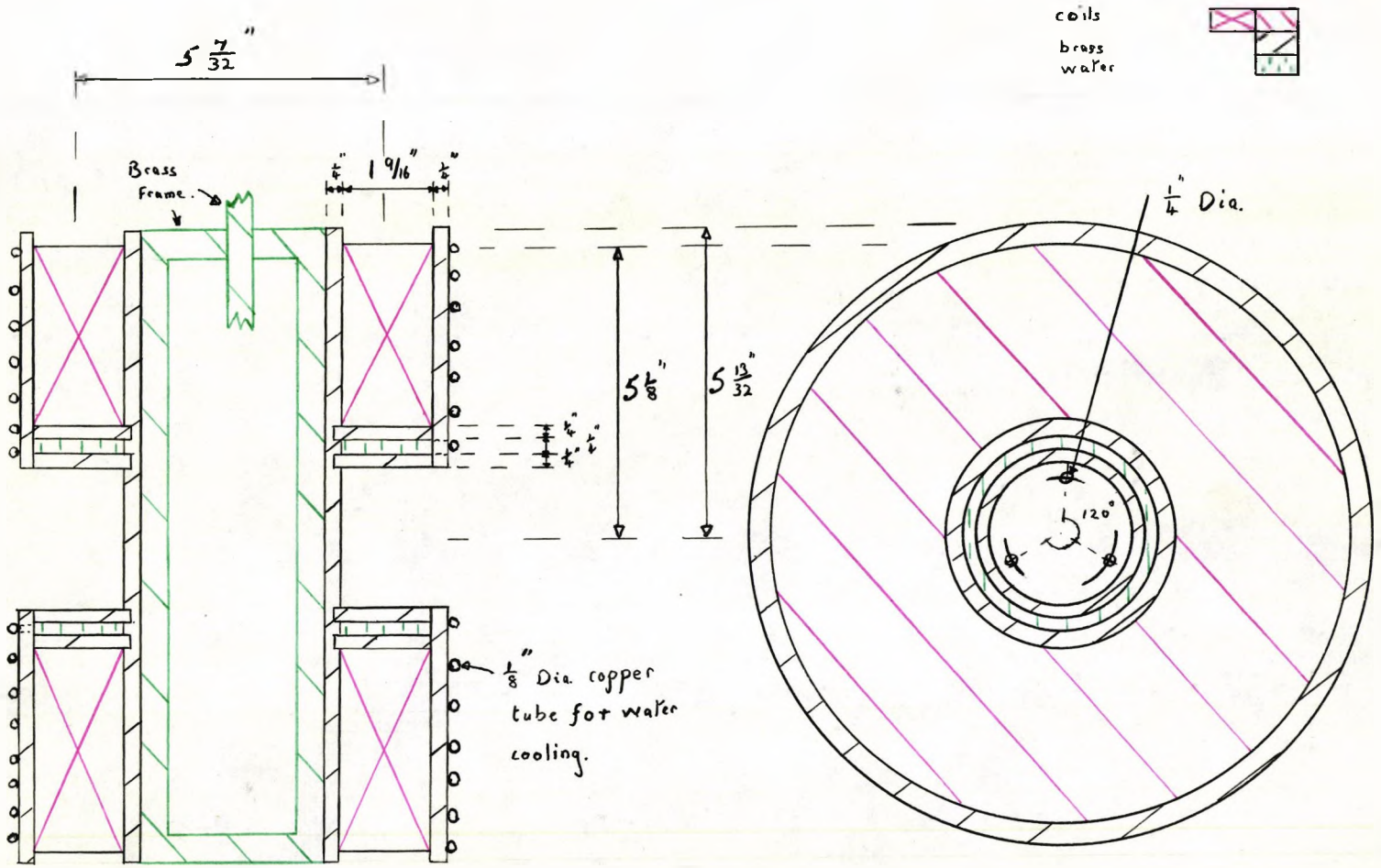

FIG. 2.7 Details of the Coils for the Main Reference Field.

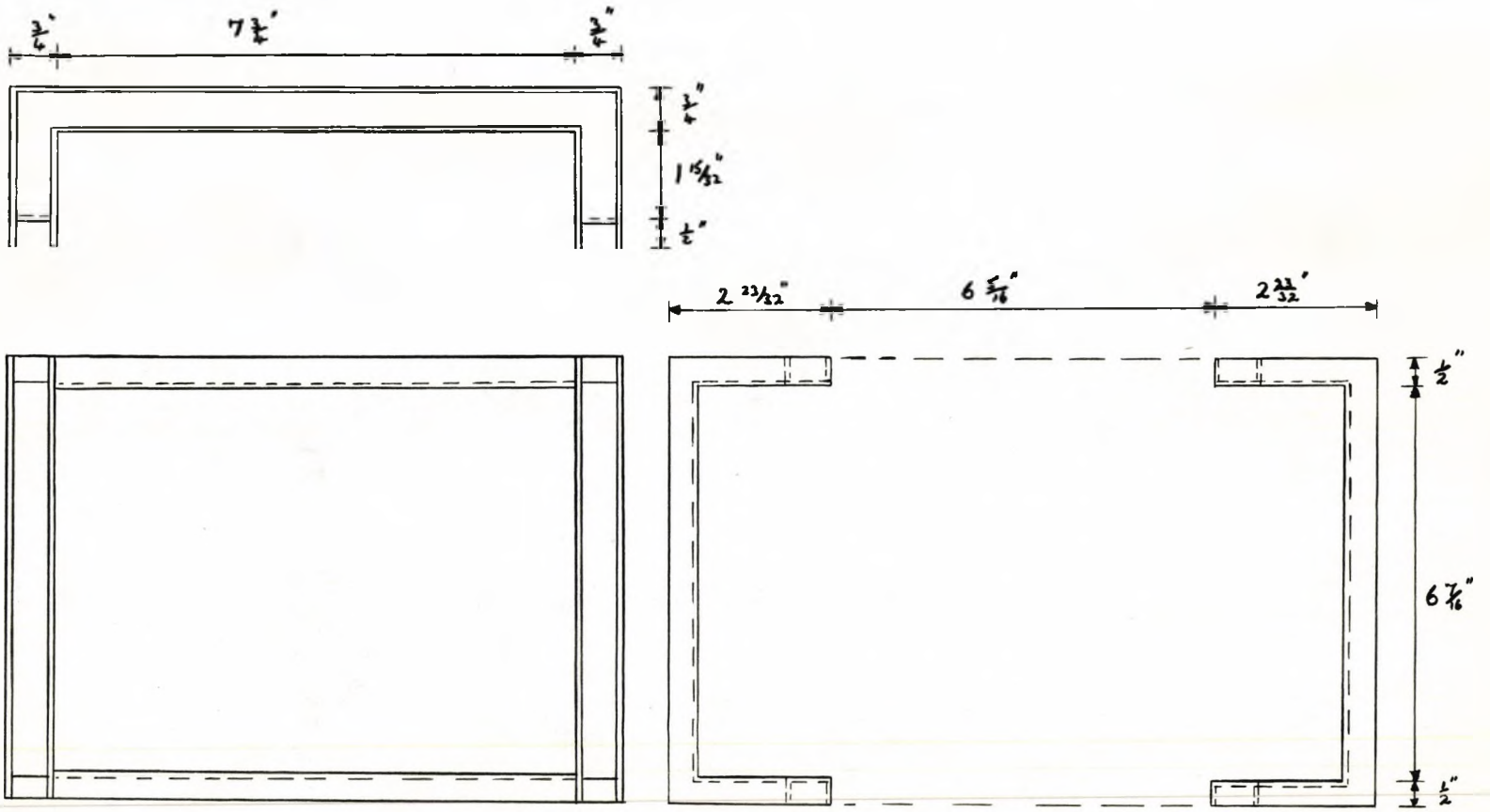

FIG. 2. 8 Details of the Coils for the Auxiliary Reference Field.

FIG. 2.9 The Assembled Coils.

which stretched across the laboratory. Because of this rotating shaft, the reference field was not movable and so he had to make a correction for the residual magnetic field in the laboratory.

Here we decided to use a combination of some of the features of both Hedgran's and Langer and Scott's methods. Two synchronous motors were used and the reference field was built on a stand so that it could be aligned with the magnetic field in the laboratory. An auxiliary field was built to phase the two spinning coils. By making the reference field capable of rotation about the axis of rotation of the spinning coil, the magnitude of the auxiliary field need never be more than 2% of the reference field. The correction to the reference field is then only $2:10^4$.

The spinning coils were wound so that both had the same number of Ampere-turns. That in the reference field had 2,800 turns of 41 B.S.S. Gauge, double silk covered wire, tapped at 1017 turns. The coil in the spectrometer had 3,550 turns of 40 B.S.S. Gauge, single silk covered wire, tapped at 1,084 turns. Both coils were tapped after 1,000 turns so that they also had an Ampere-turns product one-tenth that of the whole coil thus allowing a wide range of fields to be measured without changing either coil.

The reference field is provided by two pairs of coils, Figs. 2.7, 2.8 and 2.9. The main coils, shown in Fig. 2.7, were circular and the separation of their centres was 5.22 inches, that is, slightly greater than the Helmholtz separation. Each coil contained 614 turns

Distance from the centre of the coil. (cms.)	0	0.635	1.135	1.635	2.135	2.035	3.135	3.635	4.135
Field (oersted)	100.00	100.20	100.40	101.05	101.67	102.40	104.04	104.96	105.98
Mean Field (oersted)	100.00	100.1	100.2	100.5	100.9	101.7	102.1	102.6	102.9

TABLE 2.1. Axial Uniformity of Field from Helmholtz Coils.

15 B.S.S. Gauge, double cotton covered wire and had a resistance of 2.5 ohms. The power dissipation was 12.5 watts in each coil when the current was 2.24 Amps. The field produced by this current was 100 gauss.

To check the uniformity of the field, a few calculations of the field strength were made for points along the axis, these are given in table 2.1. The change over the radius of the spinning coil ($\frac{3}{4}$ inch) was less than 2%, while the mean value of the field over the area of the coil is 0.9% greater than the value at the centre. These coils were mounted on a brass box which could be rotated about the axis of rotation of the spinning coil and driving shaft. This allowed the relative phase of the two spinning coils to be adjusted to within one degree of the required angle.

To give a fine control over the phasing of the spinning coils, a second pair of coils was mounted to produce a field at right angles to the main field. These were shaped in accordance with designs used by Harris (40) and Lyddane and Ruark (41). These coils could be fitted easily to the box supporting the main coils. The equation given in both papers were complicated, so a simple form, derived in Appendix A, was used to calculate the fields for several dimensions of the coils. In the final design, each coil contained 630 turns of 30 S.W. Gauge, double silk covered wire and had a resistance of 144 ohms, the wires were covered with shellac varnish to keep them in place. A field of 2.2 gauss could be produced by a current of 0.1 Amp.

Stage 1

$R_a = R_b = 131\ k\Omega$
$C_a = C_b = 0.050\ \mu F.$
$R_c = 65.5\ \Omega \quad C_c = 0.100\ \mu F.$

Stage 2

$R_a = R_b = 124\ k\Omega$
$C_a = C_b = 0.050\ \mu F.$
$R_c = 62\ k\Omega \quad C_c = 0.100\ \mu F.$

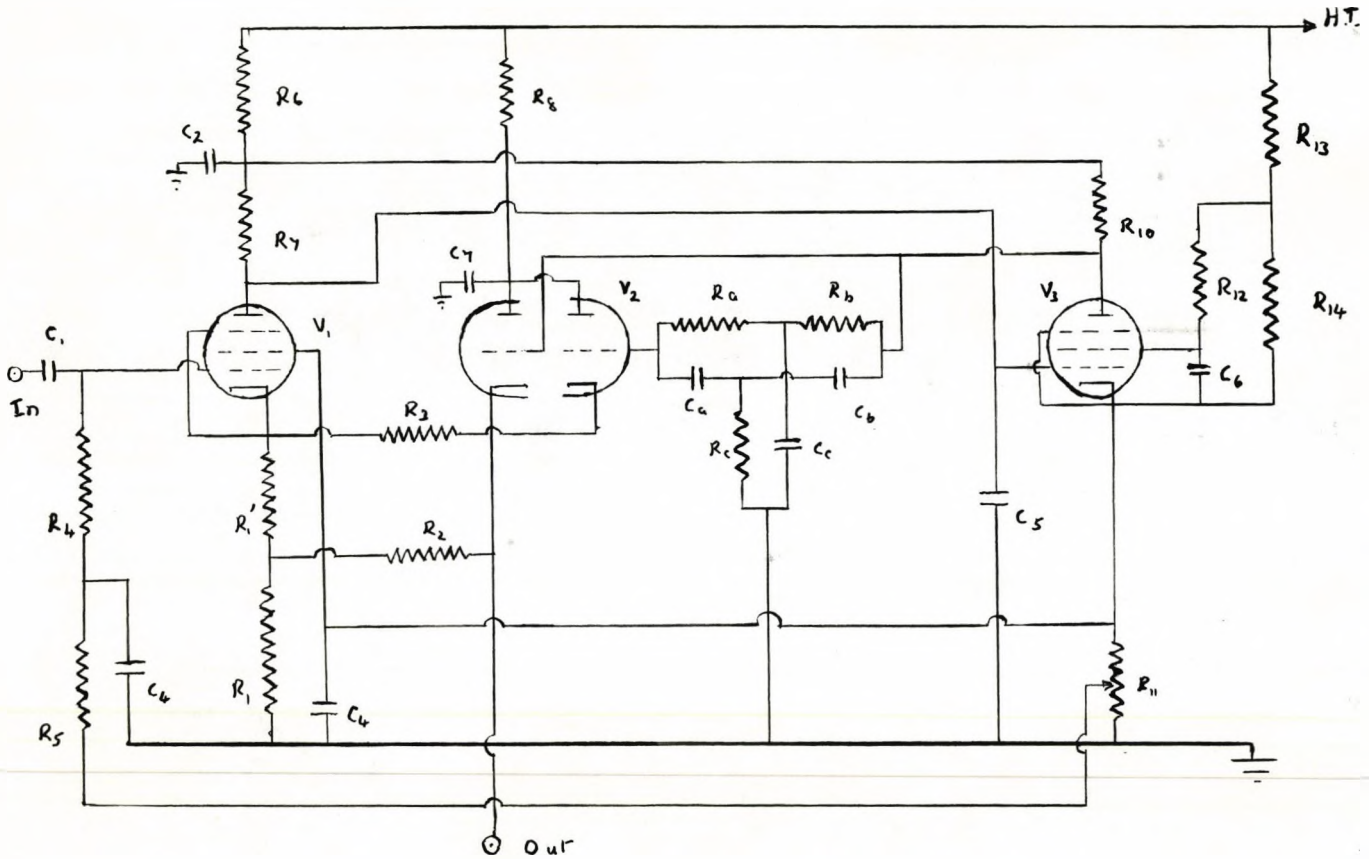

V_1 - 6 SJ 7
V_2 - 6 SN 7
V_3 - 6 SJ 7

R_1 - 1 kΩ
R_1' - 1 kΩ
R_2 - 610 kΩ
R_3 - 11·6 kΩ
R_4 - 1·0 MΩ
R_5 - 100 kΩ
R_6 - 47 kΩ
R_7 - 500 kΩ
R_8 - 47 kΩ
R_9 - 10 kΩ
R_{10} - 500 kΩ
R_{11} - 2 kΩ
R_{12} - 10 kΩ
R_{13} - 22 kΩ
R_{14} - 2 kΩ

C_1 - 0·2 μF.
C_2 - 2 μF.
C_3 - 1 μF.
C_4 - 1 μF.
C_5 - 0·01 μF.
C_6 - 1 μF.
C_7 - 2 μF.

FIG. 2.10 Circuit Diagram for one Stage of the Amplifier.

The output from the spinning coils was fed into an amplifier similar to that designed by Sturtevant (42). The circuit diagram is shown in Fig. 2.10. The amplifier consisted of two similar circuits with resonant frequencies of 24.3 c/s and 25.7 c/s, staggered to give a maximum gain at 25.0 c/s and a bandwidth of 2 c/s for a power loss of 3 db. The theory of stagger-tuned circuits has been given by Terman (43). The gain and frequency of each stage could be controlled by independent networks. The gain was controlled by resistors R_1, R'_1, R_3, R_4, and was chosen to be 10^5. The frequency was controlled by the twin-T networks R_a, R_b, R_c, C_a, C_b, C_c. Figs. 2.11 and 2.12 show the response of each stage and the combined response when the amplifier is correctly tuned. The frequency was found to depend on the setting of R_{11}, the gain control, but by adjusting this resistor, the frequency could be set to the correct value. The gain was measured and was 160 for each stage, the overall value being 25,000.

The output from the second stage was rectified and fed into a microammeter. A shunt was provided so that the sensitivity of the amplifier could be altered. There were two sensitivity ranges, the less sensitive giving an output of 10 divisions for an input signal of 97 microvolts. Such an input was equivalent to the signal which would result from a change of 7.6×10^{-3} gauss in one of the fields. This range was linear only over the lower portion of the scale. The more sensitive range yielded 10 divisions output for an input of 14.2 microvolts and was equivalent to a change of 1.1×10^{-3} gauss in one

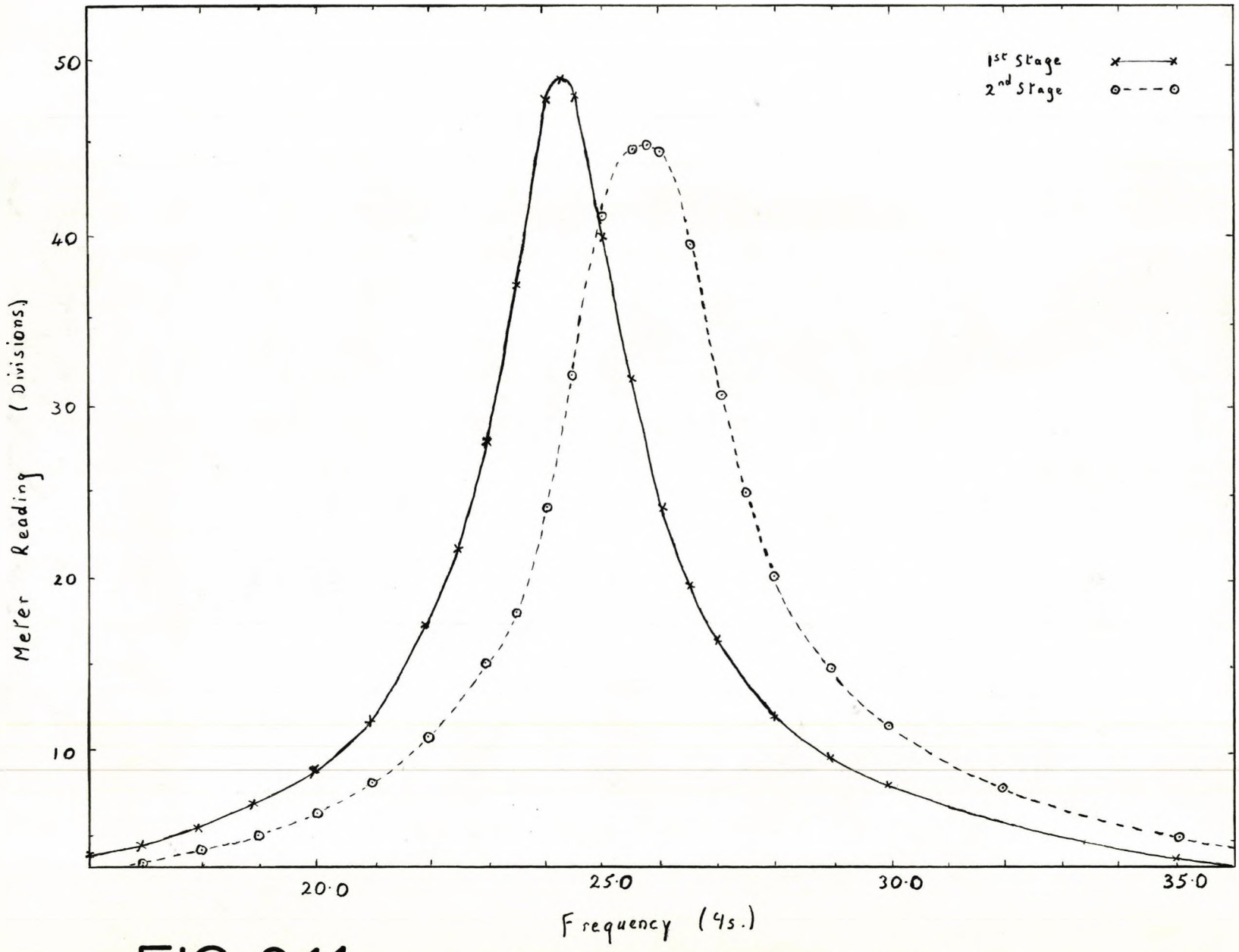

FIG. 2.11

The Response of Each Stage of the Amplifier.

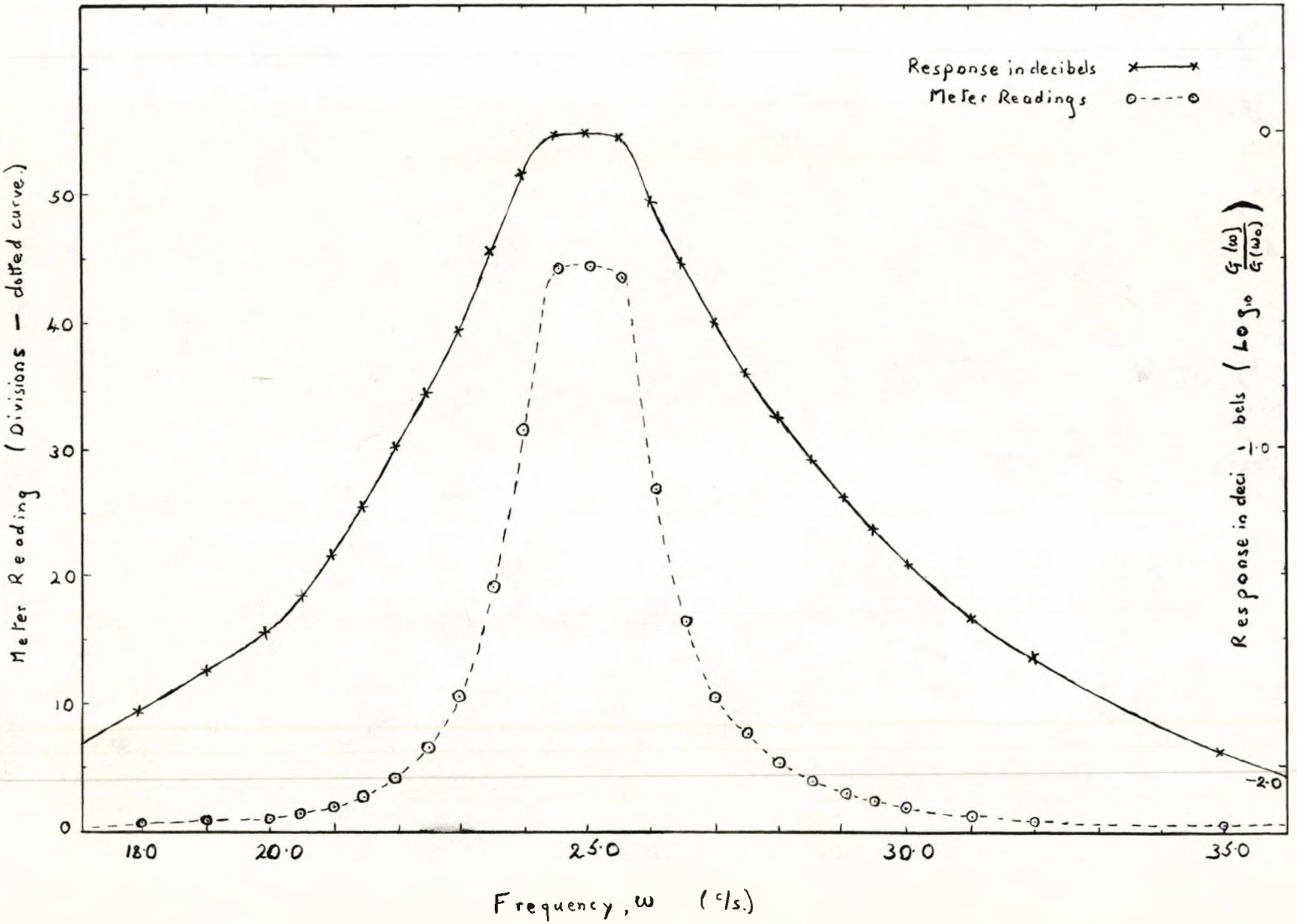

FIG. 2.12 The Response of the Complete Amplifier.

field. Since the lowest field to be measured was 13 gauss, fluctuations of 10 divisions in the output on the more sensitive range would limit the accuracy to 1:10^4.

When the apparatus was first used, carbon brushes were used on brass slip rings. These were stated to be very good by Bäckstrom (39) but I found them unsatisfactory. The output from the reference field could not be reduced to zero, even when there was no applied field. The axis of rotation had been aligned with the direction of the stray field in the laboratory so that the reading should have been zero. The pointer of the output meter flickered rapidly about a non-zero value. Several explanations were possible for this behaviour:-

1. Interference from stray fields.
2. Variations in the magnetic field in the laboratory.
3. Vibrations in the frame.
4. Earthing troubles.
5. Amplifier instability.
6. Brush noise.

The effect of stray fields was tested by moving a transformer carrying current near the spinning coil. No effect was apparent unless the transformer was in contact with the reference coils. It is therefore unlikely that any stray field would affect the output from the spinning coil. The stray magnetic field in the laboratory was shown to be too constant to cause the trouble. A cathode ray tube was placed parallel to the field in the laboratory and the

FIG. 2.13 The Frame used to support the Coils and Motor.

deflections of the spot were observed. They were barely large enough to be detected and from a calculation it was deduced that the fluctuations in the field were less than 0.004 gauss.

A more solid frame was built, that shown in Fig. 2.13, but it did not have any effect on the output. The earths were rewired without changing the behaviour of the output. The output, when a beat frequency oscillator supplied the signal was so steady that no movement of the pointer of the output meter could be detected. It was thus assumed that the amplifier was behaving correctly.

When the brush pressure was altered, there was little change in the behavious of the pointer, but when the number of brushes was increased to three per ring there was a great improvement. Not only was the amplitude of the flicker reduced but the output could be brought to the zero. The troubles were not cured because, when the apparatus was left running the reading steadily increased and could no longer be reduced to sero. Soon after this it was found that this trouble occurred when the coil was shorted thus demonstrating that it was due to the brushes. Walker (44) showed that the contact resistance between copper and carbon is dependent upon the direction of the current. Since the slip rings became hot when run for any length of time, it seemed likely that the contact voltage of each ring and set of brushes would be different from the others. This difference would give rise to an a.c. signal if the temperatures of the rings varies.

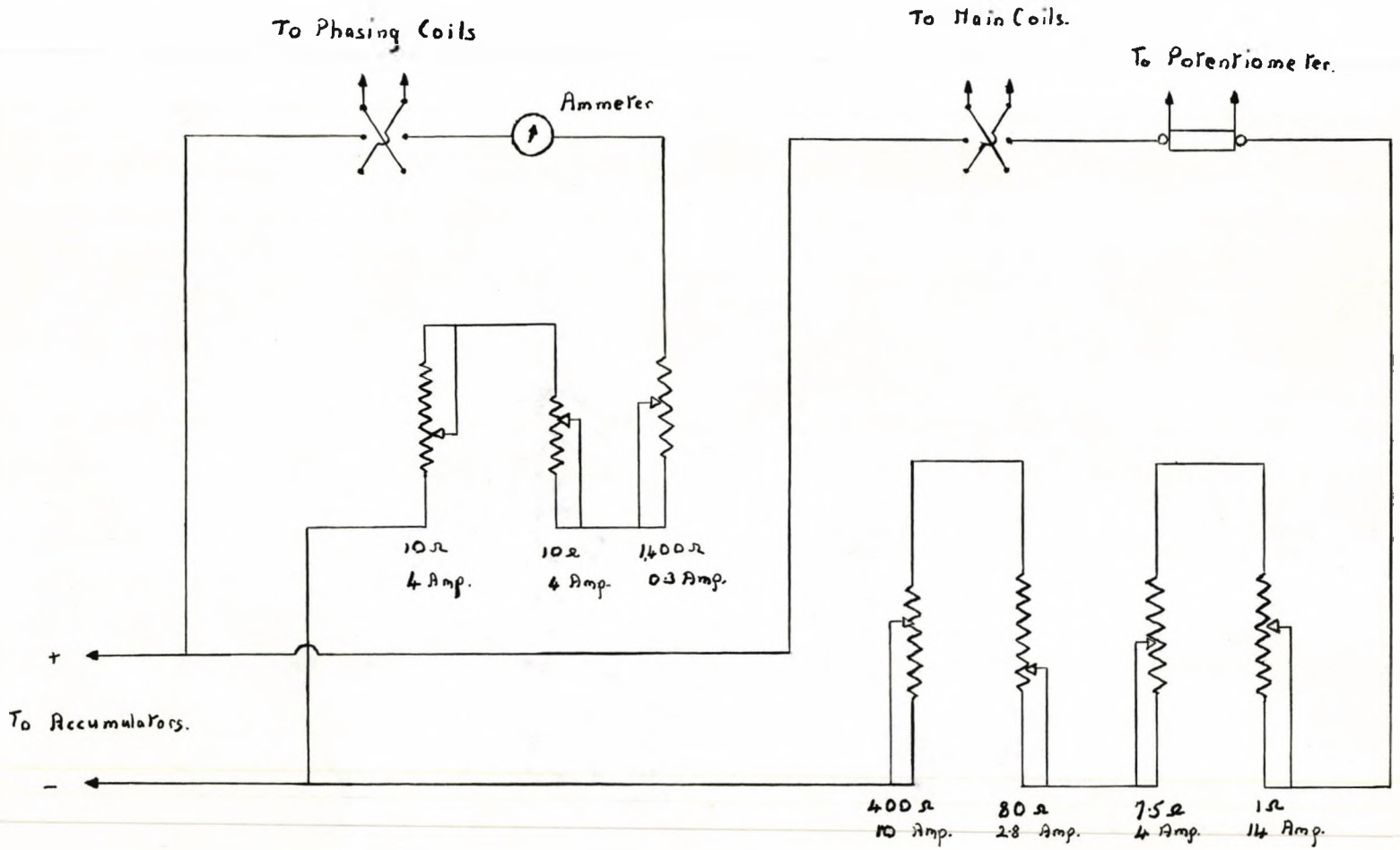

FIG. 2.14 The Reference Field Control Circuit.

To check that the trouble was due to the carbon brushes, a silver wire was soldered to the ends of two brass blocks which were placed in the brush holders. The result was conclusive, the reading could immediately be reduced to zero and maintained there indefinitely. To improve the contact and to reduce wear, a silver plate was soldered to the ends of the brass blocks and three brushes were put on each ring. The two spinning coils were than used together. As there was usually a remanent field in the spectrometer, a current was passed through the reference field to balance the field in the spectrometer. The circuit for the reference field is shown in Fig. 2.14. It was designed to be used with the same supply voltage as that used in the spectrometer circuit.

At first, it was found difficult to detect the minimum in the output of the amplifier because the sensitivity of the amplifier was so great. If the two coils were not 180 out of phase, the minimum signal was too large for the amplifier and overloaded it. When the minimum had been found the phasing field was altered to reduce the reading further and then the main field was altered again to obtain the lowest reading. Once the position of the reference field had been set, it was easier to detect the minimum when the apparatus was used again. The sensitivity was such that, to move the pointer from a maximum reading on the output meter through the minimum to the maximum on the other side of the point of balance required a current change of only 3:1,000.

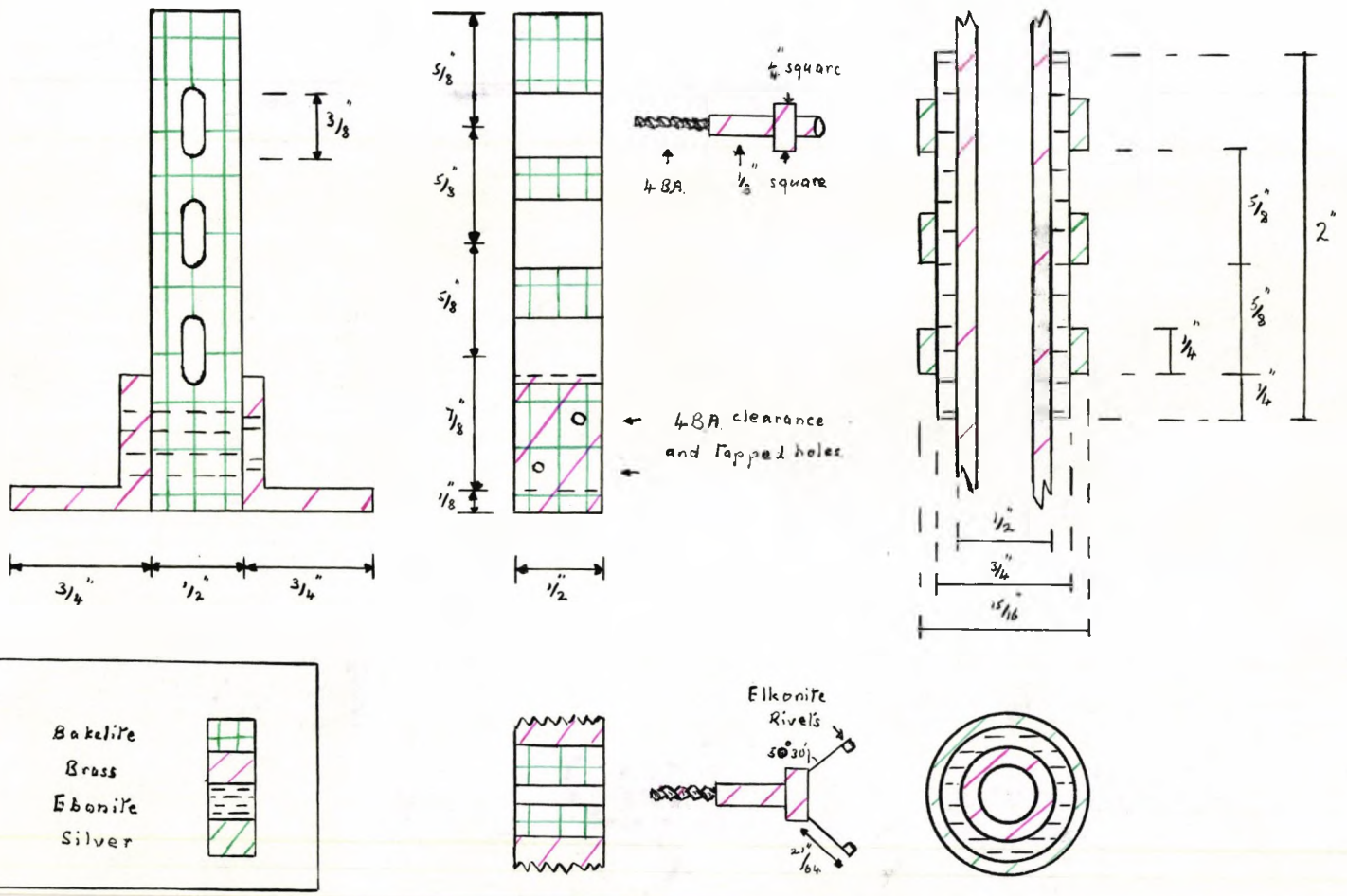

FIG. 2.15 The Design of the Final Set of Slip-rings and Brushes.

The pointer was not steady but oscillated irregularly with an amplitude of about 10 divisions. The unsteadiness of the pointer was thought to be due to the brush design. The brushes were rectangular blocks sliding in brass holders which allowed a lot of side play in the brushes. I thought this to be undesirable so I considered other designs and decided to copy one by Johnson Matthey (45) using the materials suggested in another of their leaflets (46). The slip rings were machined from a silver tube and were turned when they had been mounted in position on the shafts of the two driving systems. The radii of the slip rings was decreased to reduce the speed of contact of the surfaces, but this could not be reduced below the figure of 120 cms./sec. recommended by Morton (47).

The brushes were made from elkonite (silver-graphite) rivets which were fixed to phosphor-bronze springs. The dimensions conform to specifications laid down in the leaflets by Johnson Matthey Ltd. The design of the whole assembly is shown in Figs. 2.15 and 2.6. These materials were chosen to give low thermo-e.m.f.'s, little noise and a low rate of wear. The pressure on the brushes could be altered by using spacers between the head of the brush and the bakelite holder. These brushes were never given a complete test because time did not permit such a test.* The zero reading was checked for the coil in the reference field and was found to be stable against flicker and long term drift.

Mr. Kamal took over the apparatus and completed the final testing of it. Without any further modification he was able to make reproducible measurements of the field to 1:25,000.

Chapter III.

Apparatus and Techniques.

1. Apparatus.

The internal arrangement of the spectrometer and the rest of the equipment will be described in this chapter.

It is possible to gain access to the vacuum chamber at five points, through holes in the centre of the top and bottom plates and through three ports in the wall of the vacuum chamber. The source is put into the spectrometer through the first port, shown in the Fig. 3.1. Connections to the Geiger-Müller tube are made through the second port and while the third port is used to make adjustments to the focal plane shutter and the Geiger-Müller tube. When Barry first made measurements on the shape of the field, a cylindrical rod was placed along the axis of the spectrometer. This rod was later used to support the source, shutters and the counter tube and formed a very convenient place from which to measure radial distances.

There are five shutters and four baffles, which are used to define the solid angle used and to keep the number of scattered particles to a minimum.

The positions of the shutters are shown in Fig. 3.1. The first shutter s_1, lies at an angle of 47.5° to the radius through the source. It was designed to open symmetrically about the median plane ($z = 0$) and may be controlled through the lid. The maximum aperture is 20 cms., when $z = \pm 10$ cms. The radial extent of the aperture may

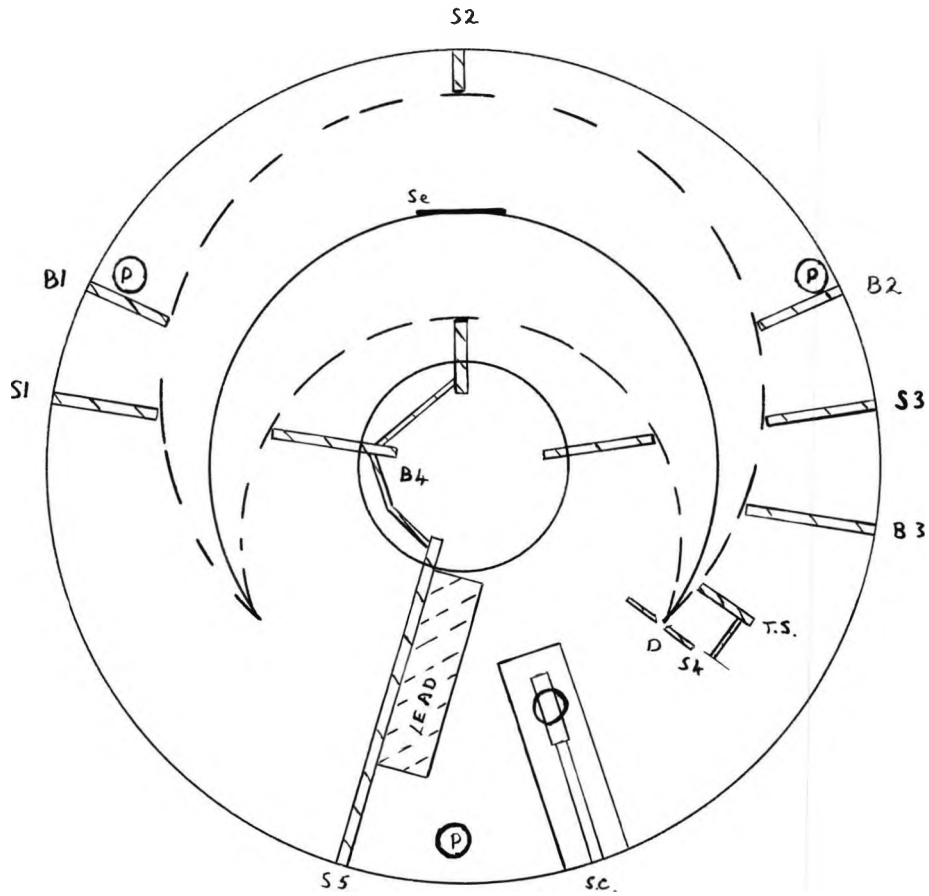

S. Source.
Se. Septum.
S1 - S5. Shutters.
S.C. Spinning Coil.
D. Detector.
P. Pole Separators.
T.S. Trochoid Stopper.
B1 - B4. Baffles.

FIG. 3.1 The Internal Arrangement of the Spectrometer.

only be altered by inserting metal strips into a slot behind the vertical shutters. The maximum radial ex ent gives a radius of 55 cms. at an angle of 127°, i.e., in the azimuthal plane mid-way between the source and the image, the half-angle $\Omega_{\frac{1}{2}}$. The minimum radial extent at 47.5° gives a radius at the half-angle of 20 cms.. Because the field deviated from the theoretical shape in the extreme regions of the spectrometer, two strips were inserted along either ed e of the first shutter to limit the maximum and minimum radii at the half-angle to 50 cms. and 25 cms. respectively.

The second shutter, s_2, was placed at the half-angle. This was designed to reduce the number of particles which reach the detector after being scattered by the walls of the vacuum chamber. The third shutter, s_3, and the four baffles B_1 to B_4, also serve to reduce the number of scattered electrons. In a field similar to that in this spectrometer, β-rays with lower energy than that of the mean ray will follow trochoidal prbits. To eliminate these particles, a septum, Sp, 10 cms. wide was placed tangentially to the path of the mean ray (r_o = 40 cms.) at the half-angle and a stop, T, designated "trochoid stopper", was placed in front of the focal plane.

Shutter s_4 was a variable slit which was placed in the focal plane. Two bevelled brass plates slid in grooves so that both the width and the position of this slit could be altered. In every experiment the slit width was set equal to the source width and the

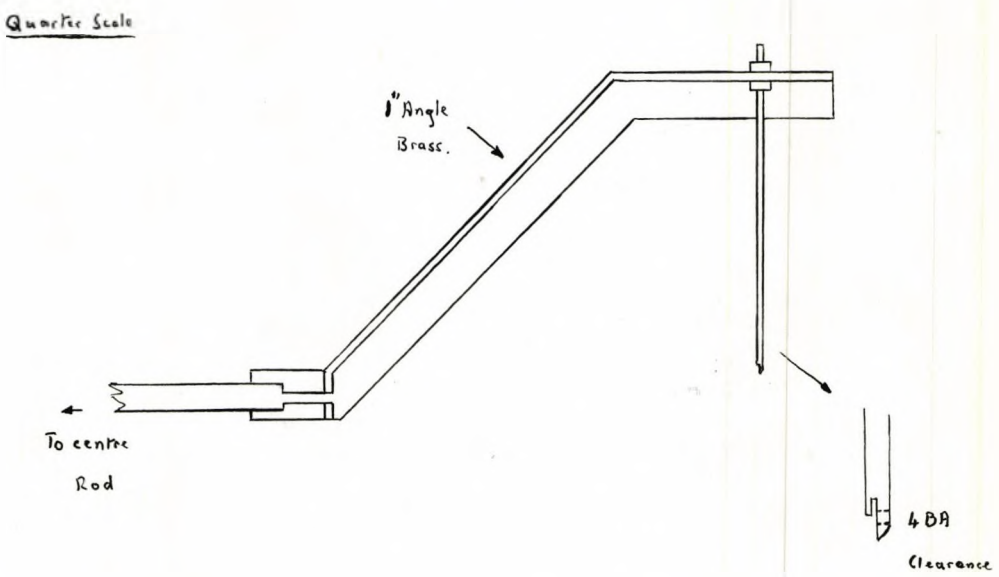

FIG. 3.2 The Arm supporting the Source and Frame.

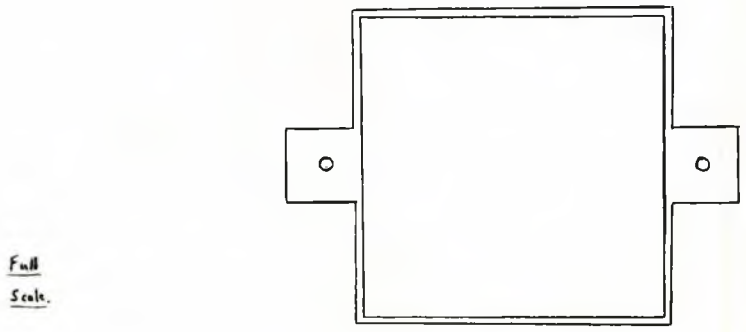

FIG. 3.3 The Frame used to support the Source.

height was always the maximum permissible, 1.6 cms. This shutter and the Geiger-Müller tube were mounted on a moveable arm. The shutter could be set in the focal plane by a rack and pinion control through the third window. The resolution was measured with the shutter at several different angles and the arm was then set to give the best resolution.

A fifth shutter, S_5, was placed behind the source to stop β-rays traversing the field in the wrong direction from reaching the counter tube. This shutter was placed as far away from the source as was possible to keep the number of electrons back-scattered from it to a minimum. The distance was limited by the position of the spinning coil and the need to place lead blocks between the source and the counter tube to reduce the number of γ-rays reaching the counter tube, so contributing to the background count rate.

The source was mounted on a frame and supported by an arm fixed to the central rod. Since a near object subtands a large solid angle at the source, it may scatter a large number of particles into the focussed beam. The arm was designed to give a rigid support for the frame, using a little material as possible to keep down the scatter. The arm was made from angle-brass which was bent so that it would lie close to the upper pole face, as shown in Fig. 3.2. A Thin rod was helf by this arm at a radius of 40 cms. and the frame was suspended from the end of it. The frame was cut from wither 1/16 in. of 1/32 in. sheet brass and was 4 cm. square with sides

1/16 in. wide and is illustrated in Fig. 3.3. The sources were mounted on the frame on thin conducting foils.

To register the intensity of the β-rays, a Geiger-Müller tube was used with a 1014A pre-amplifier* and a 1009A scaler*. The pre-amplifier paralysis time was set to 300 microseconds which was longer than either the paralysis time of the scaler or the dead + recovery time of the counter tube. The voltage was supplied by a 1033A power pack*.

The first Geiger-Müller tubes used were end window tubes. The windows were either of 0.0005 in. or 0.00025 in. Mylar foil onto which a thin layer of aluminium had been evaporated to make them conducting. To seal the windows onto the ends of the tubes, a rubber solution was used; 'Dunlop' rubber solution was found to give better results than 'Bulldog' solution. The solution was applied liberally to form a ring round the end of the tube and then allowed to dry. This formed a good gasket against which the window was held by a clamping ring. These tubes were filled outside the spectrometer and thus had to withstand atmospheric pressure; the filling mixture was 9 cm. Hg. argon + 1 cm. Hg. alcohol. Due to the presence of minute holes in the windows the gas leaked out of the tubes so the tubes had to be refilled once a week. The counters had plateaux with lengths greater than 100 volts, the slopes being 0.06%/volt.

---

* A.E.R.E. Harwell design Nos. (E. K. Cole).

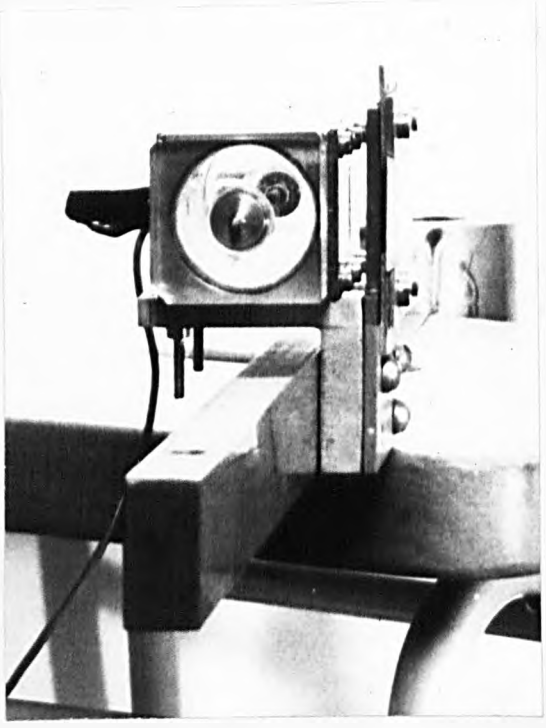

FIG. 3.4 The Side-window Geiger-Müller Tube.

To avoid the dead space due to the beads in these tubes, two side window tubes were designed one of which is shown in Fig. 3.4. The difference between the two tubes was in the sizes of the windows. One was 0.2 in. wide by 0.625 in. high and was designed to be used in the measurement of internal conversion lines, the other was 0.75 in. wide by 0.625 in. high and was designed to be used when β-spectra were measured. An extension was made to the filling system, enabling these tubes to be filled inside the spectrometer. The G.M. tube was connected to the vacuum chamber through a tap so that it could be evacuated with the vacuum chamber; the greatest pressure across the window was thus the pressure of the filling mixture.

Perspex was originally used to cover the ends of the tubes and to support the central wire anode but was replaced by glass because it was found that the perspex absorbed the alcohol as fast as it was fed into the tube. With glass ends, the counters had plateaux more than 100 volts long over which lengths there was no measurable increase in the counting rate.

The vacuum chamber was evacuated through the lower cover plate of the spectrometer. The pumping system was rather slow for such a large vacuum tank, it consisted of a rotary pump (1S50 Edward's High Vac.) of only 50 litres per minute and a 2 in. diffusion pump (203 Edward's) giving 70 litres per second. The time taken to reach a pressure of 10^{-4} mm.Hg. was about five hours. A pressure of 10^{-5} mm.Hg. or better was used and could be reached after about sixteen hours.

2. Source Preparation.

If a true energy spectrum is to be obtained, it is necessary to pay great attention to the preparation of the sources. Distortion may arise in the measured spectrum from straggling due to (a) source thickness, (b) electrons back-scattered from the supporting backing and (c) a retardation and loss of energy brought about by source charging. When these distortions were not important (e.g. when the focussing properties of the spectrometer were being measured) a thick backing of gold foil 35 mgm./cm.^{2} was used. For measurements on the spectra of Yttrium-91 and Cerium-144 the sources were mounted on aluminium backings less than 50 micro gram/cm^2 thick.

A pot containing Radio-thorium provided a source of Th(B+C+C+C+D), Thorium active deposit, which was used in the study of the behaviour of the spectrometer and which was also used to calibrate the field in the spectrometer. To prepare a source, a metal foil 5 cm. long by 1 cm. wide was placed on a perspex jig and covered by a sheet of mica in which a slot, the dimensions of the required source, had been cut. This was placed on the pot of Radio-thorium, and a negative potential was applied between the foil and the lead shielding round the pot. The field caused Th A to collect on the foil. The Th A decayed rapidly to Th B which has a half-life of 10.6 hours. The strength of the source was 75% of the maximum possible after about sixteen hours (this quantity could be conveniently collected overnight). If the source was left longer, the thickness increased

without a corresponding increase in the activity hence there was no point in collecting for longer periods.

When the foil had been activated, it was removed from the perspex jig and fixed to the frame either with a nut and bolt (in the case of the thicker foils) or with a thin layer of rubber solution. When a source was used to calibrate the spectrometer, the thickness of the foil was 140 micrograms/cm^2 aluminium leaf (the thinnest available). Since this leaf had no mechanical strength it was stuck on a thin film of zaponlak 10 micrograms/cm^2 thick.

The sources of Yttrium-91 and Cerium-144 were obtained from the Radio Chemical Centre, Amersham, and arrived, in acid solution, in small sealed bottles. To prepare sources to mount in the spectrometer, a film of zaponlak 10 micrograms/cm^2 thick was placed on the frame and a semi-opaque layer of aluminium was evaporated onto this film to render it conductive. The thickness of this aluminium layer was estimated to be less than 30 micrograms/cm^2. Because the film is hydrophobic the acid solution will not spread on the surface. To enable the solution to spread and thus ensure that the source is as uniform as possible, a drop of insulin was put on the film and spread over the central area of the film, a technique first used by Schaefer and Harkner (48) and later, by Langer (49). The excess insulin was removed with a pipette. By evaporating a known quantity of insulin to dryness, the thickness of the layer on the film could be estimated. The maximum thickness

of the layer was estimated to be 50 microgram/cm^2..

The source of Y-91 was then made by removing a small quantity of solution from the bottle and putting a few drops of the solution onto the insulin which was in the shape of a square with sides 1 cm. long. The solution was left to evaporate and then a few more drops were placed on the film. This process was repeated until the strength of the sources was about 1 millicurie. From the data supplied by the Radio Chemical Centre, the thickness of the source, which was in the form of Yttrium Chloride, could be calculated. The thickness of the Y-91 source itself was estimated to be 20 micrograms/cm^2, thus with the insulin the total thickness of the source is $<$ 70 microgram/cm^2.

The Ce-144 source was obtained to study some of the internal conversion lines arising from the decay of Ce-144 to Pr-144. Since I wanted to use as high a resolution as possible, the width of the source was made 1 mm. wide and 1 cm. long. Because of the long half-life of Ce-144 (185 days) the strength of the source was made 1/10 millicurie which was the activity contained in one drop of the solution. The thickness of this source was calculated to be 100 micrograms/cm^2. and with the insulin and the film, the total thickness of the source was calculated to be 150 micrograms/cm^2. This thickness was calculated to broaden the base width of a line by 0.15% at 100 KeV and by 0.35% at 27 KeV. A second, stronger source was prepared with dimensions 2 mm. x 16 mm., but owing to

its thickness, the resolution was about 0.5%.

3. Calibration of the Spectrometer and the Estimation of Errors.

In order to ascertain the momentum or energy of a β-line or the momentum selcted in a β-spectrum, it is necessary to calibrate the field of the spectrometer. If both ρ and B are determined accurately, it is possible to calculate the momentum absolutely. It is, however, difficult to make both these measurements at the same time. If a fixed radius ρ is used in the spectrometer, the momentum may be compared with other momenta by measuring the relative values of the field B.

I chose the latter method. Since the strength of the field was measured by rotating a coil at a fixed frequency, the outputs could be compared directly. Th(B+C+C+C+D) emits five β-lines whose energies are accurately known. These lines, the A-, B-, F-, L- and X-lines, which are standard lines, were used to calibrate the spectrometer. The spectrometer was calibrated each time the spectra of Y-91 or Ce-144 were measured, to eliminate any errors due to changes which might otherwise have occurred, such as for example a change in phase of the commutator. The geometrical size of the calibrating source was made identical with that of the source being measured so that the line shapes would resemble each other as closely as possible. The sources of Thorium-active deposit was prepared on aluminium leaf 140 micrograms/cm^2 to reduce the back-scattering to a minimum.

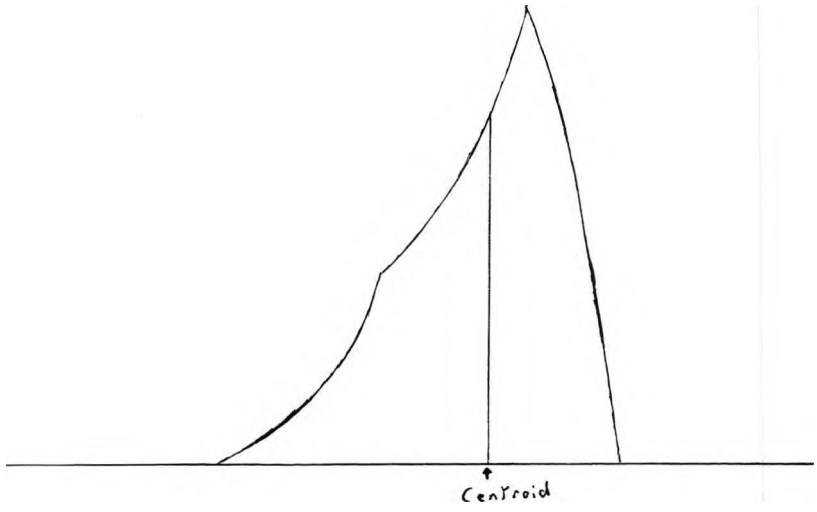

FIG. 3.5 The Profile of a β-line.

The output from the rotating coil could be read on the potentiometer to better than $1:10^4$. The accuracy was limited to $1:10^3$ however, because of oscillations of this magnitude in the output. There is also an error in the estimation of the exact position of a β-line. Fig. 3.5. shows a theoretical line shape for a semi-circular spectrometer, that for a double focussing spectrometer should be very similar. If one is measuring the momentum of an internal conversion line, one may choose any point on the line to serve as a reference point. The high energy edge, which is formed by rays travelling near to the mean radius, is well defined. The point at which this edge intersects the background is also well defined and is usually taken as the reference point. When a thin source is used to calibrate the field, there is little loss of energy in the source so that this reference point may be used as a measure of the momentum and energy of the line. With a thick source, all the rays will lose a small amount of energy leaving the source, hence this point can no longer be used as a measure of its energy. Because the sources were always thin, the point of intersection of the high energy edges with the background were always well defined the experimental curves and could be read with an accuracy of $1:10^3$.

Beta-spectra present a different problem. Here, the momenta of the ray contributing to the counting rate at a particular setting of the field have a spread in energy due to the aberrations

in the spectrometer. If the number of β-rays emitted by the source is regarded as constant over the momentum range accepted then the number of rays present with a given momentum in that range is proportional to the shape of the line, some-times known as the window curve, at that momentum. The most probable momentum is the one which should be used to represent the momentum of the rays being measured. I choose to use the centroid of the β-lines to calibrate the spectrometer when measuring β-spectra because then there are equal numbers of rays with momenta higher and lower than the momentum of the centroid. The accuracy with which the centroid could be determined was 1:300.

When the errors in measuring the unknown spectra and the errors in calibration were combined, the figures for the accuracy of measurements of β-spectra and internal conversion spectra were $3{:}10^3$ and $2{:}10^3$, respectively.

Besides these errors, there is a statistical error due to the counting of a finite number of particles. For a count of N particles, the error is $\sqrt{N}$, or as a percentage, $1/\sqrt{N}\%$. It was possible to keep the statistical error for the β-spectra between $\frac{1}{2}\%$ and 1% over most of the range of energies. Only at low and high energies, near the ends of the spectra where the counting rates were very low, was this not possible. When the results were plotted in the form of a Kurie-plot, although the points were scattered about a straight line, the error in the momentum calculated from a least mean squares fit was small. The final value for the end point of the β-spectrum of Y-91 was the mean of several determinations.

It is necessary to measure the intensities of the β-lines in internal conversion spectra in order to decide to which type of transition each β-ray belongs. Because the Ce-144 source was weak, the counting rate was low and the errors were as large as 2 to 3%. To measure the intensities of lines very close together, such as those arising from conversion in the L_I, L_{II}, L_{III} subshells, little error will be introduced if the heights of the lines are compared directly. Only when the window of the G.M. tube absorbs electrons and the efficiency of the counter changes rapidly with energy will this method have to be corrected. For lines with very different momenta, the spectrometer must be calibrated to be able to correct the results for the absorption of electrons in the window of the G.M. tube and possibly for changes in the transmission. I calibrated the spectrometer for this change in efficiency of detection by measuring the intensities of the A-, B- and F- lines from a source of Thorium active deposit and comparing them with the results obtained by Flammersfeld (50). The errors in the measurement of the intensities was estimated to be 10% except for the low energy line of Ce-144 at 27 KeV the intensity of which was estimated to have an error of 25% because it was very close to the cut-off of the window of the G.M. tube.

Chapter IV.

The Behaviour of the Spectrometer.

1. The Performance of the Spectrometer.

The behaviour of the spectrometer has been determined under a variety of conditions, and these results are supplementary to those of Barry[23]. The behaviour will be described in terms of the three criteria, defined in Chapter I, and transmission, luminosity and resolution (eq'ns (1.2), (1.3) and (1.7)).

The resolution is defined as the ratio $R_o = \frac{\Delta r}{r_o}$ (4.1)

where Δr is the image width and r_o the mean radius. Since the mean radius was constant in the spectrometer and the field was varied, the ratio of the change in field, ΔB, to the field B was of more interest. This ratio $\frac{\Delta B}{B}$ is related to the ratio $\frac{\Delta r}{r_o}$ by the formula for the dispersion, equation (1.8),

$$\frac{\Delta B}{B} = \frac{4\,\Delta r}{r_o}$$

hence from (1.7),

$$\frac{\Delta B}{B} = \frac{s+h}{r_o} + \frac{|4\alpha_2 - 3|\,\beta^2}{48\,r_o^2} + \frac{|2 - 16\alpha_2|\,\phi^2}{3} + \frac{|16\alpha_2 - 6|\,\psi^2}{3} \qquad (4.2)$$

+ higher order terms.

The angles ϕ, ψ, Ω and the directions r and z are shown in fig. 4.1. In this spectrometer, $\alpha_2 = \frac{1}{6}$, therefore,

$$\frac{\Delta B}{B} = \frac{s+h}{r_o} + \frac{5h^2}{96\,r_o^2} + \frac{4}{3}\psi^2 \qquad (4.3)$$

The resolution is thus independent of the radial angle of

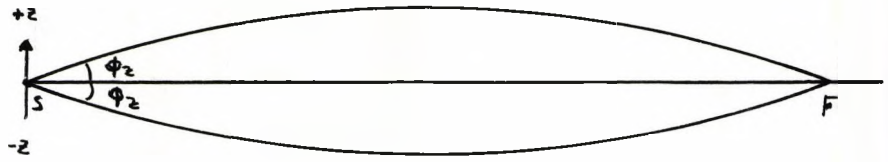

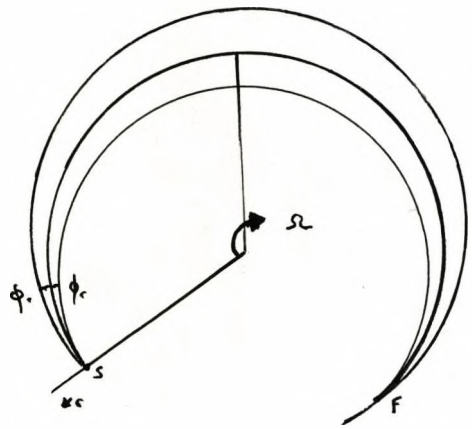

FIG. 4.1 The Definition of the Coordinate System used.

emission ϕ, hence the radial aperture.

This value of the resolution is the base resolution, that is, the total width of the image divided by its momentum. In practice, it is very difficult to measure the base resolution accurately because although the high energy edge is well defined, the low energy edge of the line trails away and approaches the background counting rate assymptotically. The resolution usually quoted is the half-height resolution which is defined as the width of the image at half the peak height of the line divided by its momentum. This is well defined and is always less than the base resolution. The half-height resolutions measured experimentally will be compared with the calculated value for the base resolution.

The experimental data on the performance of the spectrometer was obtained with sources of thorium active deposit and also with a source of Y-91. The data is summarised in tables 4.1 to 4.5 and is illustrated by figs. 4.2 to 4.7.

Table 4.1 is a summary of the first extensive measurements made with the spectrometer. The most prominent internal conversion lines of a Thorium active deposit were measured to determine how the resolution depended on the momentum. The spectrometer had been set on Branch I of a 30 amp. hysteresis cycle. Columns 1 and 2 give the name of the line (following Ellis's notation (51)) and its momentum. Column 3 shows the measured output of the spinning coil and column 4 the ratio of the output to the momentum. The resolution is given

Spectrometer set on Branch I of a 30 Amp. Hysteresis Cycle.
Source:- 1 cm. x 1 cm.; Slit Width:- 1 cm.; Transmission:- 1.47%
Predicted base line width:- 2.25%.

Line	Momentum $B\rho$ (Gauss.- cm.)	Spinner Output of the centroid (volts).	$\frac{\text{Spinner Output}}{B\rho}$	Resolution at half-height (%)	$\frac{\text{Relative height x res.}}{\text{area.}}$
A	534.2	0.1221	2.286×10^{-4}	1.4	1.01
B	652.4	0.1496	2.292 "	1.6	0.89
E	1,110	0.2554	2.309 "	1.0	1.00
F	1,388.4	0.3202	2.306 "	0.9	1.01
H	1,697	0.3916	2.308 "	0.8	0.90
I + Ia	1,753.9	0.4044	2.306 "	0.8	0.91
L	2,607.2	0.6030	2.313 "	0.7	0.99
M	2,891	0.6675	2.309 "	0.7	0.91

TABLE 4.1. Resolution and Centroid Readings of a ThB Source for High Transmissions.

in column 5 and in column 6 the ratio of the area of a line to the product of its height and half-width.

The resolution was not constant, but decreased with increasing momentum. For high momenta, the resolution was about one third of the calculated value for the base resolution but at low momenta, the half-height resolution was only two-thirds the value of the base resolution. There are three possible explanations, (1) that the broadening was caused by the natural width of the lines, (2) that the source was thick and rays leaving it were degraded and (3) that the broadening was due to aberrations which were dependent on the strength of the field.

The natural line width of the F-, I- and L-lines of Thorium active deposit have been measured and were found to be less than 0.1%[52]. Allowing for the lower energy of the B-line, its natural width should not be more than 0.3%. This is not enough to account for the observed difference between the resolutions of the B- and L-lines. The sources were always freshly prepared and were invisible to the eye; narrow sources similarly prepared for high resolution gave resolutions from 0.1 to 0.2%, cf. table 4.3. It is therefore unlikely that the broadening was caused by source thickness.

The third possible cause is that the aberrations in the spectrometer depend on the field strength. In Chapter II, the possibility of an interaction between the field due to the iron poles and the fringing field due to the exciting coils was discussed.

It was concluded that a change in the field shape may occur and that as the field strength increased, the shape should become constant. If the field shape alters, the aberrations will alter and hence the resolution also. The resolution should therefore change in such a way that it becomes constant at high fields, which was what happened.

In columns 3 and 4, the value of the output of the spinning coil quoted was the value corresponding to the centroid of the line measured. It can be seen from column 4 that the output of the spinning coil was not strictly proportional to the momentum. Since the resolution was not constant, the way in which the aberrations altered could have effected the value of the centroid. There is thus no reason why the output of the spinning coil should be proportional to the momentum if the shape of the field changes.

The ratio in column 6 is a comparison between two methods used to measure the area (and hence the intensity) of a line. The areas of a line, measured by two methods were compared by taking their ratio. The ratios for different lines were compared by normalizing them to the ratio for the E-line, This line was chosen because it was measured in most of the runs whereas the stronger F-line was sometimes too strong to measure. Because of scatter and aberrations, there is a low energy tail to a β-line which is ill-defined and therefore difficult to measure. Since both the half-width and the height of a line are well defined, their product should be a measure of the intensity provided that the line profile does not

Spectrometer set on Branch I of a 30 Amp. Hysteresis Cycle. Source:- 1 cm. x 1 cm.; Slit:- 1 cm.; Transmission: 0.25 % Predicted base line width 1.4 %		
Line	Momentum $B\rho$ (Gauss-cm.)	Resolution at half-height (%)
B	652.4	1.37 %
E	1,110	1.00 %
L	2,607.2	0.74 %

TABLE 4.2. Resolution of a Wide Source of THP for Low Transmission.

Spectrometer set on Branch I of a 30 Amp. Hysteresis Cycle Source:- 1 mm. x 1 cm. high; Slit:- 2 mm.; Transmission:-1.47% Predicted base line width 1.25%.		
Line	Momentum B (Gauss - cm.)	Resolution half-height (%)
B	652.4	0.84 %
E	1,110	0.56 %
F	1,388.4	0.50 %
L	2,607.2	0.30 %
M	2,891	0.35 %
X	9,986.1	0.17 %

TABLE 4.3. Resolution of a Narrow Source for High Transmissions.

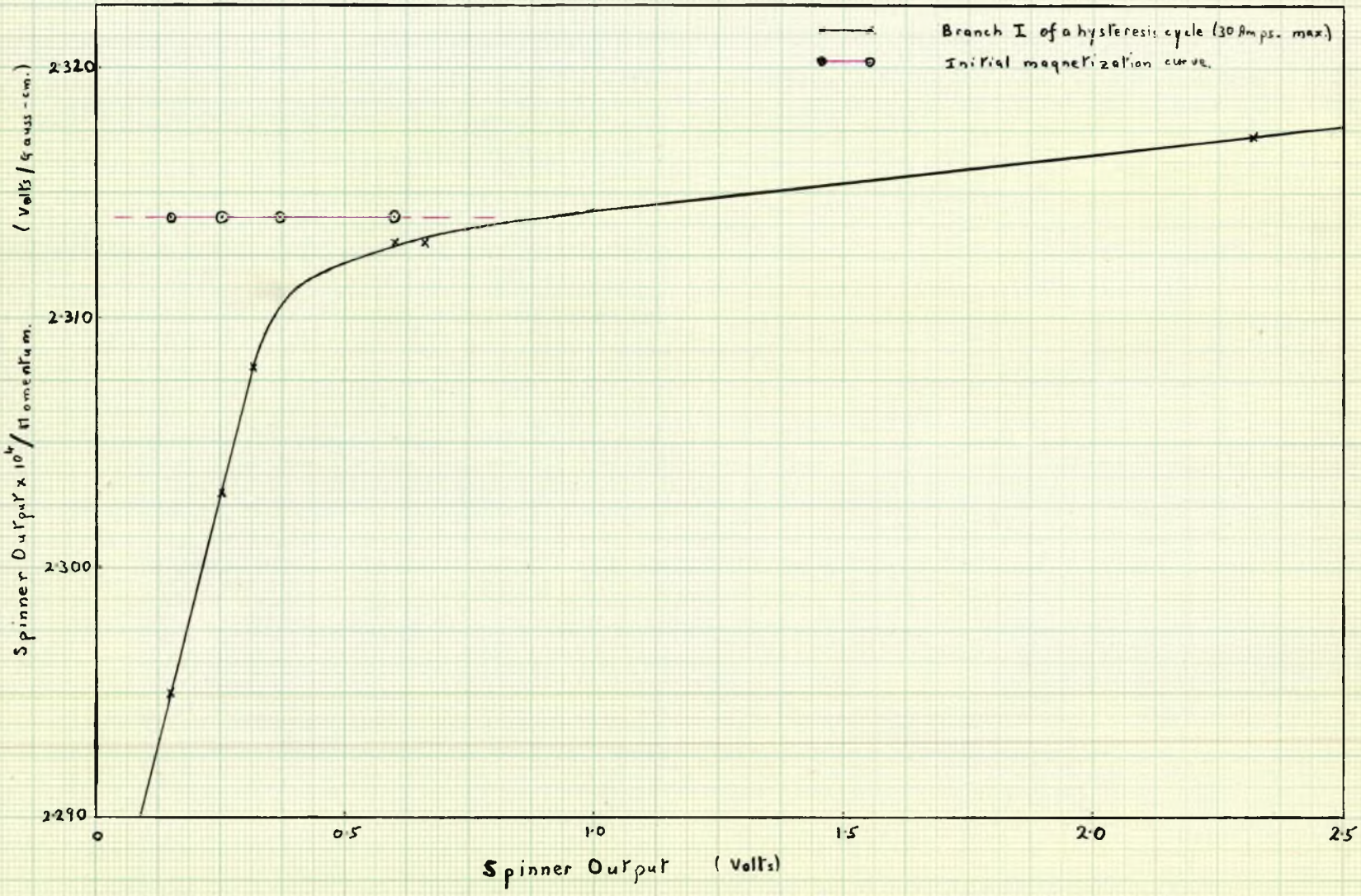

FIG. 4.4

The Ratio of the Output of the Spinning Coil to the Momentum plotted as a Function of the Momentum.

alter. The products for the lines measured, were evaluated to see whether they were still a measure of the intensity of the lines. These values were compared with the areas of the same lines measured with a planimeter. The results show that the areas of the lines measured by the two methods agree to 10%, so the intensities of β-lines were measured by calculating the areas from their heights and half-widths.

Table 4.2 gives the results of measurements made with a low transmission and table 4.3 the results of measurements made with a narrow source and high transmission. The resolutions in table 4.2 are similar to those in table 4.1, whereas the base resolution has been reduced by two-fifths. The fact that there has been no decrease in the resolution may have been due to the change in aberrations caused by a change in field shape. The resolution is much improved in table 4.3, but again, there is an increase in the resolution at low momenta comparable with the increases shown in tables 4.1 and 4.2.

When sufficient data had been obtained, the mean values for the ratios of the outputs of the spinning coil to the momenta were calculated and have been plotted against the momentum in fig. 4.4. From this curve, the true momentum for any value of the output could be determined.

Because these results indicated that the shape of the field was dependent upon its strength, I decided to set the field in a

Source:- 1 cm. x 1 cm.; Slit:- 1 cm. wide;
Transmission:- 1.47%

Line	Momentum B ρ (Gauss-cm)	Spectrometer set on Branch I of a 30 Amp. Hysteresis Cycle.			Spectrometer set using the Initial Magnetization Curve		
		Spinner Output (volts)	Spinner Output / Momentum (volts/Gauss-cm)	Resolution at half-height (%)	Spinner Output (volts)	Spinner Output / Momentum (volts/Gauss-cm)	Resolution at half-height (%)
B	652.4	0.1486	2.278×10^{-4}	1.47 %	0.1509	2.313×10^{-4}	1.19 %
E	1,110	0.2547	2.295×10^{-4}	1.13 %	0.2567	2.313×10^{-4}	1.02 %
G	1,596	0.3685	2.309×10^{-4}	0.91 %	0.3691	2.313×10^{-4}	0.89 %
L	2,607.2	0.5996	2.309×10^{-4}	0.78 %	0.6029	2.313×10^{-4}	0.73 %

TABLE 4.4. Behaviour of the Spectrometer on the Setting of the Field.

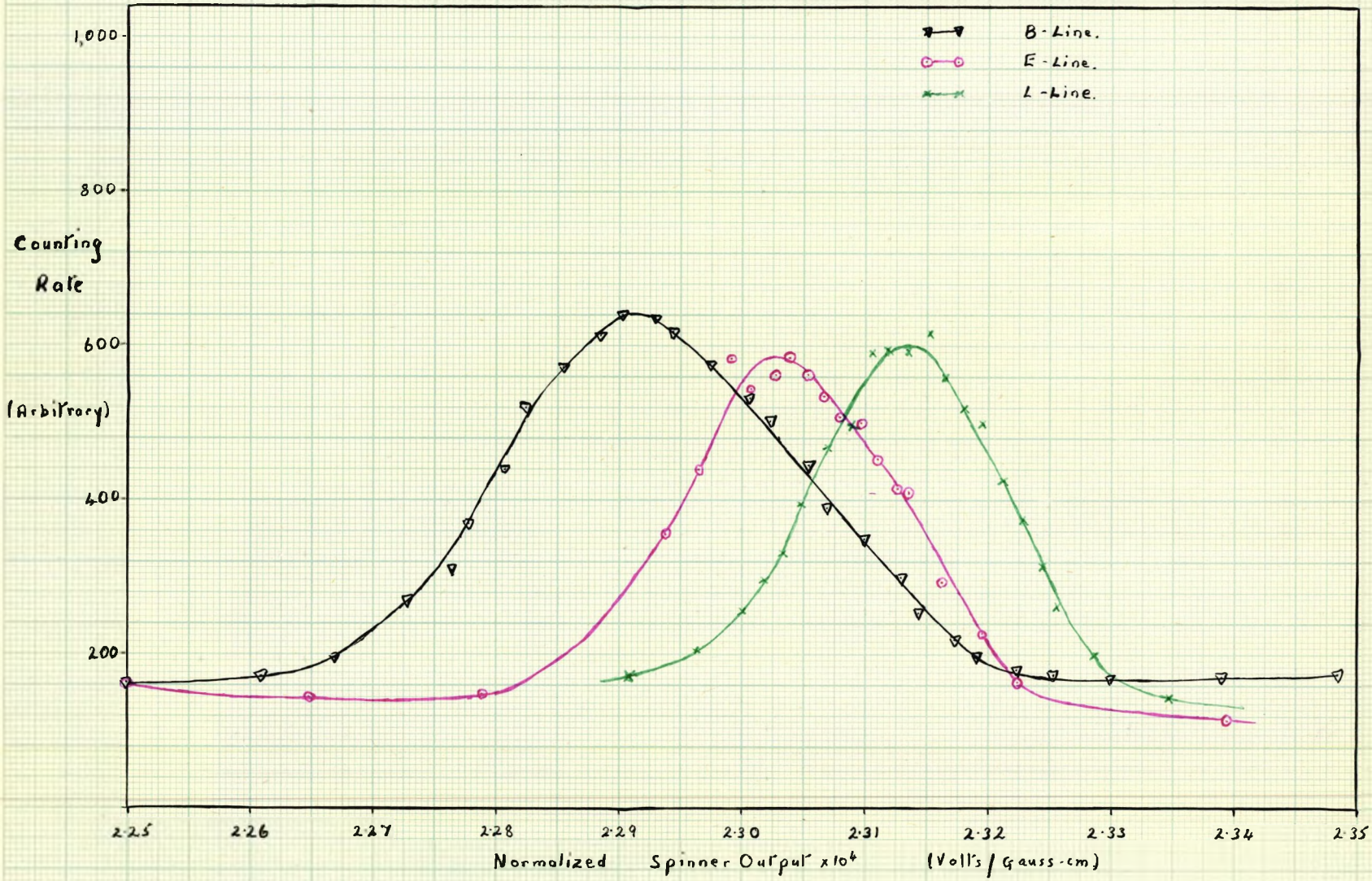

FIG. 4.2

The Positions of Three β-lines when the Spectrometer is set on Branch I of a 30 Amp. Hysteresis Cycle.

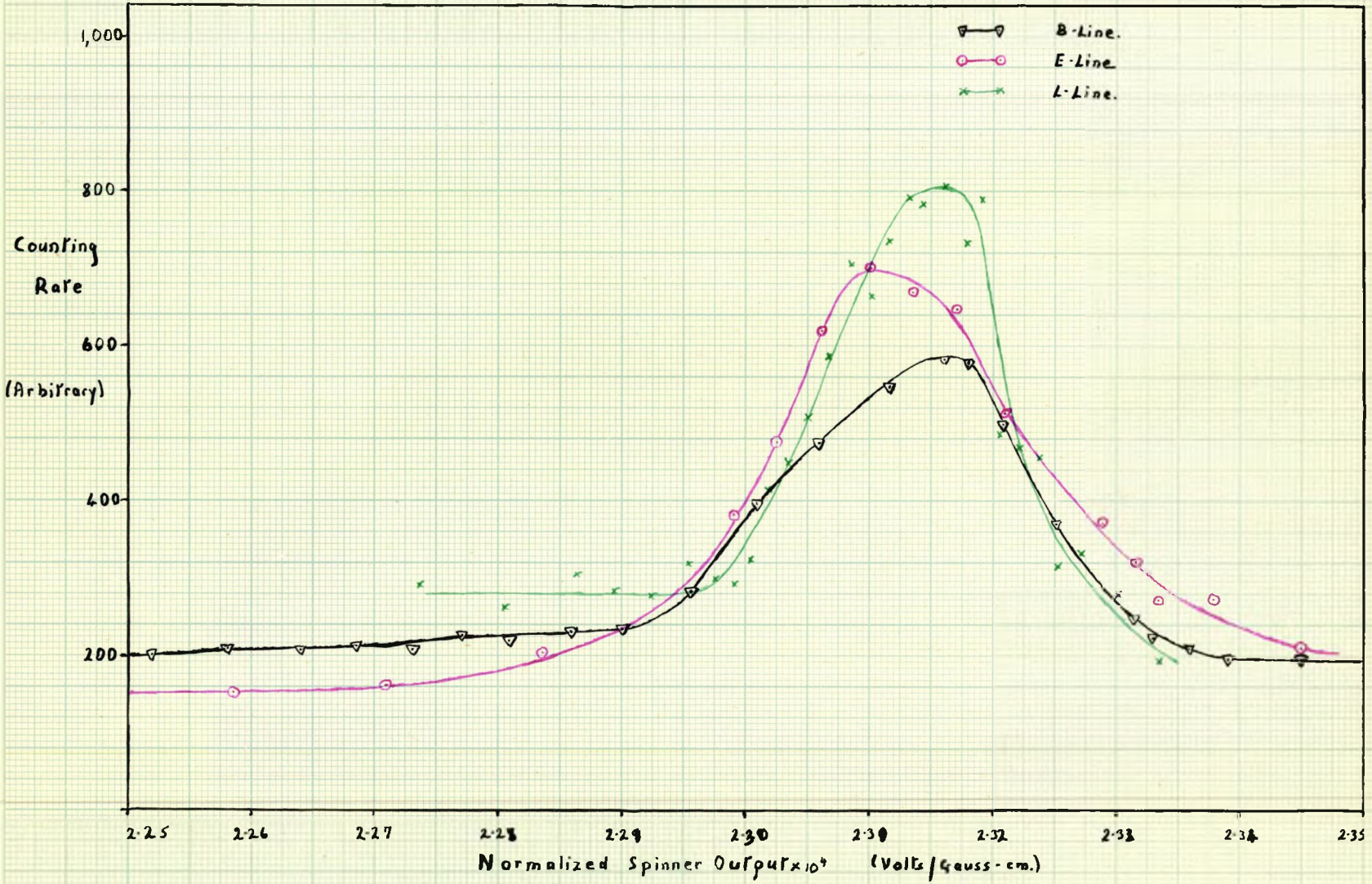

FIG. 4.3

The Positions of the same β-lines as those in Fig. 4.2 with the Spectrometer set on the Initial Magnetization Curve.

different way to see what effect the setting of the field had on the performance of the spectrometer. Hedgran et al. (11) and Stoker et al. (18) using similar spectrometers both used the initial magnetization curve so I decided to try the same method. Having carefully de-magnetized the magnet, a fresh source of Thorium active deposit was placed in the spectrometer and the B-, E- and L- lines were measured in that order (that of ascending field strength). The spectrometer was then de-magnetized again and a 30 amp hysteresis cycle was established. The same lines were measured using the same source so that a direct comparison could be made between the two sets of results. The results of this experiment are set out in table 4.4 and the lines are shown in figs. 4.2 and 4.3.

Although the resolution was only slightly better when the spectrometer was used on the initial magnetization curve, the output of the spinning coil was proportional to the momentum. When the spectrometer was set on the initial magnetization curve, there was still a broadening of the B- and E- lines compared with the L- line, indicating that the field shape still altered but to a lesser extent than when Branch 1 of a hysteresis cycle was used.

Some measurements showing the behaviour of the spectrometer operated at high resolution, are given in table 4.5 and the line profiles of the B- and F- lines obtained when the spectrometer was set on the initial magnetization curve shown in figs. 4.5 and 4.6. Once again there is a broadening of the lines at low momenta. The

Spectrometer set on Branch I of a 30 Amp. Hysteresis Cycle. Source:- 1 mm. x 1 cm. high; Slit:- 1 mm. wide; Transmission:- 0.1%. Predicted Base Resolution:- 0.4%.		
Line	Momentum B ρ (Gauss-cm.)	Resolution at half-height (%)
B	652.4	0.21%
F	1,388.4	0.13%
I	1,753.9	0.14%
L	2,607.2	0.11%

TABLE 4.5. Resolution of a Narrow Source of ThB with Low Transmission.

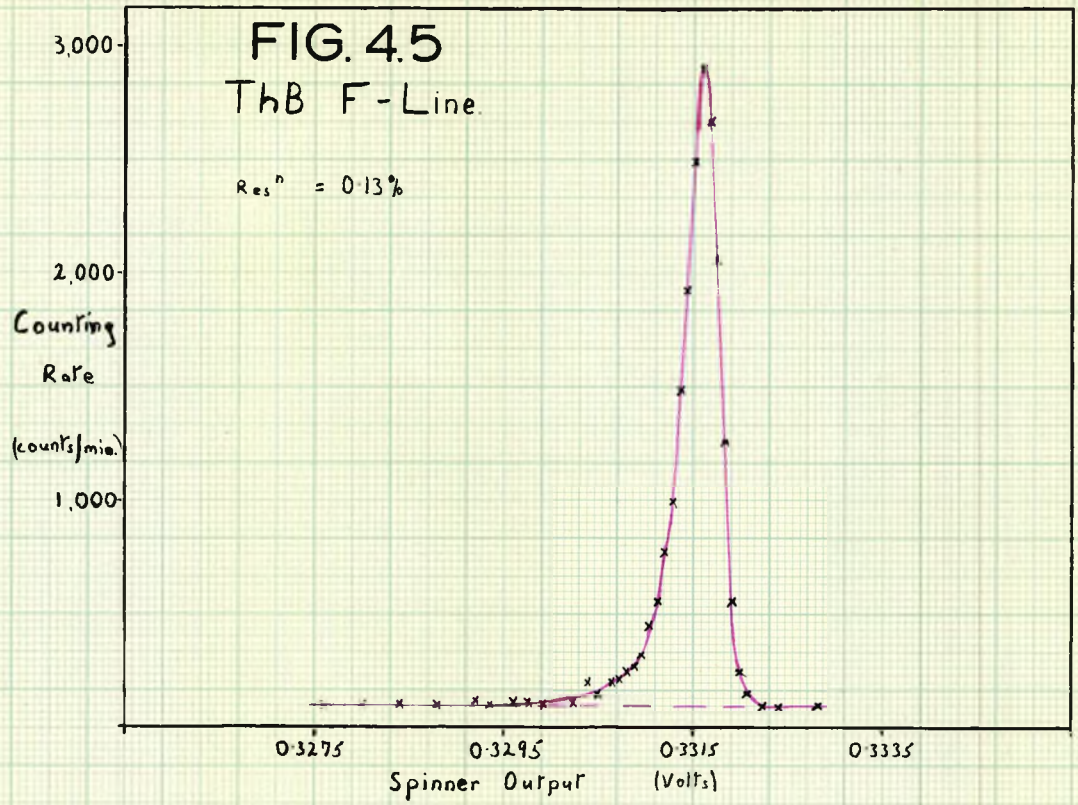

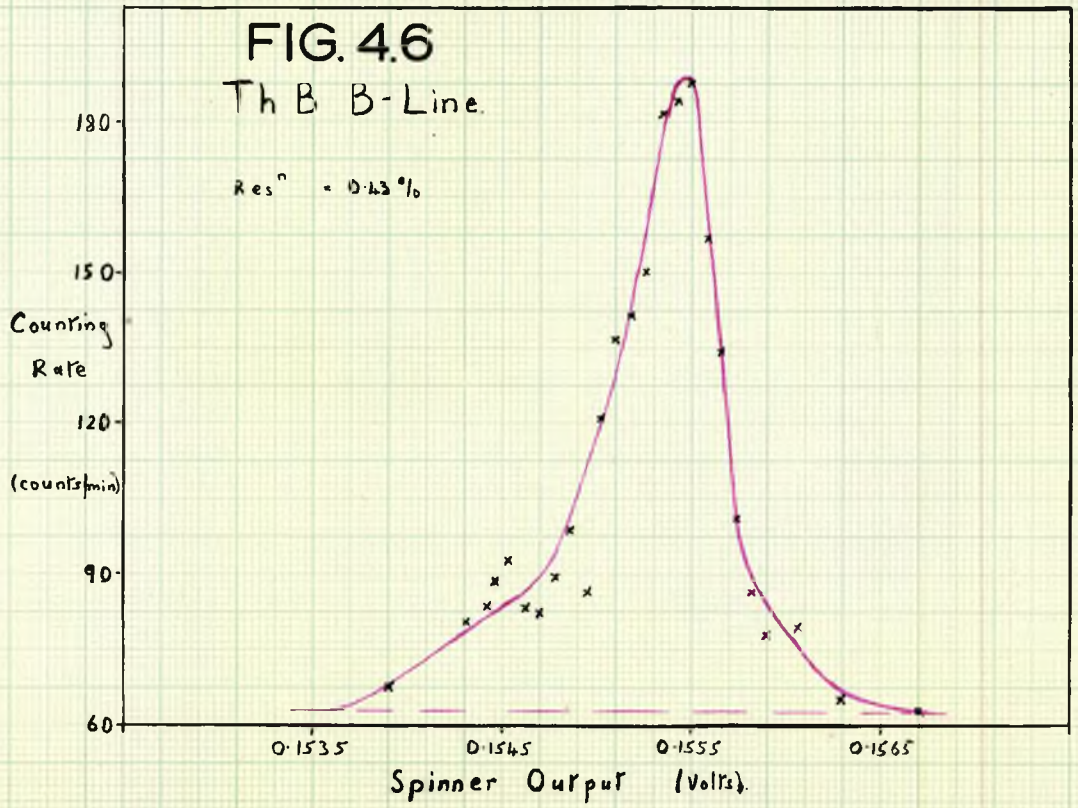

FIGS. 4.5 & 4.6 Line Profiles at High Resolution.

difference in the resolutions obtained when the field was set on the initial magnetization curve and when it was set on Branch I of a hysteresis cycle may be explained if the field shape changes. If the field shape changes, there will be astigmatism in the image and the focus will alter causing the resolution to alter also. If the field shape is not the same when the field is set by different methods the resolutions of the same lines will be different. Thus, depending on the position of the focal plane, the changes in resolution using different methods to set the field may be entirely different.

Bergkvist (53) suggested that if the field shape altered, the transmission should alter, so that, if the field were to be set by different methods the counting rates should depend upon the way in which the field was set. Using a source of Y-91, the field was set using the initial magnetization curve and also using Branch I of a 30 amp hysteresis cycle. A small difference in the counting rates was observed at energies below 160 KeV. The low energy ends of the Kurie plots of two such runs are shown in fig. 4.7. Since below 200 KeV the window of the counter tube absorbed some of the β-rays, a correction would have to be made to the spectrum below this energy. The correction for the change in transmission could then be included with the correction for the absorption in the window in a single correction factor which would have to be determined experimentally.

2. The Change in the Field Shape.

The consequences of a change in field shape were discussed

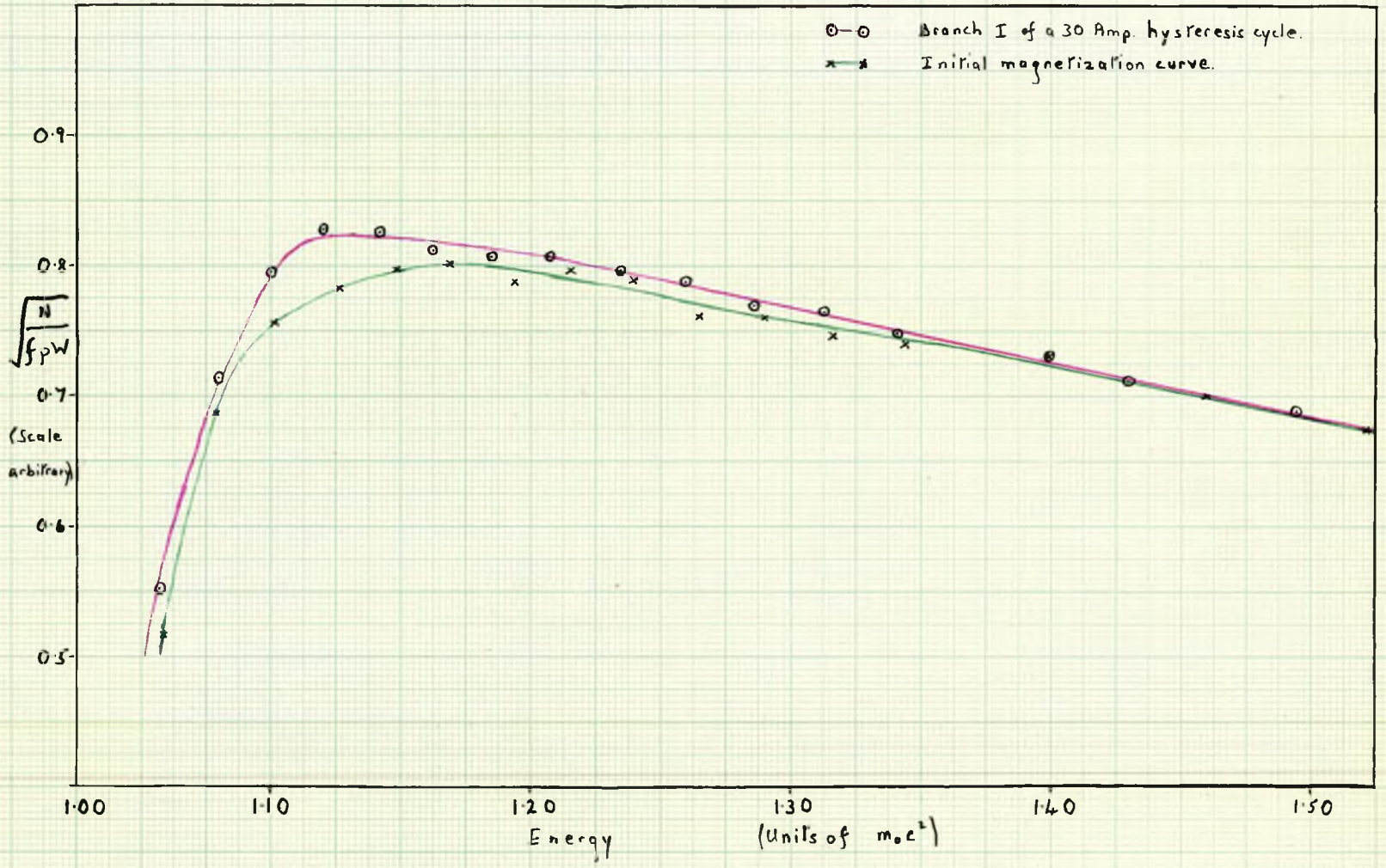

FIG. 4.7 The Dependence of the Counting Rate on the Method used to set the Field.

by Bergkvist in a recent paper. This paper although mainly theoretical concluded with some results verifying a change in the field shape in the spectrometer at Uppsala. He started with some equations given in a paper by Svartholm (16) but ended with a very complicated expression for the change in field shape. To measure the change in field shape, he derived an expression for the dispersion and another for the dependence of the image position on the change $\delta\alpha_1$, in the parameter α_1, he then equated the two equations and solved for $\delta\alpha_1$. The dependence on the parameter $\delta\alpha_2$ cannot be derived without developing further the original equations of Svartholm.

I attempted to derive a simpler formula for the change $\delta\alpha_1$, but arrived at the expression for the dispersion except that I disagreed with Bergkvist's expression over the sign of a small order term. Following the notation of Svartholm except for a change from α_1 to $\alpha_1+\delta\alpha_1$ which was the notation used by Bergkvist to describe the change in the parameter α_1, the formula for the dispersion is :-

$$\rho^* = \delta\left[\frac{2}{\lambda_r}\left(1 - \frac{\delta\alpha_1}{\lambda_r}\right) + \frac{\pi\beta\cos\theta}{2\lambda_r}\left(1 - \frac{\delta\alpha_1}{2\lambda_r}\right)\right] \qquad (4.4)$$

ρ^* is the image displacement $\frac{\Delta r}{r_0}$ for a change $\delta.p = p - p_0$ in the momentum, $\lambda_r = 1 + \alpha_1$ and $\beta\cos\theta$ is the angle of emission in the radial plane, that is ϕ_r, in Chapter I and part I of this chapter. Bergkvist obtained $+\frac{\delta\alpha_1}{2\lambda_r}$ for the last term in this expression. I believe that this difference, which will change the dispersion by

less than $\frac{1}{4}$, arises from a difference in the point at which small order terms were neglected. For double focussing, $\alpha_1 = -\frac{1}{2}$ and $\delta\alpha_1 = 0$ then

$$\rho^* = \delta\left[4 + \frac{\pi\gamma\cos\theta}{\sqrt{2}}\right] \tag{4.5}$$

If $\gamma\cos\theta$ is small $\rho^* = 4\delta$, which is the same expression as (1.8).

Equation (4.4) was the basis on which an experiment was designed to measure the change in the field shape of the spectrometer. In order to compare the results with those obtained by Berglvist, the changes in the field shape were also calculated by his method. He related the difference in the field required to focus rays taking different paths in the spectrometer to the displacement in the image positions due to the change in the shape of the field. This change is given by the formula:-

$$\rho^{(1)} = -\frac{\gamma\cos\theta}{2\sqrt{\lambda_r^3}}\,\pi\,\delta\bar{\alpha}_1\left[1-\delta\bar{\alpha}_1\right] + \frac{\gamma^2\cos^2\theta}{3\lambda_r}\left[1-\frac{\delta\bar{\alpha}_1}{\lambda_r}\right] - \frac{4\gamma^2\cos^2\theta}{3\lambda_r^2}\left[\frac{1}{2}+\frac{3}{2}\alpha_1+\alpha_2\right]\left\{1+2\frac{\delta\bar{\alpha}_1}{\lambda_r}\right\}^2 \tag{4.6}$$

$\rho^{(1)}$ is the displacement of the image in the focal plane. To determine the value of $\delta\bar{\alpha}_1$ it is necessary to equate $\rho^{(1)}$ to ρ^* and to solve for $\delta\bar{\alpha}_1$. To calculate the dispersion and the image displacement, it is necessary to know the angles of emission of the rays taking different paths in the spectrometer. These were calculated using the equation:-

$$\rho = \frac{\gamma\cos\theta}{\sqrt{\lambda_r}}\sin\Omega\sqrt{\lambda_r} + \frac{\gamma^2\cos^2\theta}{2\lambda_r^2}\left(1-\cos\Omega\sqrt{\lambda_r}\right)f_{11} + \frac{\gamma^2\cos^2\theta}{6\lambda_r}\left(\frac{f_0}{\lambda_r}-1\right)\left(\cos 2\Omega\sqrt{\lambda_r}-\cos\Omega\sqrt{\lambda_r}\right) \tag{4.7}$$

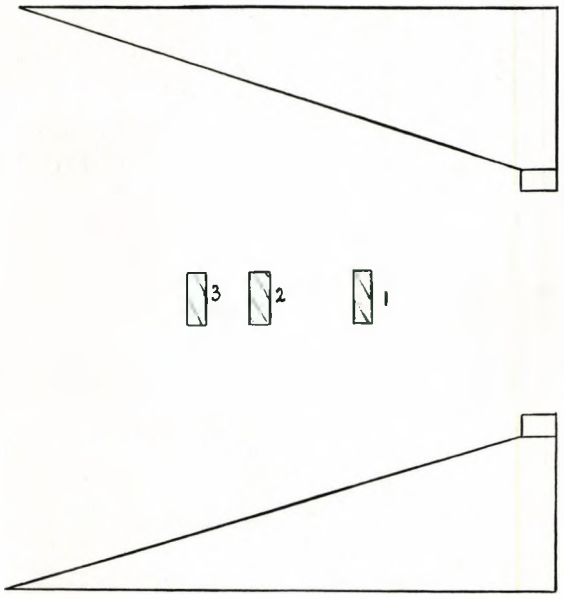

FIG. 4.8 The Three Positions of the Aperture used in the Measurements on the Changes in Field Shape.

$f_{11} = -\frac{1}{2} - \frac{3}{2}\alpha_1 - \alpha_2, \Omega$ is the angle between the leading shadow and the source and is the ratio of the radial position of the shadow to the mean radius. By substituting for α_1, α_2, Ω, $r_{min.}$ and $r_{max.}$ $\rho \cos\theta$ in the expression for the $\delta\alpha_1$ between the mean trajectory and chosen trajectory whereas by my method, both the mean value and the actual value of the change can be measured for any chosen trajectory. It is thus possible to gain much more information by my method than by that of Terghvist. These methods are not the only methods used to measure the change in field shape, they are complementary to the method used by Barry, who measured the changes in the astigmatism of the spectrometer.

I decided to measure α_1 for three different trajectories in the spectrometer, for the mean radius and for the two extreme trajectories in the plane of symmetry, for which $Z = 0$. To measure the dispersion, a narrow source of Thorium active deposit 1 mm. wide by 1 cm. long was used to give good resolution. A double slit - slit widths 1 mm. separation 9 mm. - was placed in the focal plane and the change in field strength required to focus a line at each slit in turn was measured. Knowing Δr and ΔB (r_0 being constant) the dispersion could be calculated and from that the value of α_1. When α_1 had been calculated for one field strength, using equation (4.4), this value was substituted back in equation (4.4) to evaluate $\delta\alpha_1$ for a different field strength.

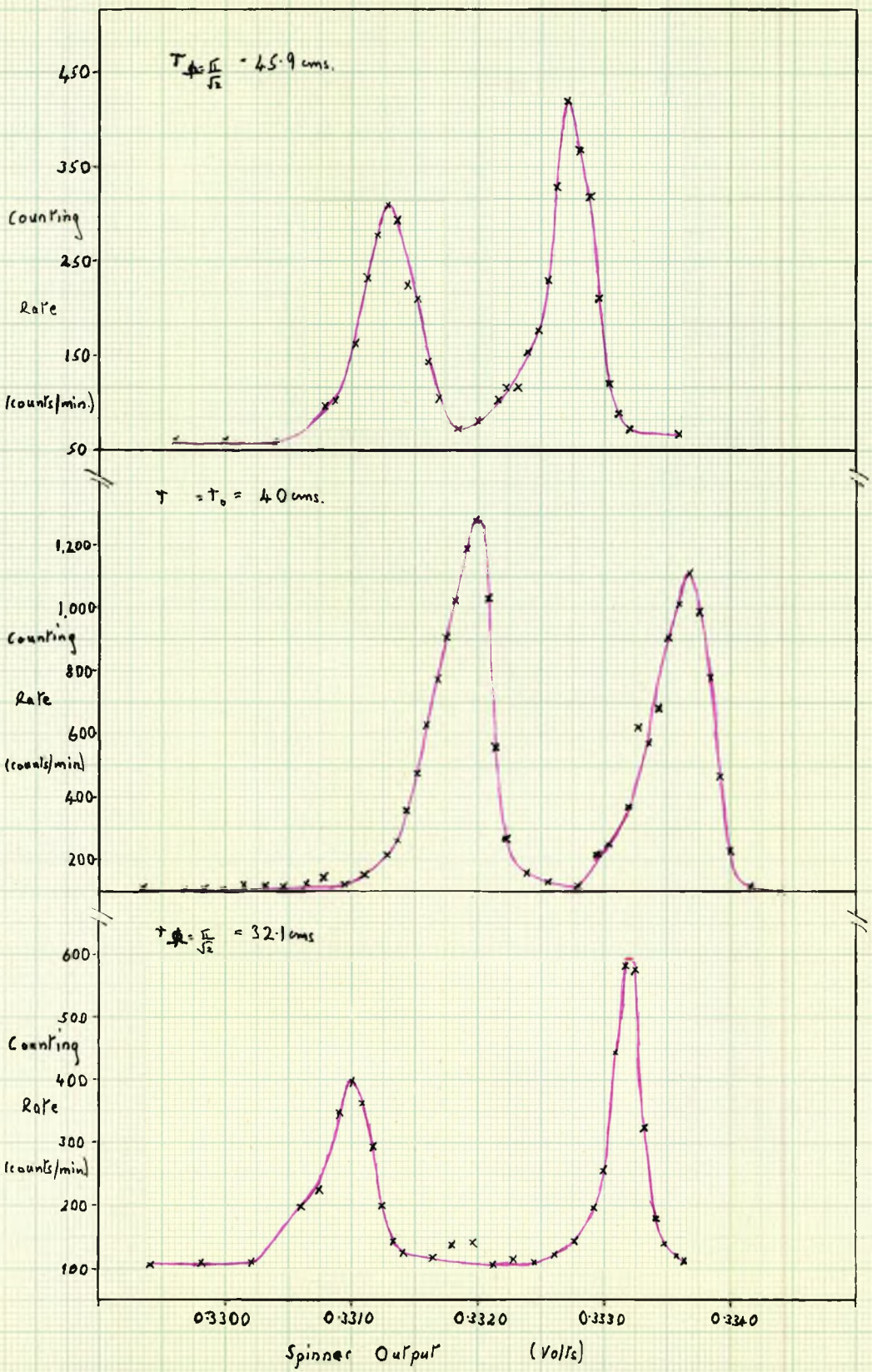

FIG. 4.9 The Dispersions for the Three Positions of the Aperture.

The sources could not be positioned with sufficient accuracy to make measurements on the position of the image on successive runs so the following method was adopted to measure the image positions from one source using the three different trajectories. The trajectories were defined by shutter, S_1, which was stopped down by two aluminium sheets chosen to give a radial width of 2 cms. These sheets were placed in a groove behind the shutters defining the vertical height and could be moved across the shutter by two strings attached to a rod sliding through a Wilson seal in window 3. The position of the aperture could thus be controlled and was set at positions 1, 2 and 3 in Fig. 4.8. in that order. The vertical extent of the aperture was 2.5 cms giving a transmission of 0.1% of a sphere.

The measurements on the changes in the field shape were made at four energies, those corresponding to the B-, F-, I- and L-lines of Thorium active deposit. No other lines were strong enough to be measured easily. Fig. 4.9 shows the dispersion of the F-line for the three trajectories round the spectrometer.

The first step in the calculations was the evaluation of α_1, using equation (4.4), from the dispersion of the central rays for which $\chi_0 \cos\theta = 0$. The value for the L-line was calculated on the assumption that $\delta\alpha_1 = 0$, then using the value derived for α_1, the values of $\delta\alpha_1$ were calculated for the other three lines. The values of $\delta\alpha_1$ and α_1 are set out in table 4.6 for the two methods used to produce the field in the spectrometer.

Source:- 1 mm. x 1 cm. high; Slit:- two slits 1 mm. wide, 9 mm. apart; Transmission:- 0.1%.					
Line	Momentum $B\rho$ (Gauss - cm)	Spectrometer set on Branch I of a 30 Amp. Hysteresis Cycle		Spectrometer set using the Initial Magnetization Curve	
		$\delta\alpha_1$	α_1	$\delta\alpha_1$	α_1
B	652.4	-0.051	-0.57 (7)	-0.053	-0.54 (4)
F	1,338.4	-0.013	-0.53 (9)	-0.025	-0.51 (6)
I	1,753.9	-0.013	-0.53 (9)	-0.010	-0.50 (1)
L	2,607.2	0	-0.52 (6)	0	-0.49 (1)

TABLE 4.6. Change of α_1 for the central rays ($\phi_r = 0$)

Spectrometer set on Branch I of a 30 Amp. Hysteresis Loop			
Line	Momentum, $B\rho$ (Gauss-cm.)	$r_{(max)}$	$r_{(min)}$
B	652.4	0.169	- 0.300
F	1,388.4	0.191	- 0.312
I	1,753.9	0.191	- 0.312
L	2,607.2	0.195	- 0.315

TABLE 1.7. Radius of Curvature.

The angles of emission ϕ_{max} and ϕ_{min} were then calculated using equation (4.7), assuming the values obtained by the above method for α_1. When the values of $\alpha_1 + \delta\alpha_1$ had been calculated for the non-central trajectories these angles of emission were re-calculated. Only in the case of the B-line was the value of angle ϕ_{max} altered appreciably and then it was by 10%. This change in the angle resulted in a change of about 6% in $\delta\alpha_1$. The values of the angles at the energies of the four lines are set out in table 4.7.

The change in $\delta\alpha_1$ for the non-central trajectories was calculated in two ways. The first way was to use the value of α_1 in table 4.6 and substitute this in equation (4.4) and calculate the value of $\delta\alpha_1$. The second method was to use the value of α_1 for the central trajectory of the L-line and calculate the difference $\delta\alpha_1$ from this value of α_1. The two methods gave results for $\alpha_1 + \delta\alpha_1$ which agreed to better than 2%. The values for $\delta\alpha_1$ and $\alpha_1 + \delta\alpha_1$ are set out in table 4.8 for the two methods used to set the field.

The mean changes $\bar{\delta\alpha_1}$ for the non-central trajectories were calculated by equation (4.4) to equation (4.6) and the results are given in table 4.9 for the case when the field was set on Branch I of a 30 amp hysteresis cycle. Comparing these values with those in table 4.8, $\bar{\delta\alpha_1} \approx \frac{\delta\alpha_1}{4}$. These values for $\bar{\delta\alpha_1}$ are comparable with those quoted by Bergkvist.

Since this study was made to obtain a qualitative account of the nature of the changes in the field shape, no attempt was made to

Line	Momentum $B\rho$ (Gauss-cm)	Spectrometer					
		Set on Branch I of a 30 Amp. Hysteresis Cycle			Set using the Initial Magnetization Curve		
		r = 31.1 cms.	r_o = 40 cms.	r = 45.9 cms.	r = 31.1 cms.	r_o = 40 cms.	r = 45.9 cms.
B	652.4	- 0.55 (5)	- 0.57 (7)	- 0.70 (3)	- 0.56 (6)	- 0.54 (4)	- 0.60 (9)
F	1,388.4	- 0.50 (6)	- 0.59 (9)	- 0.59 (3)	- 0.49 (9)	-0.51 (6)	- 0.54 (0)
I	1,753.9	- 0.50 (3)	- 0.53 (9)	- 0.59 (4)	- 0.51 (0)	- 0.50 (1)	- 0.54 (4)
L	2,607.2	- 0.52 (6)	- 0.52 (6)	- 0.56 (6)		- 0.49 (1)	

TABLE 4.8. Changes in the Parameter α with Changes in Field Strength and Method of Setting the Spectrometer.

Spectrometer set on Branch I of a 30 Amp. Hysteresis Cycle			
Line	Momentum $B\rho$ (Gauss-cm.)	r = 31.1 cms.	r = 45.9 cms.
B	652.4	- 0.57 (1)	- 0.60 (7)
F	1,388.4	- 0.53 (4)	-.0.55 (0)
I	1,753.9	- 0.53 (5)	- 0.55 (1)
L	2,607.2	- 0.52 (3)	- 0.52 (3)

TABLE 4.9. Values of α, based on the Mean Change, $\delta\alpha_1$ in the Parameter α_1.

estimate the errors. It was felt that because of the number of approximations in the theory the figures themselves could not be an exact expression of what was happening but that viewed as a whole, they were an indication of the behaviour of the spectrometer.

Comparing the results for $\alpha_1 + \delta\alpha_1$, when the field was set at different points on Branch I of a hysteresis cycle (table 4.8) the value of changes most at low energies. The results for $\alpha_1 + \delta\alpha_1$ when the spectrometer is set on the initial magnetization curve are closer to the theoretical value for α_1 of - 0.500 but they still increase at low energies, although not quite as markedly as they do when Branch I of a hysteresis cycle is used. From these results is was verified that the field shape changed as the energy of the focussed rays increased and that this change in field shape affected the resolution and the transmission at low energies. Since a correction for the change in transmission could always be made, it was concluded that the spectrometer behaved reliably.

CHAPTER V.

The Beta-spectrum of Yttrium-91 and the Internal Conversion Spectrum of Cerium-144.

1. The Beta-spectrum of Yttrium-91.

The β-spectrum of Y-91 was chosen because it had already been measured and was well known. A measurement of the spectrum would confirm that the spectrometer was behaving correctly over the whole energy range of the spectrum besides yielding a fresh determination of its maximum energy.

Y-91 was the first isotope to be identified belonging to the class of unique first forbidden transitions (54). This type of transition has a simple shape factor which, at the time the spectrum was measured, could only be calculated approximately. The shape factor, when applied to the results, yielded a linear Kurie plot. Other reports (55), (56), agree with this interpretation although Agnew (57) also stated that a unique second forbidden shape factor yielded a durie plot which was linear except at the high energy end. Since then, Rose et al. (58) have published a set of tables which allows the shape factor to be calculated exactly.

The energy spectrum of a forbidden β-transition may be written:-

$$N(W)\,dW = \left(g^2/2\pi^3\right) F(Z,W)\, p\, W\, (W_0 - W)^2\, S \qquad (5.1)$$

where:- N(W)dW is the number of rays in the energy interval W to W + dW, g is a coupling factor, F(Z,W) is a term allowing for the Coulomb effect due to the charge of the nucleus, p and W are the momentum and energy, respectively, of the β-ray and S is a shape factor.

A more convenient way of presenting the data is in the form of a Kurie plot. In this, the function $\sqrt{N/FpW}$ is plotted against the energy. While, for an allowed transition, the Kurie plot should be linear, there is no reason why it should be necessarily so in the case of a forbidden transition. The shape factor for a first forbidden transition may be written as the sum of two partial shape factors,

$$S_1 = S_1^{(1)} + S_1^{(2)} \qquad (5.2)$$

$S_1^{(1)}, S_1^{(2)}$ are the partial shape factors corresponding to spin changes in the nucleus of one and two units of angular momentum respectively. Whilst the shape factor $S_1^{(2)}$ may contribute to the total shape factor when the spin changes by only one unit of angular momentum, it is not possible for the shape factor $S_1^{(1)}$ to contribute to the total shape factor when the spin change is two units of angular momentum. The shape factor is thus unique when the spin changes by two units of angular momentum and the transition is known as a unique first for bidden transition. Similarly, there are unique second, third, fourth, etc., transitions.

The shape factor for a unique first forbidden transition arises from either tensor or axial-vector coupling between the initial and final states of the nucleus and may be written:-

$$S_1^{(1)} = \left\{ (W_0 - W)^2 L_0 + 9 L_1 \right\} \left(1 + \frac{b}{W}\right) \qquad (5.3)$$

and Uhlenbeck (59),

L_0, L_1 are radial wave functions, first used by Konopinski, (W_0-W) is the momentum of the neutrons (in units of m_0c^2), L_0 and L_1 have now been tabulated by Rose et al.(58). The term $(1 + \frac{b}{W})$ is a Fierz interference term (69) which is included to allow for a possible interaction between the tensor and axial-vector types of coupling.

An approximate expression for the shape factor may be written:-

$$S_1^{(2)} = \{(W_0-W)^2 + (W^2-1)\} \qquad (5.4)$$

If the function $N/FS_1^{(2)}, pW$ is plotted against energy, the graph should be a straight line provided that b = 0. This is known as a modified Kurie plot. A more sensitive way of plotting the result is to plot the function $N/FS_1^{(2)}, pW(W_0-W^2)$ against energy. This function should be constant, again provided that b = 0, hence any small deviations show up more easily than in the modified Kurie plot.

Experimental Procedure.

The sources used were less than 70 micrograms per cm^2. thick and were mounted on backings with thicknesses less than 40 micrograms per cm^2. thick. The maximum transmission was 1.5% of a sphere and the momentum resolution was better than 1% for a β-line from a source with a size of 1 cm^2. and a slit width of 1 cm.

To ensure that any errors would be minimised, the spectrum was measured under a variety of conditions. The transmission was altered to change the counting rate so that, if for any reason,

the counting losses were greater than calculated from a measurement of the paralysis time of the scaler, there would be a discrepancy between the results for different counting rates. The best fit was given when the paralysis time was 300 microsecs. which was the measured value. The peak counting rate was varied between 6,500 counts/min. and 13,000 counts/min., the corrections for scaling losses at these counting rates were 3% and 6% respectively.

The field was set both on Branch I of a 30 Amp. hysteresis cycle and on the initial magnetization curve. Above 160 Kev both methods yielded the same results. The spectrometer was calibrated by measuring the momenta of the B-, E-, G- and L-lines of a Thorium active deposit using sources with identical dimensions to those of the Y-91 sources. The centroid of the β-lines was chosen as the reference point for the calibration of the momenta as discussed in chapter III.

The background counting rate, due to cosmic rays, scatter from the walls of the spectrometer and spurious pulses from the G-M tubes increased from 15 counts/min. at low fields to 45 counts/min. above the maximum energy of the β-rays. The increase was assumed to be linear. This background counting rate was only a fraction of the peak counting rate and the corrections applied for it yielded consistent results despite the variations in the peak counting rate.

The statistical accuracy was kept within either 0.5% or 1.0% for the highest counting rates, but for a few points near the ends

of the spectrum the counting rates were so low that it was impossible to obtain such accuracy.

Once the counting rate had been corrected for scaling losses and background, a correction was made for the decay of the source. The half-life of Y-91 is 57.5 days (61) the maximum correction which had to be applied was 1.0%. Because the momentum interval accepted by the focussing slit is proportional to the momentum, the counting rate must be divided by the momentum to give the true particle distribution as a function of momentum.

The values for the Coulomb Factor were taken from a set of tables compiled by Fano (62). These values had to be modified slightly because of the screening effect of the electrons in the atomic shells. Again, the values were taken from Fano's tables, but they were also compared with those of Reitz (63) with which they agreed well. Corrections for the finite nuclear size (64) and the de Broglie wave-length (65) were considered, but both were found to be less than 0.1%.

The Kurie-plot of Y-91 is shown in fig. 5.1. together with the modified Kurie-plot. The Kurie-plot was extrapolated to determine the maximum energy of the spectrum. The shape factors could than be calculated and applied to the experimental data. A straight line was obtained with the exact expression for the shape factor, as shown in Fig. 5.1., but the plot was definitely non-linear when the approximate expression for the shape factor was used.

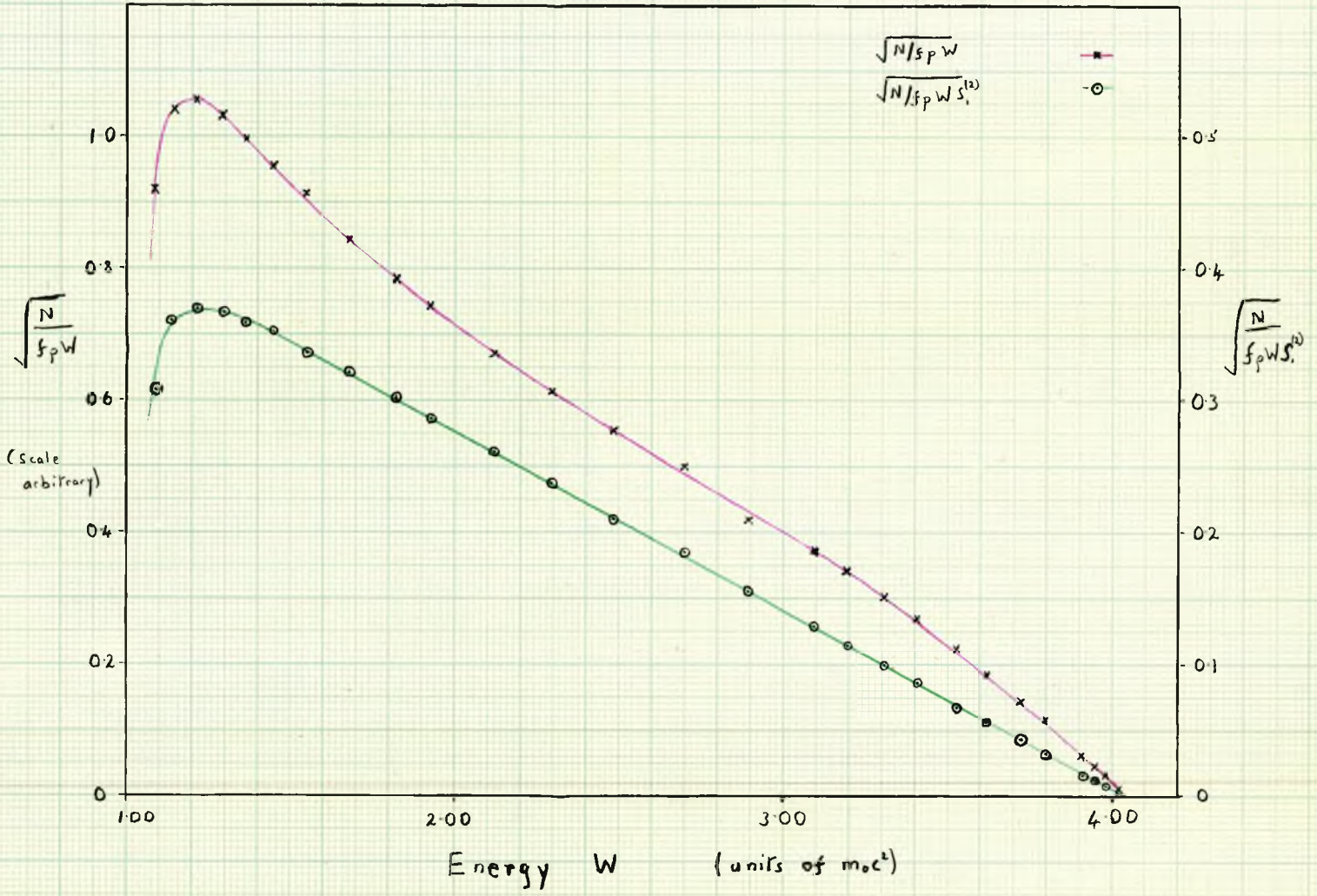

FIG. 5.1 The Kurie Plot of Y-91 and the modified Kurie Plot including the Shape Factor $S_1^{(2)} = (W_0 - W)^2 L_0 + 9L_1$

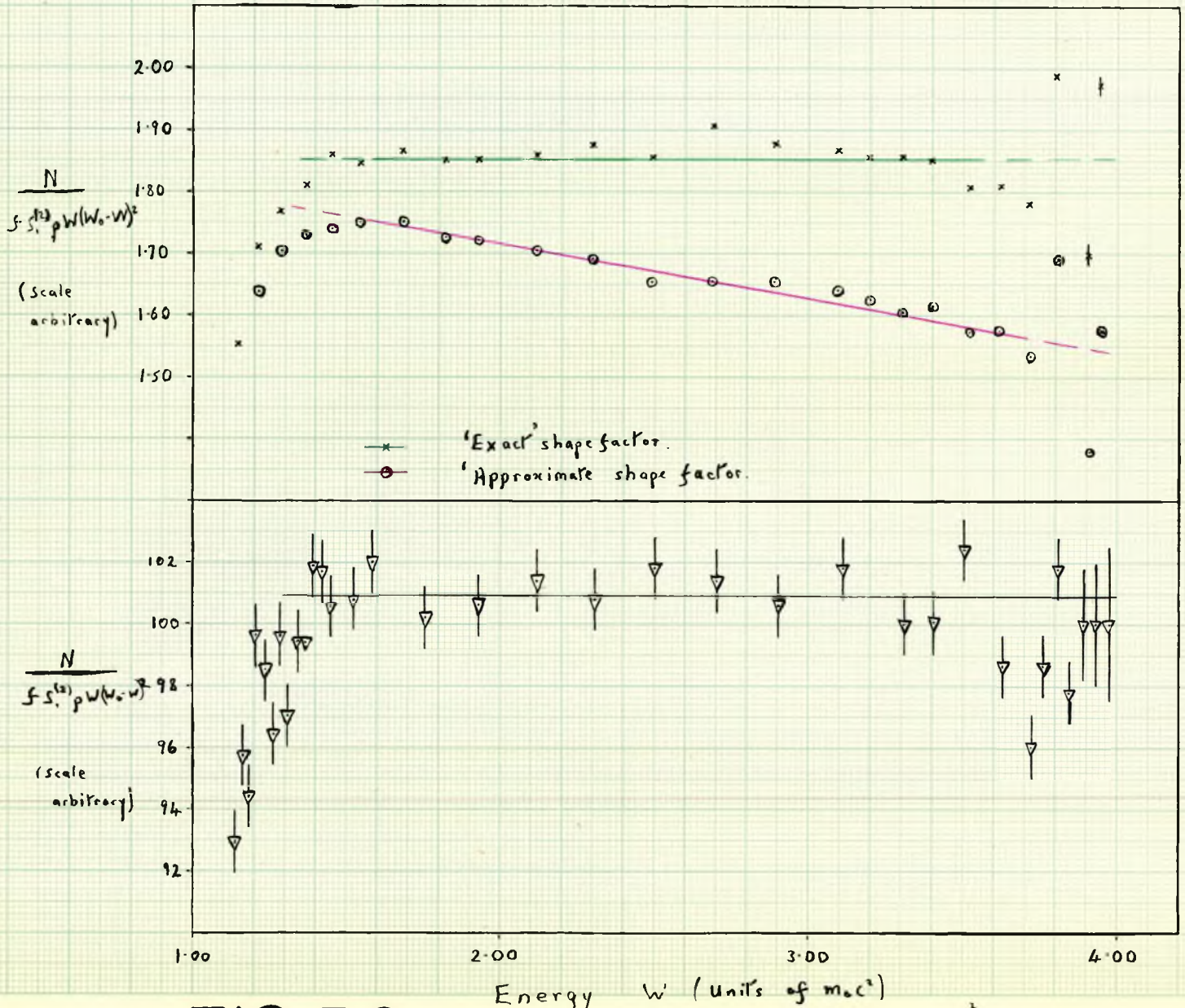

FIG. 5.2 Two Plots of the Function $N/fS_1^{(2)}W(W_0-W)^2$ against Energy W.

Fig. 5.2 shows two graphs of the function $N/FS_1^{(2)}pW(W_o-W)^2$ against energy, W. With the exact expression for the shape factor, this function was found to be constant from W = 1.400 to W = 4.000 (0.200 Mev to 1.500 Mev), whereas with the approximate expression for the shape factor, there was an 11% decrease over this energy range. A similar plot was made using the unique second forbidden shape factor and was found to resemble closely the plot in which the approximate shape factor was used, thus ruling out this interpretation.

Since measurements, by Barry (23), on the β-spectrum of Phosphorous-32 agree with the latest reported results (66) it was concluded that the spectrometer was functioning correctly.

The maximum energy of the β-spectrum of Y-91 was determined to be 1.547 $\pm$ 5 Mev. From the plot of $N/FS^{(2)},pW(W_o-W)^2$ against W the limits on the interference term, b, were determined to be $-0.03 < b < 0.05$.

Y-91 has been reported to decay by β-emission with maximum energy of 0.330 Mev and with a frequency of 0.2% of the decays. This β-ray is followed by a γ-ray with an energy of about 1.200 Mev. (61), (67) and (68). Using a 3 millicurie source and a resolution of about 0.2% a search was made for internal conversion electrons, photo-electrons and Compton-electrons between 1.100 Mev and 1.250 Mev. No peaks could be found which corresponded to any of these phenomena. The limit placed on the frequency of internal conversion was 3 conversion electrons per 10^7 disintegrations.

2. The Internal Conversion Spectrum of Cerium-144.

The internal conversion spectrum of Ce-144 was first brought to mind when the measurements of the change in field shape were being made. Because of the low transmission, a fresh source of Thorium active deposit had to be prepared each day. A search was made for an isotope with a long half-life having also several low energy internal conversion lines which could be used instead of those from the Thorium active deposit. Ce-144 was one of the few isotopes, readily available, which decayed by β-emission followed by several low energy γ-transitions. The energy of the most energetic internal conversion lines is 132 Kev which is lower than the value which was desired (about 250 Kev). Ce-144 was not used in the measurements on the changes in the field shape, however, because it was found that the reported energies and intensities of the internal conversion lines differed widely. Since the lines from Thorium active deposit were known accurately and could be found very quickly, sources of Thorium active deposit were used despite the inconvenience of having to prepare new sources. I decided to study some of the internal conversion lines of the ce-144 spectrum in order to establish the nature of the transitions and to clarify the decay scheme.

There is some agreement that there are γ-transitions with energies of 134 Kev, 80 Kev, 53 Kev, 41 Kev and 34 Kev. The strongest transition, the 134 Kev transition is an M1 transition (69) to (78) although Kelly (70) suggested that it was an E2 transition. The 80 Kev transition is the second strongest transition, but opinion was

divided over its nature. Porter and Cook (72) and Emmerich, Auth and Kurbatov (73) concluded from the α_K/α_L ratio that it was a M2 transition. Cork, Brice and Schmid (75) from a measurement of both the α_K/α_L ratio and the $\alpha_{L_I}/\alpha_{L_{III}}$ ratio reached the same conclusion. On the other hand, Pullman and Axel (76) from the α_K/α_L ratio and from a measurement of the value of α_K suggested that this transition was a M1 transition. This interpretation has been supported by Hickock, McKinley and Fultz (77) who measured the value of α_K and by Freeman (78) who measured both α_K and the α_K/α_L ratio.

Only Hickock et al. attempted to identify the nature of the 53 Kev transition. From their measurements of the value of α_K the transition should have been an E1 transition but this interpretation conflicted with their measurements on the coincidence spectra. No attempt to identify the nature of either the 34 Kev or the 41 Kev transition has been made.

Three γ-transitions with energies of 145 Kev (75), 231 Kev (71) and 46.8 Kev (69) have been reported only once while Freeman (78), recently, has reported two more weak transitions with energies of 66 Kev and 86 Kev. Three more transitions with energies of 60 Kev, 95 Kev and 100 Kev have been reported by more than one group. These three transitions arise from different interpretations of two groups of internal conversion lines, one at 52 Kev and the other at 58 Kev. Keller et al, Emmerich et al and Cork et al, interpret the group of lines at 52 Kev as the K-shell conversion line of a 95 Kev γ-ray

and the L-shell conversion lines of a 59 Kev γ-ray. The group of lines at 58 Kev is interpreted as the combination of the K-shell line of a 100 Kev γ-ray and the M-shell lines of the 59 Mev transition by Keller et. al., Emmerich et. al, Porter et. al. and Pullman et. al.

The measurements on the coincidence spectra conflict. Hickock et. al. and Pullman et. al. found that the 53 Kev and the 80 Kev γ-rays were in coincidence. Freeman detected coincidences between the 80 Kev γ-ray and the internal conversion lines of the 53 Kev transition. Pullman et. al. also detected coincidences between the 34 Kev γ-ray and the 100 Kev γ-ray. Cork et al, on the other hand, detected coincidences between the 134 Kev transition and the 34 Kev, and 41 Kev transitions, while Freeman detected coincidences between the 134 Kev γ-ray and the L-shell conversion lines of the 34 Kev transition.

There are at least three β-transitions from the Ce-144 nucleus to levels in the Pr-144 nucleus. There is one to the ground state with an energy of 319 Kev (intensity 75%), one to a level at 80 Kev which is in coincidence with the 80 Kev γ-transition, this transition has a maximum energy of 240 Kev (5%) and one to a 134 Kev level with a maximum energy of 186 Kev (20 %). Freeman reports a fourth β-transition with an energy of 135 Kev with an intensity of 12% the intensities of the other transitions being reduced correspondingly. This β-transition feeds a level at 166 Kev.

With a resolution of 0.2% all the L-shell conversion lines could be clearly separated, thus one might hope to identify the

nature of the transitions. The intensities of the internal conversion lines from a β-transition depends both on energy of the transition and on the multipolarity of the transition. It is not always possible to determine the type of transition from a measurement of the α_K/α_L ratio (α_K, α_L are the K- and L-shell internal conversion coefficients), because the lines from these shells have widely different energies and measurements may be effected by such phenomena as the absorption of the electrons in the window of the G-M tube. Often too, it is not possible to distinguish between different types of radiation because the α_K/α_L ratios are very similar. A much more sensitive indication of the order of the multipolarity of the radiation is the $\alpha_{L_I}/\alpha_{L_{II}}/\alpha_{L_{III}}$ ratio. Because the lines are close together, window absorption does not usually affect the results. The intensities of the L-shell internal conversion lines are completely different for all types of radiation up to E5 and M5 multipolarities, thus if the L-shell internal conversion lines can be separated, it should be possible to identify the type of transition. I decided to measure the intensities of the K-shell lines, those of the L-shell lines and where necessary the intensities of the M-shell conversion lines.

Results.

A source of Ce-144 was prepared on a Zaponlak film with a thickness of about 130 micrograms/cm^2. thick. The strength of the source was 1/20 millicurie. The resolution decreased from 0.40% at 27 Kev to 0.25% at 126 Kev due to the astigmatism in the

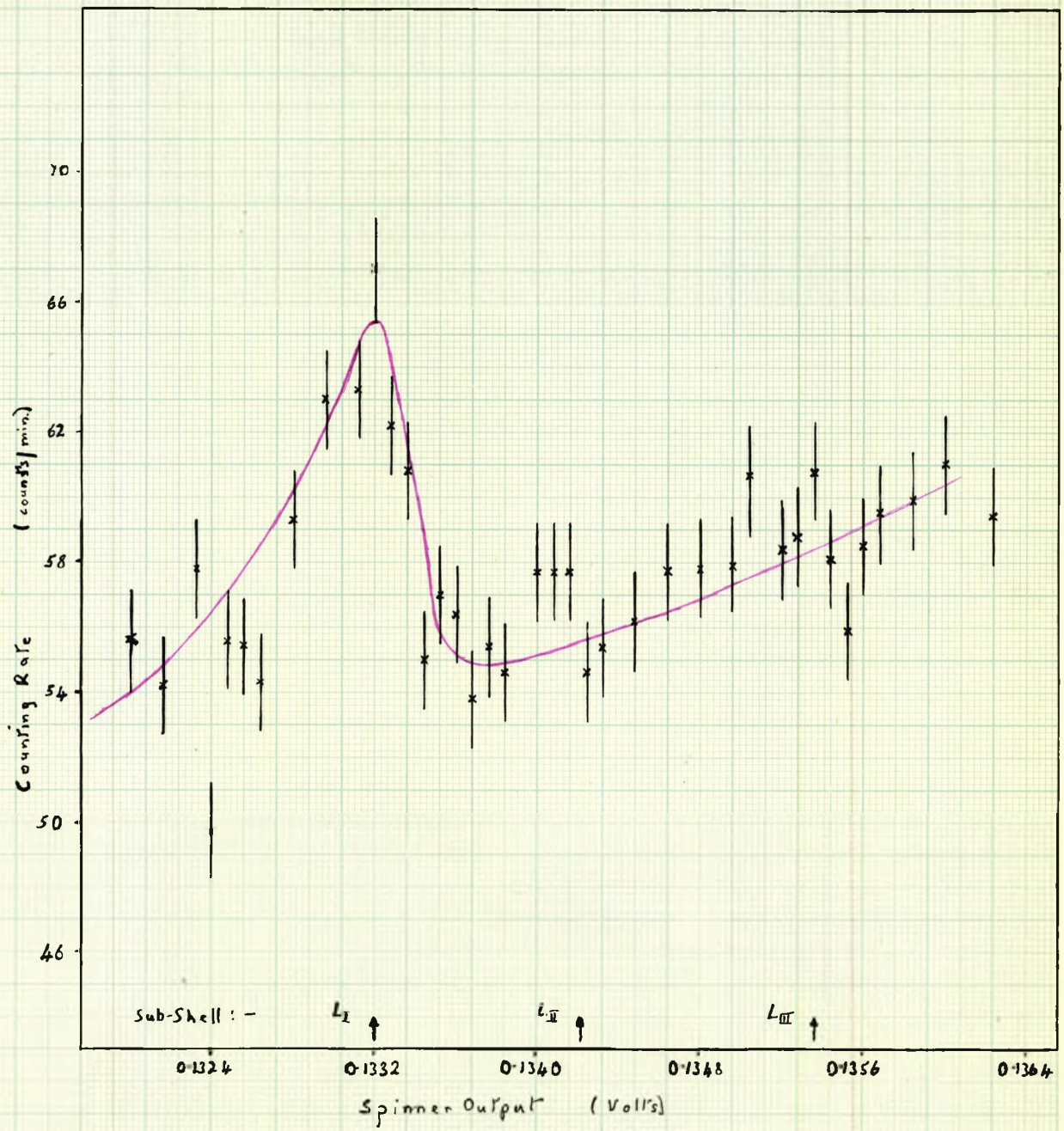

FIG. 5.3 The L-shell Conversion Lines of the 33·7 Kev. Transition.

FIGS. 5.4 & 5.5

The L-shell Conversion Lines of the 40·6 Kev. and 53·3 Kev. Transitions.

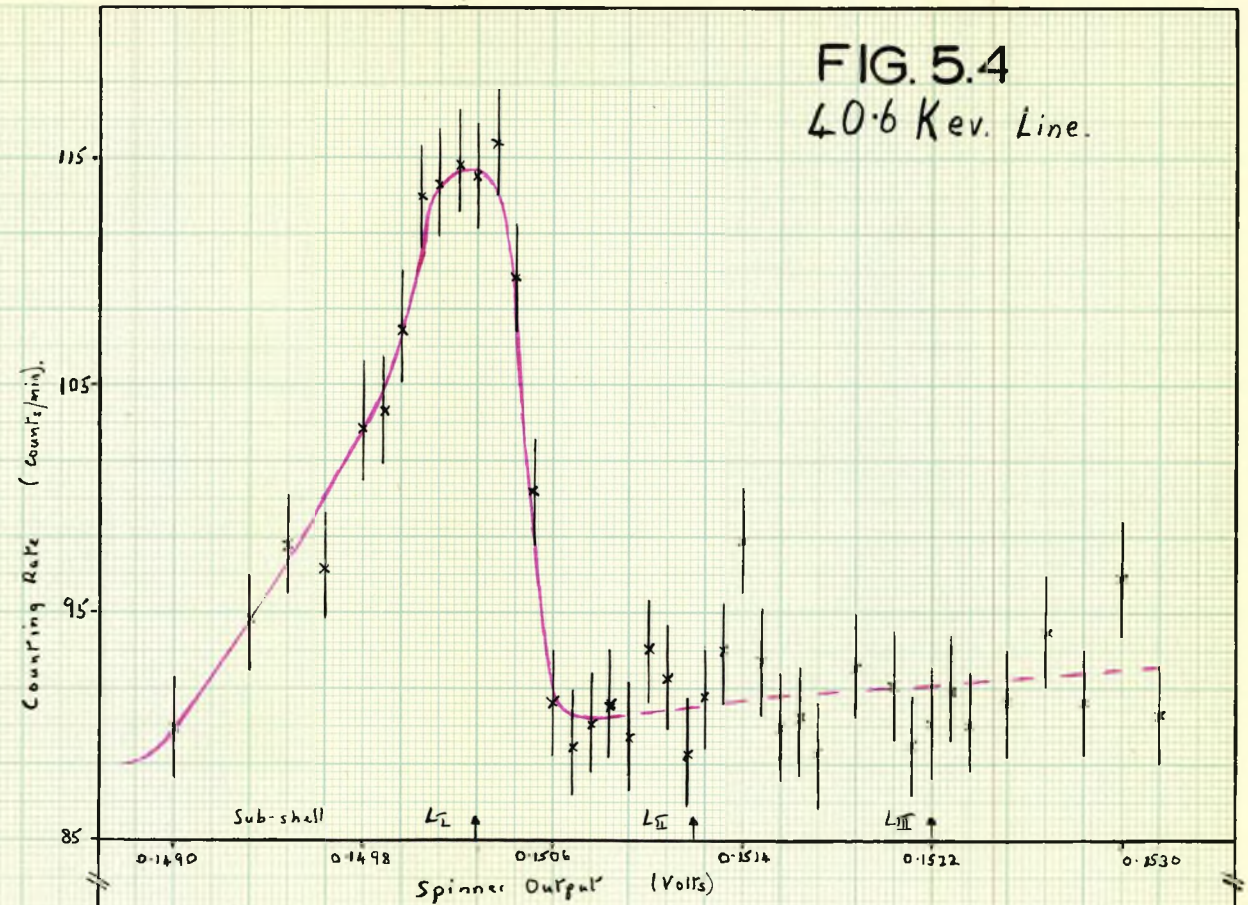

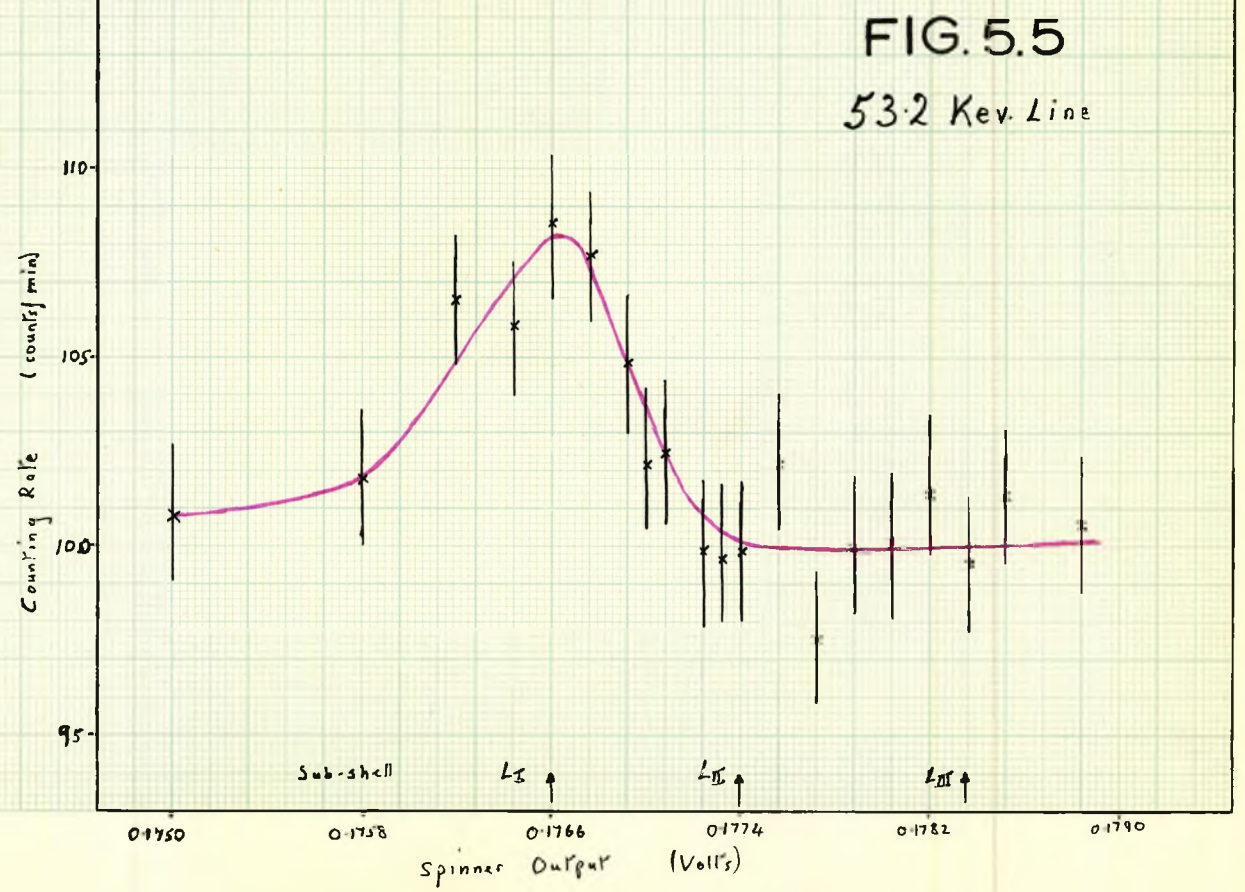

FIGS. 5.6 & 5.7

The L- and M-shell Conversion Lines of the 59·1 Kev. Transition.

FIG. 5.6

M - shell.

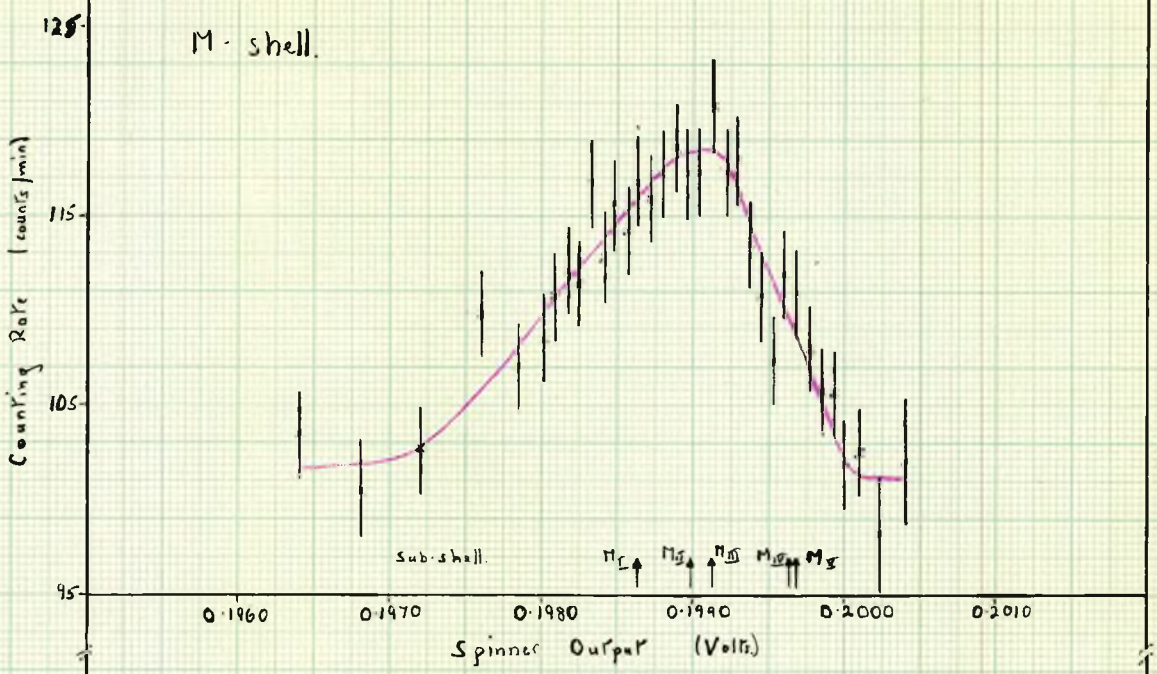

FIG. 5.7

L - Shell.

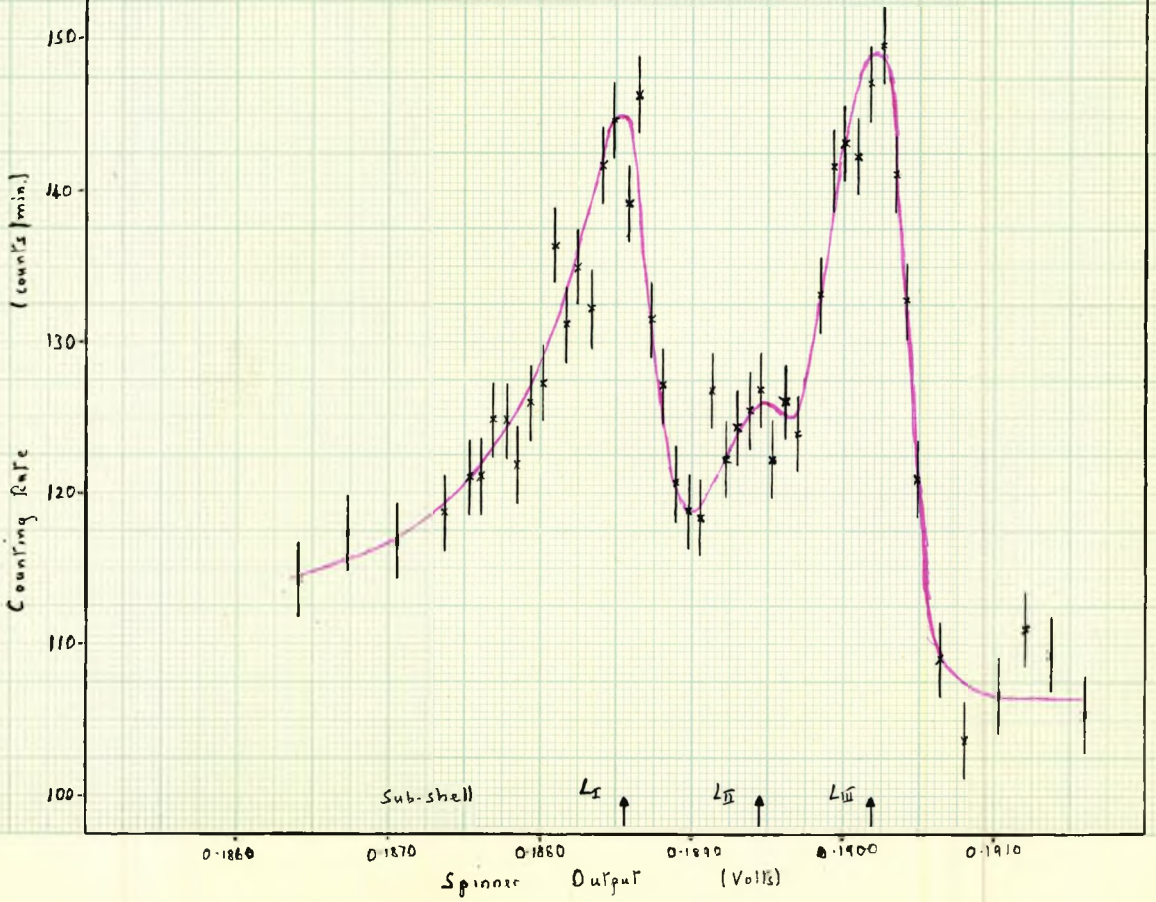

FIGS. 5.8 & 5.9

The K- and L-shell Conversion Lines of the 80·1 Kev. Transition.

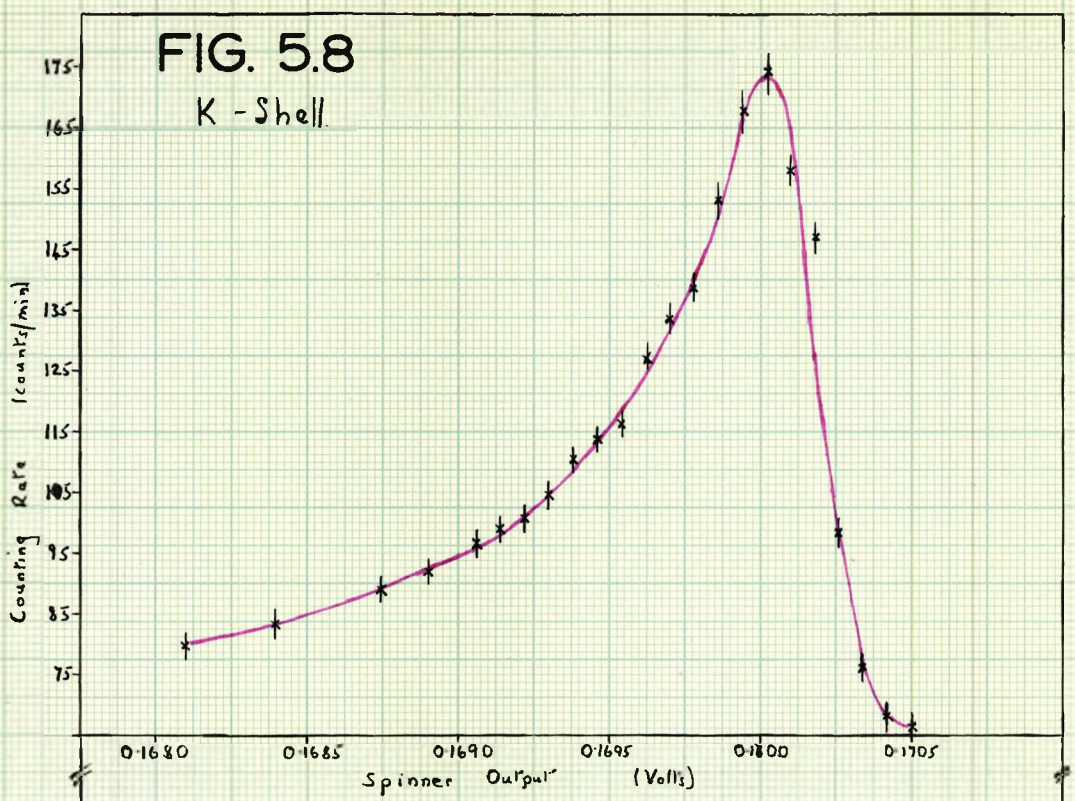

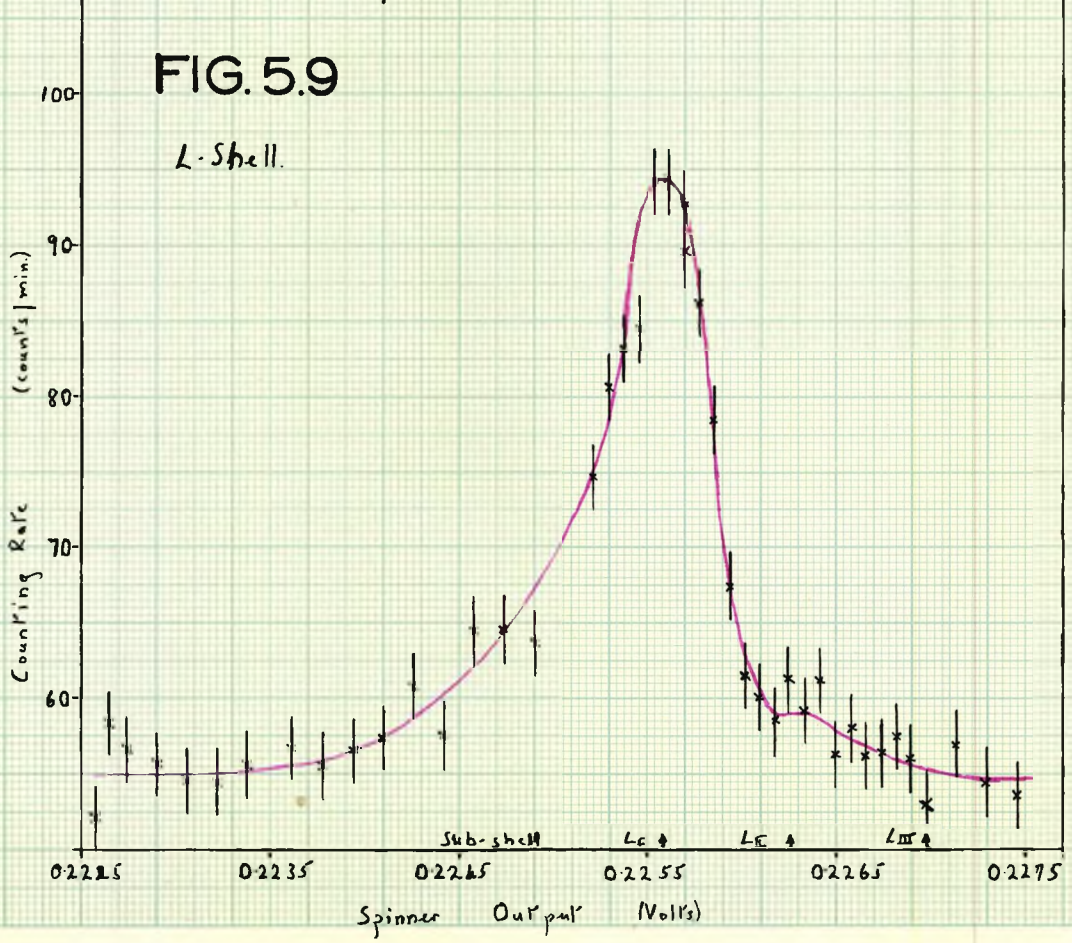

FIGS. 5.10 & 5.11

The K- and L-shell Conversion Lines of the 133·6 Kev. Transition.

FIG. 5.10

K - Shell.

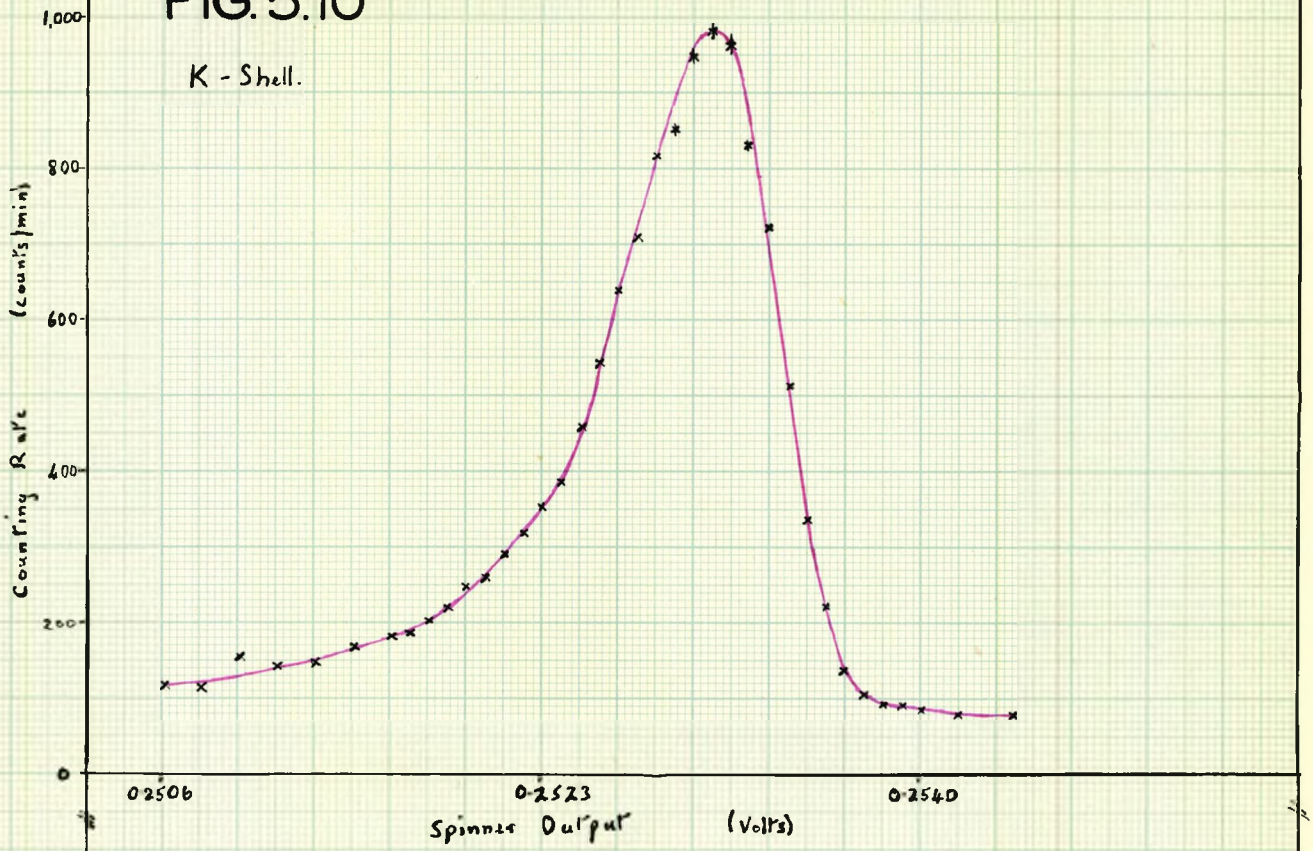

FIG. 5.11

L - shell

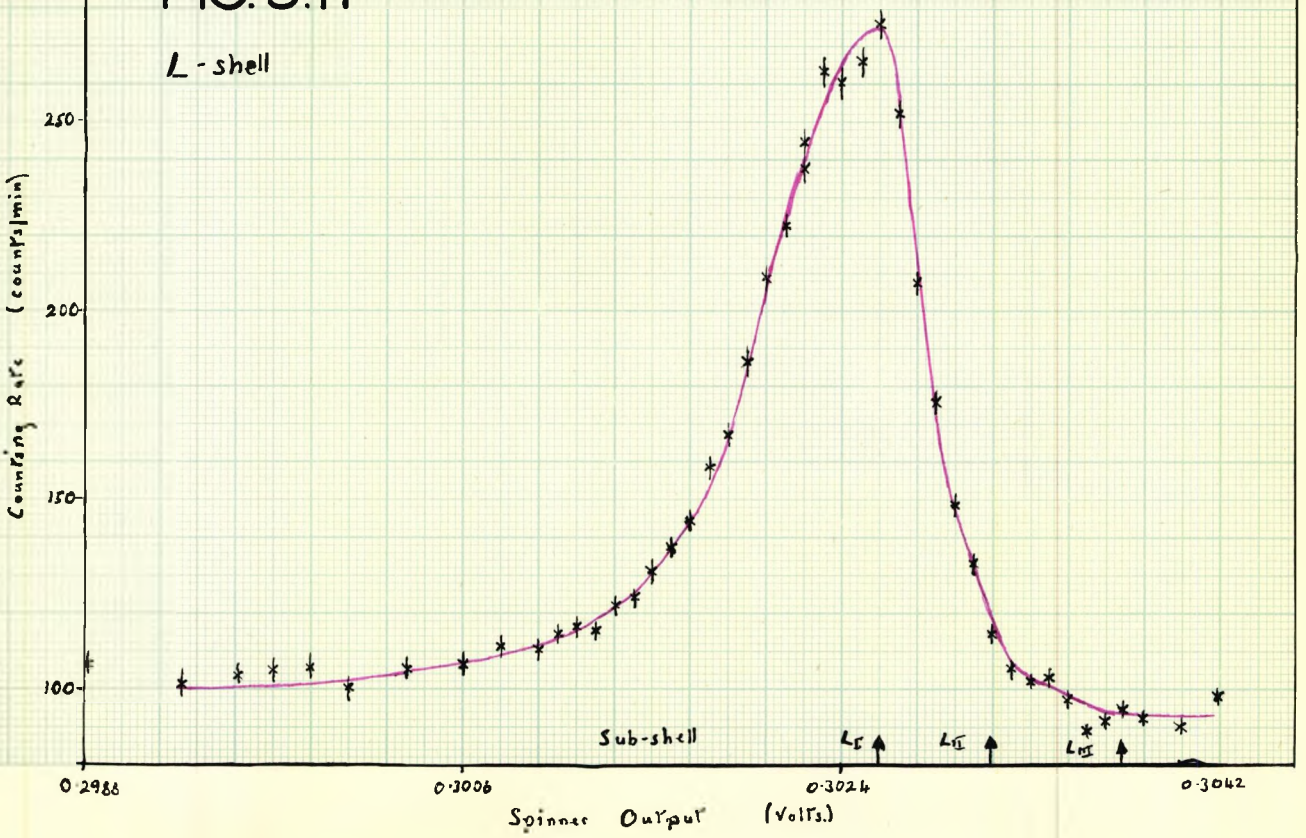

spectrometer. The transmission was set to 0.1% of a sphere and with a source of Thorium active deposit, the resolution for a source 1 mm. wide was 0.13% at 148 Kev, indicating that some of the width of the Ce-144 internal conversion lines was due to the thickness of the source.

The spectrometer was de-magnetized after every run to ensure the maximum reliability in the measurement of the momentum. Most of the measurements were made with a side-window G-M tube which was designed for the experiment. Table 5.1 gives a list of the lines measured; a more accurate table is given in Appendix B. Column I, table 3.1., contains the output of the spinning coil; column 2, the energy of the conversion line; column 3, the shell or sub-shell which the conversion took place; column 4, the energy of the transition and column 5, the estimated intensity of the line. The line profiles are shown in Fig. 5.3 to 5.11. The transitions are listed in order of energy in table 5.2 in the first column. The second and third columns give the experimental and theoretical values for the α_K/α_L and $\alpha_{L_I}/\alpha_{L_{II}}/\alpha_{L_{III}}$ ratios and column 4 gives the multipolarity of the transition. The relative intensities of the transitions are given in column 5. These were calculated from the theoretical values of the internal conversion coefficients given by Rose (79), from whose tables the ratios quoted in table 5.2, were calculated.

No internal conversion lines could be found which corresponded to a transition with an energy between 90 Kev and 98 Kev, so that if

TABLE 5.1. Energies and Intensities of the Measured β-lines of Pr-144.

Spectrometer set using the Initial Magnetization Curve
Source:- 1 mm. x 1 cm. high, $\frac{1}{20}$ millicurie Ce-144. Detector slit:- 1 mm. wide x 1.6 cm. high.
Transmission:- 0.1%
Calibration:- 0.3320 volts ≡ 1,388.44 Gauss cm. (F-Line of ThB).

Line		Shell	γ -ray	
Spinner output (volts)	Energy (kev)		Energy (kev)	Intensity
0.1338	26.8	L_I	33.7	(10±2.5) %
0.1506	33.8	L_I	40.6	(12±1.2) %
0.1603	38.1	K	80.1	(59±6) %
0.1776	46.4	L_I	53.2	(1.6±0.2) %
0.1888	52.2	L_I	59.1	(3.2±0.3) %
0.1905	53.1	L_{III}	59.1	(4.0±0.4) %
0.1996	57.9	M_{III}	59.1	(3.7±0.4) %
0.2256	73.0	L_I	79.9	(9.0±0.9) %
0.2547	91.6	K	133.6	(100±10) %
0.3044	126.8	L_I	133.6	(12.5±1.3)%
–	88.3	L_I	95	< 0.1%
–	92.9	L_I	99.7	< 0.5%

Transition (kev)	α_K/α_L and $\alpha_{L_I}/\alpha_{L_{II}}/\alpha_{L_{III}}$ ratios		Interpretation	Total Intensity
	Experimental	Theoretical		
33.7 ± 0.1	1/< 0.09/< 0.04	1/0.081/0.018	M1	6.6 ± 1.7
40.6 ± 0.1	1/< 0.10/< 0.02	1/0.079/0.017	M1	7.7 ± 0.8
53.3 ± 0.1	1/< 0.14/< 0.05	1/0.078/0.016	M1	7.1 ± 0.1
59.1 ± 0.1	1/0.144/1.27	1/0.153/1.52	M3	7.1 ± 0.1
80.1 ± 0.1	α_K/α_L - 5.7/1	α_K/α_L - 8.2/1	M1	45 ± 4.5
	$\alpha_{L_I}/\alpha_{L_{II}}/\alpha_{L_{III}}$ - 1/< 0.12/< 0.03	$\alpha_{L_I}/\alpha_{L_{II}}/\alpha_{L_{III}}$ - 1/0.074/0.015		
133.6 ± 0.1	α_K/α_L - 7.5/1	α_K/α_L - 8.3/1	M1	100 ± 10
	$\alpha_{L_I}/\alpha_{L_{II}}/\alpha_{L_{III}}$ - 1/< 0.074/< 0.03	$\alpha_{L_I}/\alpha_{L_{II}}/\alpha_{L_{III}}$ - 1/0.071/0.014		
99.7			E1	< 0.4

TABLE 5.2. Summary of Transitions and their Estimated Intensities.

there were a γ-ray with an energy of about 95 Kev it must be a weak transition. With regard to the L-shell conversion lines of a γ-ray of 100 Kev, the statistical accuracy was very poor and although there did appear to be a very slight increase in the counting rate at the right energy, the increase was less than the statistical variation. An upper limit has been placed on the intensities of both these transitions, assuming that they were both E1 transitions. If these transitions are not E1 transitions then their intensity will be less than the figures quoted for an E1 transition.

The group of lines at 58 Kev was not completely resolved. The lines were due to conversion in the M shell of the 59 Kev transition but there is also a possibility that the intensity may be partly accounted for by a K-shell conversion line from the γ-ray of 100 Kev.

The energies of these transitions are in good agreement with those of Cork et al, who also used high resolution. My values for the $\alpha_{L_I}/\alpha_{L_{III}}$ ratios of the 80.1 Kev and 133.6 Kev transitions differ from theirs, but since the lines were well resolved, there was no difficulty in calculating the intensities. These transitions could only be M1 transitions from their $\alpha_{L_I}/\alpha_{L_{III}}$ ratios. Cork et al pointed out in their paper that their results for the intensities of the lines at 52.2 Kev and 53.1 Kev agree with the theoretical ratio for the L-shell lines an M3 transition with an energy of 59 Kev but they decided that this interpretation was unlikely. I found three lines which could be interpreted as the L_I-, L_{II}-, and L_{III}-conversion

lines of a 59.1 Kev γ-ray so that it is improbable that these lines are due to only two transitions. This argument is strengthened by the failure to observe conversion lines arising from the L-shell of a 95 Kev γ-ray and the complexity of the M-shell conversion lines. The 33.7 Kev, 40.6 Kev and 53.2 γ-rays must all be M1 transitions because in all other types of transition there is appreciable conversion in the L_{III}-subshell.

Whilst Rose's tables were being computed, the theory of internal conversion was developed further. Rose's tables were based on the assumption that the nucleus was static, that is, that the internal conversion coefficients do not depend on the nuclear shell structure. Church (80) and Rose and Green (81) have developed the theory to allow for such dynamic effects as those of nuclear shell structure while Sliv (82) has analysed the effect of the finite size of the nucleus. Because of the computation necessary, it has not been possible to evaluate the dynamic effects. Since these dynamic effects depend on the structure of the nucleus, one must postulate the most likely nuclear configurations otherwise the number of tables required would be large. The effect of the finite size of the Pr^{144} nucleus on the internal coefficients should be small for a M1 transition.

My results for the α_K/α_L ratios are lower than the predicted figures and by themselves, are not sufficient evidence to allow an interpretation of the transitions. I could not measure the ratios, except those of the 59.1 Kev transition, with sufficient

accuracy to be able to compare them critically with the theoretical values. Within the statistical limits, however, the agreement was good. In view of this agreement, it is assumed that the nuclear shell structure does not play an important part in the decay of the excited states of Pr-144.

Level Schemes.

The six transitions measured may be explained by a simple level scheme for the Pr-144 nucleus. All the transitions arise from the decay of an excited state 133.5 Kev above the Ground State. There are three competing modes of decay, namely (i) a single transition with an energy of 133.6 $\pm$ 0.1 Kev, (ii) two γ-rays in cascade with energies of 53.2 $\pm$ 0.1 Kev + 80.1 $\pm$ 0.1 Kev = 133.3 $\pm$ 0.14 Kev and (iii) three γ-rays in cascade with energies of 33.7 $\pm$ 0.1 Kev + 40.6 $\pm$ 0.1 Kev + 59.1 $\pm$ 0.1 Kev = 133.4 $\pm$ 0.17 Kev. The mean value for the energy of this level is 133.5 $\pm$ 0.2 Kev. The agreement between the intensities of the γ-transitions is good although the intensities were only measured roughly.

Freeman found that the 33 Kev transition was in coincidence with the 133 Kev transition and hence postulated a level at 166 Kev. He could not, however, explain the intensities of the 40 Kev and 59 Kev transitions from his decay scheme nor did the intensities of the β-transition to the 155 Kev level and the intensities of the γ-rays leaving this level agree. He suggested that the level at 100 Kev was fed either by a β-transition or by a γ-ray with an energy close to

that of the 33.2 Kev γ-ray which he detected. Except for the weak γ-transitions which were not measured, his decay scheme in the latter case would be similar to mine.

The cascading γ-rays may be fitted into a scheme in different ways. Coincidence experiments can be used to sort out the order of the 80.1 Kev and 53.2 Kev γ-rays. Because the 53.2 Kev γ-ray is weaker than the 80.1 Kev transition it must decay to a level at 80 Kev. This assumption is supported by measurements of the $\beta-\gamma$ coincidences of Hickock et al and Freeman. With regard to the 33.7 Kev, 40.6 Kev and 59.1 Kev transitions, there is no information about coincidences between any of the transitions. From a consideration of the life-times of the states, the 59.1 Kev transition cannot decay from the 133.5 Kev level because , being a M3 type of transition, it would be too slow to compete with the 133.5 Kev γ-ray.

If the evidence for a 100 Kev γ-ray is accepted, then the 59.1 Kev transition must decay to the Ground State of the Pr-144 nucleus and must be fed by the 40.6 Kev transition. The 59.1 Kev could not decay from the 100 Kev level because it would be competing with the much faster 100 Kev E2 transition. It is possible to construct only one decay scheme taking into account all these considerations, this scheme is shown in Fig. 5.12. The Ground State is known to be 0^- from measurements of the spin of Pr-144 (83) and the β-transitions from the Pr-144 nucleus (84), (85). The 100 Kev transition is indicated with a broken arrow becuase it was not observed.

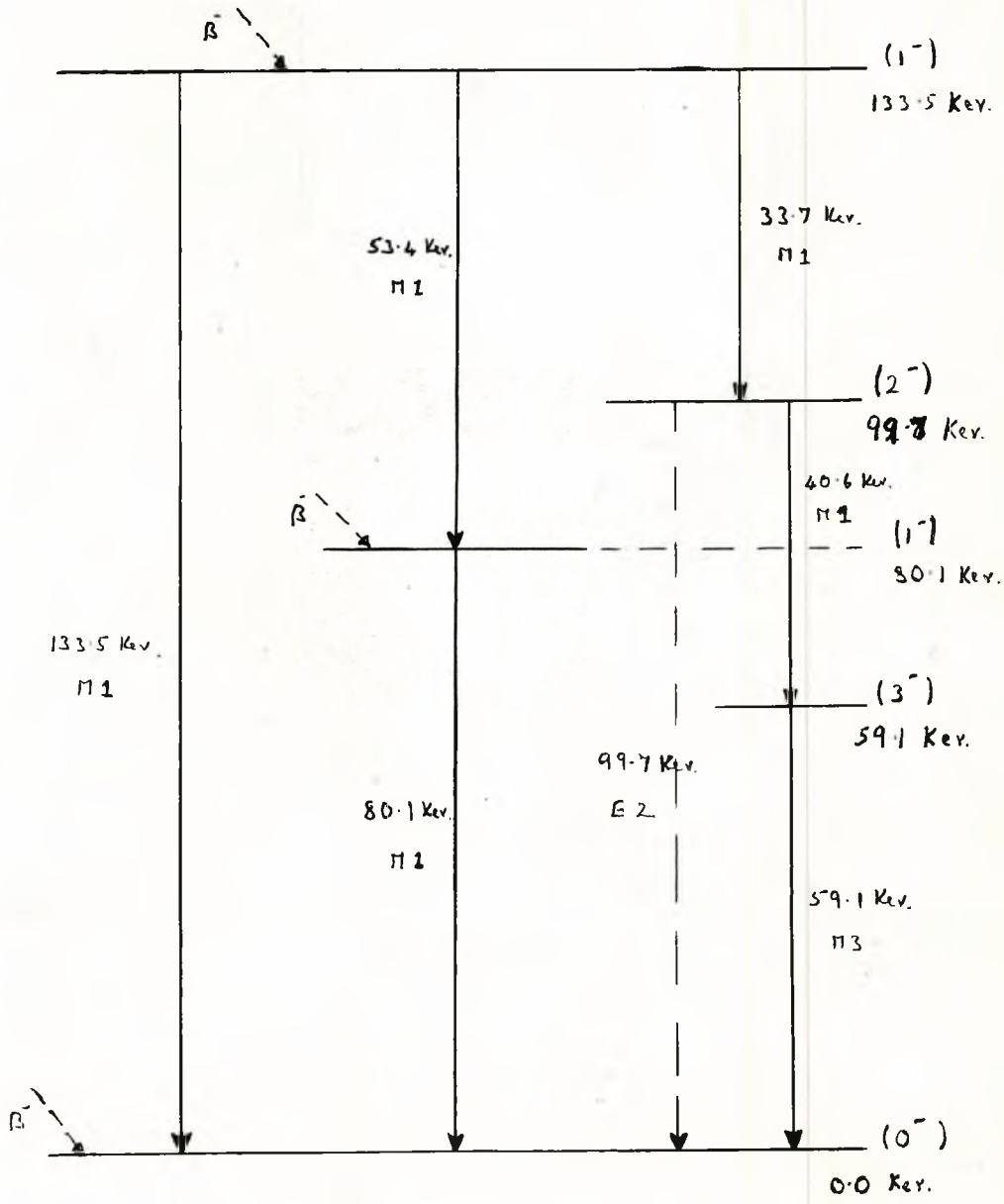

FIG. 5.12

The Level Scheme proposed for the Pr-144 Nucleus following the β-decay of Ce-144.

This decay scheme is consistent with the observed β-spectra to the ground state, the 80 Kev level and the 133.5 Kev level. Because the Ground State is 0^-, all three β-spectra must be first forbidden spectra. The spin changes are 0, 1 and 1 respectively. The transition to the 100 Kev level would be a unique first forbidden transition. In this type of transition, the logarithm of the decay constant, log(ft), is greater than for a first forbidden non-unique transition so this transition should be weaker than a non-unique first forbidden transition if the two compete in a decay scheme. There should not therefore be an observable β-transition to the 100 Kev level. A β-transition to the 59.1 Kev would be a second forbidden transition and again it should not be observable.

The decay scheme proposed has also been put forward by Graham and Geiger (86) in a recent paper in which they give the same assignments to the transition measured in this work. It is a consistent scheme with respect to the observed β-transitions, and the energies, intensities and multipolarities of the γ-transitions.

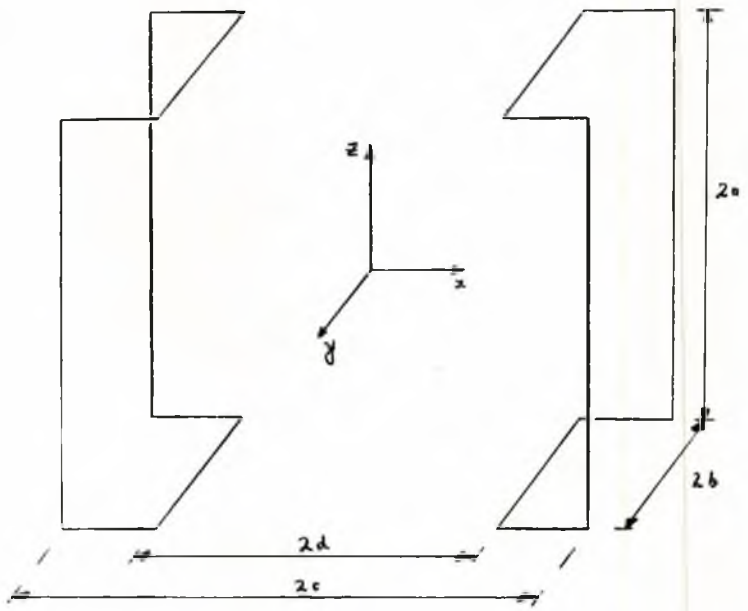

FIG. A.1

The Coordinate System used to calculate the Field Strength of the Auxiliary Coils.

Appendix A.

The formulae for the field produced by square and bent-headed coils have been given (40), (41), but they are very complicated and difficult to use. The following expression was therefore derived and used to calculate the field from a pair of coils shown in fig. A.1.

The field at a point P, distant r_o from a straight wire of length a+b is given by the formula:-

$$H = \int_a^b \frac{I\, dl \cos\theta}{r^2} = \int_a^b \frac{I\, r_o\, dl}{(r_o^2 + l^2)^{3/2}}$$

$$= \frac{I}{r_o}\left[\frac{a}{(a^2 + r_o^2)^{\frac{1}{2}}} + \frac{b}{(b^2 + r_o^2)^{\frac{1}{2}}} \right]$$

For a pair of coils such as those in fig. A.1. the field is the sum of the contributions from individual sections of the frame. The field will be divided into components H_x, H_y, along the x- and y- axes respectively. The distances a,b,c,d, specify the dimensions of the coils. For two coils each with n turns the field is:-

$$H_x = nI \left\{ \frac{(a-z)}{[(a-z)^2 + (b-y)^2 + (c-x)^2]^{\frac{1}{2}}} + \frac{(a+z)}{[(a+z)^2 + (b-y)^2 + (c-x)^2]^{\frac{1}{2}}} \right\} \frac{(b-y)}{(b-y)^2 + (c-x)^2}$$

$$+ nI \left\{ \frac{(a-z)}{[(a-z)^2 + (b+y)^2 + (c-x)^2]^{\frac{1}{2}}} + \frac{(a+z)}{[(a+z)^2 + (b+y)^2 + (c-x)^2]^{\frac{1}{2}}} \right\} \frac{(b+y)}{(b+y)^2 + (c-x)^2}$$

$$+ nI \left\{ \frac{(a-z)}{[(a-z)^2 + (b-y)^2 + (c+x)^2]^{\frac{1}{2}}} + \frac{(a+z)}{[(a+z)^2 + (b-y)^2 + (c+x)^2]^{\frac{1}{2}}} \right\} \frac{(b-y)}{(b-y)^2 + (c+x)^2}$$

$$+ nI \left\{ \frac{(a-z)}{[(a-z)^2 + (b+y)^2 + (c+x)^2]^{\frac{1}{2}}} + \frac{(a+z)}{[(a+z)^2 + (b+y)^2 + (c+x)^2]^{\frac{1}{2}}} \right\} \frac{(b+y)}{(b+y)^2 + (c+x)^2}$$

+

$$+ nI \left\{ \frac{(b-y)}{[(a-z)^2 + (b-y)^2 + (d-x)^2]^{\frac{1}{2}}} + \frac{(b+y)}{[(a-z)^2 + (b+y)^2 + (d-x)^2]^{\frac{1}{2}}} \right\} \frac{(a-z)}{(a-z)^2 + (d-x)^2}$$

$$+ nI \left\{ \frac{(b-y)}{[(a+z)^2 + (b-y)^2 + (d-x)^2]^{\frac{1}{2}}} + \frac{(b+y)}{[(a+z)^2 + (b+y)^2 + (d-x)^2]^{\frac{1}{2}}} \right\} \frac{(a+z)}{(a+z)^2 + (d-x)^2}$$

$$+ nI \left\{ \frac{(b-y)}{[(a-z)^2 + (b-y)^2 + (d+x)^2]^{\frac{1}{2}}} + \frac{(b+y)}{[(a-z)^2 + (b+y)^2 + (d+x)^2]^{\frac{1}{2}}} \right\} \frac{(a-z)}{(a-z)^2 + (d+x)^2}$$

$$+ nI \left\{ \frac{(b-y)}{[(a+z)^2 + (b-y)^2 + (d+x)^2]^{\frac{1}{2}}} + \frac{(b+y)}{[(a+z)^2 + (b+y)^2 + (d+x)^2]^{\frac{1}{2}}} \right\} \frac{(a+z)}{(a+z)^2 + (d+x)^2}$$

$$H_y = - nI \left\{ \frac{(a-z)}{[(a-z)^2 + (b-y)^2 + (c-x)^2]^{\frac{1}{2}}} + \frac{(a+z)}{[(a+z)^2 + (b-y)^2 + (c-x)^2]^{\frac{1}{2}}} \right\} \frac{(c-x)}{(b-y)^2 + (c-x)^2}$$

$$+ nI \left\{ \frac{(a-z)}{[(a-z)^2 + (b+y)^2 + (c-x)^2]^{\frac{1}{2}}} + \frac{(a+z)}{[(a+z)^2 + (b+y)^2 + (c-x)^2]^{\frac{1}{2}}} \right\} \frac{(c-x)}{(b+y)^2 + (c-x)^2}$$

$$- nI \left\{ \frac{(a-z)}{[(a-z)^2 + (b-y)^2 + (c+x)^2]^{\frac{1}{2}}} + \frac{(a+z)}{[(a+z)^2 + (b-y)^2 + (c+x)^2]^{\frac{1}{2}}} \right\} \frac{(c+x)}{(b-y)^2 + (c+x)^2}$$

$$+ nI \left\{ \frac{(a-z)}{[(a-z)^2 + (b+y)^2 + (c+x)^2]^{\frac{1}{2}}} + \frac{(a+z)}{[(a+z)^2 + (b+y)^2 + (c+x)^2]^{\frac{1}{2}}} \right\} \frac{(c+x)}{(b+y)^2 + (c+x)^2}$$

$H_y = 0$ if $y = 0$.

The field was calculated for several points on the x-axis with a = $4\frac{1}{4}$", b = $3\frac{1}{2}$", c = $5\frac{1}{2}$" and d = $3\frac{1}{2}$".

x, ins.	0	0·25	0·5	0·75	1·0
$\frac{25{\cdot}4\ Be}{I_n}$, oersted/gauss-cm	0·9576	0·9646	0·9735	0·9885	1·0088

Over the dimensions of the spinning coil ($\frac{3}{4}$" radius), the field increases by 3%.

Appendix B.

Mr. Kamal has remeasured the energies of the internal conversion lines of Pr-144 using the apparatus I designed and built to measure the magnetic field (see pp. 31 - 39); he has also estimated their relative intensities. His results are summarised below and should be compared with table 5.1.

Electron Energy, Kev.	Interpretation (shell)	Gamma Energy, Kev.		Multipolarity	Intensity %
26.77	L1	33.61		M1	
34.01	L1	40.85)	40·88	M1	12
39.91	M1	40.92)			1·8
46.54	L1	53.38		M1	
52.10	L1	58.99)	58·97	M3	8·7
57.52	M1	59.03)			3·1
38.00	K	80.00)			57
73.12	L1	79.96)	79·97	M1	6·6
78.45	M1	79.96)			1·5
91.40	K	133.40)			100
126.54	L1	133.38)	133·39	M1	16·5
131.89	M1	133.40)			5·2

There was no evidence for a 100 Kev gamma ray.

No errors have been quoted because Mr. Kamal did not send a record of the errors in his measurements.

Bibliography.

Abbreviations.

Ann.Phys. - Annals of Physics.

Ark.f.Fys. - Arkiv för Fysik.

Ark.F.Mat.Ast.o.Fys. - Arkiv för Matematik Astronomi och Fysik.

Bull.Am.Phys.Soc. - Bulletin of the American Physical Society.

Bull.Inst.Nucl.Sci."Boris Kidrich" - Bulletin of the Institute of Nuclear Science "Boris Kidrich".

Bur.St'ds.J.Res. - Bureau of Standards Journal of Research.

Helv.Phys.Acta. - Helvetica Physica Acta.

J.App.Phys. - Journal of Applied Physics.

J.E.T.P. - Journal of Experimental and Theoretical Physics. U.S.S.R.

Nucl.Inst. - Nuclear Instruments.

Phys.Rev. - Physical Review.

Proc.Reh.Conf. - Proceedings of the Rehoveth Conference on Nuclear Shell Structure.

Proc.Phys.Soc. - Proceedings of the Physical Society.

Proc. Roy. Soc.(Lond.) - Proceedings of the Royal Society of London.

Prog.Nucl.Phys.(Lond.)	-	Progress in Nuclear Physics (London).
Rep.Prog.Phys.	-	Report on Progress in Physics.
Rev.Mod.Phys.	-	Reviews of Modern Physics.
Rev.Sci.Inst.	-	Review of Scientific Instruments.
Zeits.f.Phys.	-	Zeitschrift für Physik.
N.B.S.	-	National Bureau of Standards (Washington).

References.

1. The historical data on radio-activity has been taken from:-
"Radiation and Radio-active Substances" by Sir E. P. Rutherford, J. Chadwick and C. D. Ellis, Cambridge University Press,
"The Atomic Nucleus" by R. D. Evans, McGraw Hill and
"Atomic Physics" by G. P. Harnwell and W. G. Stephens, McGraw Hill.
2. The early historical data on spectrometers has been taken from
"Beta- and Gamma-ray Spectroscopy" by K. Siegbahn, North Holland
3. C. Witcher:- Phys. Rev. 60 (1941), 32. Publishing Co..
4. M. Deutsch:- Phys. Rev. 59 (1941), 648a.
5. J. DuMond:- Ann. Phys. 2 (1957), 283.
6. E. Persico:- Rev. Sci. Inst. 20 (1949) 191.
7. K. Siegbahn and H. Slätis:- Ark.f.Fys. 1 (1949) 339.
8. L. M. Langer and C. S. Cook:- Rev. Sci. Inst. 19 (1948) 257.
9. F. Beiduk and F. Konopinski:- Rev. Sci. Inst. 19 (1948) 594.
10. K. Siegbahn and N. Svartholm:- Ark.f.Mat.Ast.o.Fys. A33 (1946). No.21.
11. A. Hedgran, K. Siegbahn and H. Slätis:- Proc. Roy. Soc. 63A (1950) 960.
12. M. Mladjenovic:- Bull. Inst. Nucl. Sci. "Boris Kidrich" 6 (1956) 54.
13. H. Slätis:- Nucl. Inst. 2 (1958) 332.
14. F. Shull and D. Dennison:- Phys. Rev. 71 (1947) 681 and 72 (1947) 256.
15. F. Kurie, J. Osaba and L. Slack:- Rev. Sci. Inst. 19 (1948) 771.

16. N. Svartholm:- Ark.f.Fys. 2 (1950) 195.

17. A. Bartlett and K. Bainbridge:- Rev. Sci. Inst. 22 (1951) 517.

18. F. Stoker, Ong. Ping Hok, E. de Hahn and E. Sizoo:- Physica 20 (1954) 337.

19. H. Huber and O. Wild:- Helv. Phys. Acta. 30 (1957) 3.

20. E. Persico and C. Geoffrion:- Rev. Sci. Inst. 21 (1950) 945.

21. P. Cavanagh:- Prog. Nucl. Phys. (Lond.) 1 (1950) 140.

22. N. Verster:- Prog. Nucl. Phys. (Lond.) 2 (1952) 1.

23. J. F. Barry:- Ph.D. Thesis, Univ. of Liverpool.

24. W. Y. Chang and S. Rosenblum:- Rev. Sci. Inst. 16 (1945) 75.

25. E. R. Andrews:- "Nuclear Magnetic Resonance", p.66, (Cambridge Monograph on Physics.)

26. J. Du Mond:- Ann. Phys. 2 (1957) 283.

27. N. J. Hopkins:- Rev. Sci. Inst. 20 (1949) 401.

28. A. S. Newton and H. X. Di Grazia:- Univ. California Radiation Laboratory, Report No. 2994.

29. G. D. Adams, R. W. Dressel and F. E. Towsley:- Rev. Sci. Inst. 21 (1950) 69.

30. J. L. Symonds:- Rep. Prog. Phys. 18 (1955) 102.

31. R. H. Dicke:- Rev. Sci. Inst. 19 (1948) 533.

32. P. P. Cioffi:- Rev. Sci. Inst. 21 (1950) 624.

33. H. R. Fechter and S. Reuben:- Rev. Sci. Inst. 26 (1955) 1108.

34. D. G. E. Martin and H. C. W. Richardson:- Proc. Phys. Soc. 63A (1950) 223.

35. J. M. Cork, R. G. Shreffler and F. B. Shull:- Rev. Sci. Inst. 18 (1947) 315.

36. L. M. Langer and F. R. Scott:- Rev. Sci. Inst. 21 (1950) 522.

37. W. G. Lamb Jr. and R. C. Retherford:- Phys. Rev. 81 (1951) 222.

38. A. Hedgran:- Ark.f.Fys. 1 (1952) 1.

39. G. Bäckstrom:- Nucl. Inst. 1 (1957) 253.

40. F. K. Harris:- Bur.St'ds.J.Res. 13 (1934) 390.

41. R. H. Lyddane and A. E. Ruark:- Rev. Sci. Inst. 10 (1939) 253.

42. J. M. Sturvant:- Rev. Sci. Inst. 18 (1948) 124.

43. F. E. Terman:- "Radio-Engineering", McGraw Hill.

44. M. Walker:- "Diagnosing of Troubles in Electrical Machinery".

45. Johnson Matthey Ltd:- leaflet No. 1300, 380.

46. Johnson Matthey Ltd:- leaflet No. 1300, 381.

47. W. M. Horton:- Rev. Sci. Inst. 20 (1949) 930.

48. V. J. Scheafer and P. Harkner:- J. App. Phys. 13 (1942) 427.

49. L. M. Langer:- Rev. Sci. Inst. 20 (1949) 216.

50. A. Flammersfeld:- Zeits.f.Phys. 114 (1939) 224.

51. C. D. Ellis:- Nature 129 (1932) 276.

52. H. Slätis:- Ark.f.Fys. 6 (1953) 415.

53. K. E. Bergkvist:- Ark.f.Fys. 12 (1957) 381.

54. L. M. Langer and H. C. Price Jr.:- Phys. Rev. 75 (1949) 1109L.
and Phys. Rev. 76 (1949) 641.

55. C. S. Wu and L. Feldman:- Phys. Rev. 76 (1949) 696.

56. J. Moreau and J. Perez y Jorba:- Comptes Rendus 235 (1952) 38.

57. H. M. Agnew:- Phys. Rev. 77 (1950) 655.

58. M. E. Rose, N. M. Dismuke and C. L. Perry:- Oak Ridge National
Report No. 1459.

59. E. J. Konopinski and G. E. Uhlenbeck:- Phys. Rev. 60 (1941) 308.

60. M. Z. Fierz:- Physik 104 (1937) 553, and H. M. Mahmoud and E. J. Konopinski :- Phys. Rev. 88 (1952) 1266.

61. B. Kahn and W. S. Lyon:- Phys. Rev. 98 (1955) 58.

62. U. Fano:- N.B.S. Applied Maths. Series No. 13.

63. J. R. Reitz:- Phys. Rev. 77 (1950) 10.

64. M. E. Rose and D. K. Holmes:- Phys. Rev. 83 (1951) 190L.

65. M. E. Rose and C. L. Perry:- Phys. Rev. 90 (1953) 479.

66. F. T. Porter, F. Wagner and M. S. Freedman:- Phys. Rev. 107 (1957) 135.

67. F. I. Boley and D. S. Dunavan:- Phys. Rev. 90 (1953) 158L.

68. M. E. Bunker, S. P. Mize and S. W. Starner:- Phys. Rev. 94 (1954) 1694.

69. H. B. Keller and J. M. Cork:- Phys. Rev. 84 (1951) 1079.

70. W. C. Kelly:- Phys. Rev. 85 (1952) 101.

71. Chang Lin-Sheng, G. John and J. D. Kurbatov:- Phys.Rev. 85 (1952) 487.

72. F. T. Porter and C. S. Cook:- Phys. Rev. 87 (1952) 464.

73. W. S. Emmerich, H. J. Auth and J. D. Kurbatov:- Phys. Rev. 94 (1954) 110.

74. W. E. Kreger and C. S. Cook:- Phys. Rev. 96 (1954) 1276.

75. J. M. Cork, M. K. Brice and L. C. Schmid:- Phys. Rev. 96 (1954) 1296.

76. I. Pullman and P. Axel:- Phys. Rev. 102 (1956) 1366.

77. R. L. Hickock, W. A. McKinley and S. C. Fultz:- Phys. Rev. 109 (1958) 113.

78. N. S. Freeman:- Phys. Soc. (Proc.) 74 (1959) 449.

79. M. E. Rose:- "Internal Conversion Coefficients" (1958), North Holland Publishing Co..

80. C. Church and J. Wenzer:- Phys. Rev. 104 (1956) 1382.

81. T. A. Green and M. E. Rose:- Phys. Rev. 110, (1958) 105.

82. L. A. Sliv:- J.E.T.P. 21 (1951) 770.

and L. A. Sliv and M. Listgarten:- 22 (1952) 29.

83. M. A. Grace, C. E. Johnson, R. E. Surlock and R. T. Taylor:- unpublished data.

see:- D. Strominger, J. M. Hollander and E. T. Seaborg:- Rev. Mod. Phys. 30 (1958).

84. M. J. Laubitz:- Proc. Phys. Soc. 69A (1956) 789.

85. D. A. Bromley:- Proc. Reh. Conf.

86. J. S. Geiger, R. L. Graham and G. T. Ewan:- Bull. Am. Phys. Soc. Series II Vol. 4 (1959) 57.